CHARACTERIZATION OF A NEW *ANOPHELES DIRUS* DELTA CLASS GLUTATHIONE S-TRANSFERASE AND INTERACTIONS WITH THE C-JUN N-TERMINAL KINASE PATHWAY COMPONENTS

RUNGRUTAI UDOMSINPRASERT

A THESIS SUBMITTED IN PARTIAL FULFILLMENT
OF THE REQUIREMENTS FOR
THE DEGREE OF DOCTOR OF PHILOSOPHY
(MOLECULAR GENETICS AND GENETIC ENGINEERING)
FACULTY OF GRADUATE STUDIES
MAHIDOL UNIVERSITY
2005

ISBN 974-04-6077-1

Thesis
Entitled

CHARACTERIZATION OF A NEW *ANOPHELES DIRUS* DELTA CLASS GLUTATHIONE S-TRANSFERASE AND INTERACTIONS WITH THE C-JUN N-TERMINAL KINASE PATHWAY COMPONENTS

……
Miss Rungrutai Udomsinprasert
Candidate

……....
Assoc. Prof. Albert J. Ketterman, Ph.D.
Major-Advisor

..……..
Asst. Prof Gerd Katzenmeier, Ph.D.
Co-Advisor

……
Prof. Duncan R. Smith, Ph.D.
Co-Advisor

..……..
Lect. Witoon Tirasophon, Ph.D.
Co-Advisor

……
Assoc. Prof. Chanan Angsuthanasombat, Ph.D.
Co-Advisor

..……...
Assoc. Prof. Rassmidara Hoonsawat, Ph.D.
Dean
Faculty of Graduate Studies

..……..
Asst. Prof. Varaporn Akkarapatumwong, Ph.D.
Chair
Doctor of Philosophy Programme in
Molecular Genetics and Genetic Engineering
Institute of Molecular Biology and Genetics

Thesis
Entitled

CHARACTERIZATION OF A NEW *ANOPHELES DIRUS* DELTA CLASS GLUTATHIONE S-TRANSFERASE AND INTERACTIONS WITH THE C-JUN N-TERMINAL KINASE PATHWAY COMPONENTS

was submitted to the Faculty of Graduate Studies, Mahidol University
for the degree of Doctor of Philosophy
(Molecular Genetics and Genetic Engineering)

On

May 4, 2005

.....
Miss Rungrutai Udomsinprasert
Candidate

.....
Assoc. Prof. Albert J. Ketterman, Ph.D.
Chair

.....
Prof. Duncan R. Smith, Ph.D.
Member

.....
Miss Peerada Prommeenate, Ph.D.
Member

.....
Assoc. Prof. Chanan Angsuthanasombat, Ph.D.
Member

.....
Lect. Witoon Tirasophon, Ph.D.
Member

.....
Asst. Prof Gerd Katzenmeier, Ph.D.
Member

.....
Assoc. Prof. Rassmidara Hoonsawat, Ph.D.
Dean
Faculty of Graduate Studies
Mahidol University

.....
Asst. Prof. Chartchai Krittanai, Ph.D.
Acting Director
Institute of Molecular Biology and Genetics
Mahidol University

ACKNOWLEDGEMENTS

I would like to express my deepest gratitude to many persons, especially my Major Advisor, Assoc. Prof. Albert J. Ketterman, for his warm guidance, invaluable advice and encouragement throughout this thesis project. I would also like to thank my co-advisors; Prof. Duncan R. Smith, Assoc. Prof. Chanan Angsuthanasombat, Asst. Prof. Gerd Katzenmeier and Dr. Witoon Tirasophon, for their valuable comments, helpful advice and discussion for this research project.

I would like to give my sincere thank to Dr. Marie A. Bogoyevitch for her great advice in my first publication. Without helpfulness and work collaboration from Dr. Saengtong Pongjaroenkit, Dr. La-aied Prapanthadara, Dr. Aaron J. Oakley and Ms. Jantana Wongsantichon, my second publication would not be succeeded. I also thank Dr.Walawut Chulalakasananukul for providing me the source of *Drosophila* adult flies.

My appreciation also is extended to Ms. Anchalee Nirachanon for her great help in managing all documents and scholarship budgets during the whole project period. I would like to special thank to all GST members, especially Dr. Jeerang Wongtrakul, Mr. Pakorn Winayanuwattikun, Ms. Ardcharaporn Vararattanavech and all my friends for their great assistance in solving problems, wonderful friendships, support and encouragement.

I am particularly indebted to the Royal Golden Jubilee Ph.D. program, conducted by the Thailand Research Fund (TRF) that provided me the good opportunity for doing this project. I also deeply thank the faculty of graduated studies for supporting me several scholarships to succeed this research project.

Finally, I am grateful to everybody in my family for their entirely care and love.

Rungrutai Udomsinprasert

CHARACTERIZATION OF A NEW *ANOPHELES DIRUS* DELTA CLASS GLUTATHIONE S-TRANSFERASE AND INTERACTIONS WITH THE C-JUN N-TERMINAL KINASE PATHWAY COMPONENTS

RUNGRUTAI UDOMSINPRASERT 4338133 MBMG/D

Ph.D. (MOLECULAR GENETICS AND GENETIC ENGINEERING)

THESIS ADVISORS: ALBERT J. KETTERMAN, Ph.D.,
CHANAN ANGSUTHANASOMBAT, Ph.D., DUNCAN R. SMITH, Ph.D.,
GERD KATZENMEIER, Ph.D., WITOON TIRASOPHON, Ph.D.

ABSTRACT

Interest in insect GSTs has focused on their role in conferring insecticide resistance. Previously from the mosquito malaria vector *Anopheles dirus,* two genes encoding five delta class GSTs have been characterized for structural as well as enzymatic activities. We have obtained a new delta class GST gene and isoenzyme from *An. dirus* which we named adGSTD5-5. The adGSTD5-5 isoenzyme was identified and only detectably expressed in *Anopheles dirus* adult female. A putative promoter analysis suggests this GST has an involvement in oogenesis. The enzyme displayed little activity for classical GST substrates although it possessed the greatest activity for DDT observed for delta GSTs. Moreover, a crystal structure showed adGSTD5-5 possessed an elongated and more polar active site topology compared to other Delta GSTs. In addition to catalytic function, GST regulate JNK (c-Jun N-terminal kinase) signal transduction by interaction with JNK itself or other proteins upstream in the JNK pathway. We have studied GSTs and their interaction with components of the JNK pathway from *Diptera*. We have evaluated the effects of all six delta class adGSTs, D1-1, D2-2, D3-3, D4-4, D5-5 and D6-6, on the activity of full-length recombinant *Drosophila* HEP (mitogen-activated protein kinase kinase 7; where HEP stands for hemipterous) and the *Drosophila* JNK, as well as the reciprocal effect of these kinases on GST activity. Interestingly, these exerted different effects on JNK activity. adGSTD1-1 inhibited JNK activity, whereas the other GST isoforms activated JNK. All adGSTs were inhibited 50–80% by HEP or JNK but adGSTD1-1 was not inhibited by JNK. However, binding constants for HEP or JNK inhibiting a GST were similar (20–70 nM). Upon GST-JNK interaction, both GST and JNK underwent conformational changes and that affected their structural and catalytic properties differently, an example is adGSTD1-1 which was stabilized by JNK whereas adGSTD2-2 was not. Furthermore, the substrate specificities of both GSTs and JNK were also altered after their co-incubation. In addition, glutathione modulated the effects of JNK on GST activity.

These results emphasize that different adGST isoforms possess different properties, both in their catalytic function and in their regulation of signaling through the JNK pathway.

KEY WORDS: *ANOPHELES DIRUS* GLUTATHIONE S-TRANSFERASE/
JUN-N TERMINAL KINASE

157 P. ISBN 974-04-6077-1

การศึกษาการทำงานของเอนไซม์กลูตาไธโอน เอสทรานสเฟอเรสในยุง *ANOPHELES DIRUS* (CHARACTERIZATION OF A NEW *ANOPHELES DIRUS* DELTA CLASS GLUTATHIONE S-TRANSFERASE AND INTERACTIONS WITH THE C-JUN N-TERMINAL KINASE PATHWAY COMPONENTS)

รุ่งฤทัย อุดมสินประเสริฐ 4338133 MBMG/D

ปร.ด. (อณูพันธุศาสตร์และพันธุวิศวกรรมศาสตร์)

คณะกรรมการควบคุมวิทยานิพนธ์: ALBERT J. KETTERMAN, Ph.D.,
ชนันท์ อังศุธนสมบัติ, Ph.D., DUNCAN R. SMITH, Ph.D.,
GERD KATZENMEIER, Ph.D., วิฑูรย์ ถิระโสภณ, Ph.D.

บทคัดย่อ

เอนไซม์กลูตาไธโอน เอสทรานสเฟอเรส (GST) ในแมลง มีความสำคัญในกลไกการดื้อต่อยาฆ่าแมลง ปัจจุบันถูกจำแนกออกเป็น 6 กลุ่ม ในอดีตเราได้ทำการศึกษาเอนไซม์จากยุงนำโรคมาเลเรีย *Anopheles dirus* 5 ชนิดในกลุ่มเดลต้าจากยีน 2 กลุ่มทั้งในเชิงของโครงสร้างและการเกิดปฏิกิริยาการทำลายสารพิษ วิทยานิพนธ์เล่มนี้เราได้ค้นพบเอนไซม์ GST ตัวใหม่ชื่อว่า adGSTD5-5 หมายถึงเอนไซม์จากยุง *Anopheles dirus* ชนิดเดลต้า กลุ่มที่ 5 ผลการทดลองพบว่าเอนไซม์ชนิดนี้เกี่ยวข้องกับกระบวนการผลิตไข่และมีปฏิกิริยาการทำลายสารพิษต่ำต่อสับสเตรทดั้งเดิม อย่างไรก็ตามเอนไซม์ชนิดนี้มีความสามารถในการเกิดปฏิกิริยาต่อ DTT ได้สูงสุด จากการศึกษาโครงสร้างของเอนไซม์ที่ตำแหน่งบริเวณเร่งของเอนไซม์ (active site) พบว่ามีส่วนยื่นและมีความเป็นประจุสูงกว่าเมื่อเทียบกับเอนไซม์ชนิดอื่นในกลุ่มเดียวกัน นอกจากนี้ GST สามารถควบคุมการทำงานของเอนไซม์ ในวิถี จูน ไคเนส (JNK) และเอนไซม์เบื้องบน (upstream kinase)ได้ ดังนั้นเราจึงทำการศึกษาความสัมพันธ์ของ GST และโปรตีนในกลุ่มจูนไคเนสในกลุ่มแมลงปีกคู่ (*Dipteran)* จากยุง *Anopheles dirus* GST กลุ่มเดลต้าหกชนิด และ *Drosophila* ไคเนสโปรตีนได้แก่ จูนไคเนส (JNK) และโปรตีนเบื้องบน (HEP) ผลการศึกษาพบว่า GST แต่ละชนิดมีผลควบคุมการทำงานของ JNK แตกต่างกัน โดยเอนไซม์กลุ่มที่ 1 ยับยั้งการทำงานในขณะที่เอนไซม์กลุ่มอื่นๆกระตุ้นการทำงานของ JNK นอกจากนี้ GST ทุกกลุ่มสามารถถูกยับยั้งปฏิกิริยาการทำงานโดย HEP หรือ JNK ประมาณ 50-80% ยกเว้น GST กลุ่มที่ 1 อีกเช่นกันที่ไม่สามารถถูกยับยั้งโดย JNK อย่างไรก็ตาม GST แต่ละกลุ่มมีค่าคงที่ในการจับกับโปรตีน HEP และ JNK ที่ใกล้เคียงกัน (20-70 nM) การศึกษาพบว่าในระหว่างที่มีการจับกันของ GST กับ JNK เอนไซม์ทั้งสองชนิดจะถูกกระตุ้นให้เกิดการเปลี่ยนแปลงของการคงสภาพของเอนไซม์ ซึ่งส่งผลโดยรวมต่อคุณสมบัติการเร่งปฏิกิริยาและคุณสมบัติทางโครงสร้าง

โดยสรุปเอนไซม์ GST ชนิดเดลต้าทั้ง 6 กลุ่ม มีคุณสมบัติแตกต่างกันทั้งการเร่งปฏิกิริยา และหน้าที่ในการควบคุมโปรตีนในวิถีของจูนไคเนส

157 หน้า ISBN 974-04-6077-1

CONTENTS

CONTENTS (continued)

CONTENTS (continued)

CONTENTS (continued)

CONTENTS (continued)

Page

LIST OF TABLES

LIST OF FIGURES

LIST OF FIGURES (continued)

LIST OF ABBREVIATIONS

ATF2	Activating transcription factor
ASK1	Apoptosis signal-regulating kinase 1
CDNB	1-chloro-2, 4-dinitrobenzene
CTAB	Cetyltrimethyltrichloroethane
CuCOOH	Cumene hydroperoxide
DCA	Dichloroacetic acid
DCNB	1, 2–dichloro-4-nitrobenzene
DTT	Dithiothreitol
EA	Ethacrynic acid
ERK	Extracellular signal regulated kinases
GSH	Glutathione
GSTs	Glutathione S-transferases
HEP	Hemipterous
IPTG	Isopropyl-β-D-thiogalactopyranoside
JNK	c-Jun N-terminal kinase
MAPK	Mitogen-activated protein kinase
PNBC	p-nitrobenzyl chloride
PNBr	p-nitrophenethyl bromide
rpm	Revolution per minute
TCA	Trichloroacetic acid
TEMED	N,N,N’,N’tetramethylene-ethylenediamine

LIST OF PUBLICATIONS

1. Oakley,A.J.; Harnnoi,T.; **Udomsinprasert,R**.; Jirajaroenrat,K.; Ketterman,A.J.; Wilce,M.C.J. (2001). The crystal structures of glutathione S-transferases isozymes 1-3 and 1-4 from *Anopheles dirus* species B. *Protein Science*. 10, 2176-2185.

2. **Udomsinprasert,R**.; Ketterman,A.J. (2002) Expression and characterization of a novel class of glutathione S-transferase from *Anopheles dirus*. *Insect Biochemistry and Molecular Biology*. 32, 425-432.

3. Wongtrakul,J.; **Udomsinprasert,R**.; Ketterman,A. (2003). Non-active site residues Cys69 and Asp150 affected the enzymatic properties of glutathione *S*-transferase AdGSTD3-3. *Insect Biochemistry and Molecular Biology*. 33, 971-979.

4. **Udomsinprasert,R**.; Bogoyevitch,M.A.; Ketterman,A.J. (2004). Reciprocal regulation of glutathione *S*-transferase spliceforms and the *Drosophila* c-Jun N-terminal Kinase pathway components. *Biochem.J.* 383, 483-490.

5 **Udomsinprasert,R**.; Pongjaroenkit,S.; Wongsantichon,J.; Oakley,A.J.; Prapanthadara,L.; Wilce,M.C.J.; Ketterman,A.J. (2005) Identification, characterization and structure of a new delta class glutathione transferase isoenzyme. *Biochem.J. In Press Immediate publication doi: 10.1040/BJ20042015*.

CHAPTER 1
INTRODUCTION

1.1 Glutathione S-transferases

Glutathione S-transferases (EC 2.5.1.18; GSTs) are a superfamily of multifunctional enzymes involved in normal cellular metabolism as well as the detoxication of various hydrophobic endogenous and xenobiotic compounds (1). The central importance of GSTs in detoxication lies in their unique capacity to conjugate glutathione with a wide variety of compounds (2). This detoxification reaction is of critical importance in cell survival. As a consequence, GSTs have been virtually found in all organisms from mammals, insects, plants, yeasts and bacteria (3). The two GST superfamilies are distinguished by being membrane-bound and cytosolic GSTs, which are different in structure, activity, intracellular distribution, and biological activity (4).

1.1.1 Membrane-bound GSTs

The membrane-bound enzymes have an evolutionarily different origin from that of the cytosolic enzymes and three enzymes, microsomal GST I (MGST1), leukotriene C4 (LTC4) synthase and microsomal GST II (MGST2), have been identified (5-7). These three proteins are similar in size. With respect to amino acid sequence, there is no apparent relationship between these three GSTs and any of the known cytosolic GST enzymes (2,8). MGST1 is a homotrimeric integral membrane protein that also forms part of the so-called MAPEG superfamily. This superfamily contains structurally and phylogenetically related enzymes involved in detoxication, protection from oxidative stress, and synthesis of prostaglandin E and cysteinyl leukotrienes (9). LTC4 and MGST2 are the only mammalian glutathione transferases which have a clearly defined physiologic substrate, leukotriene A4. However, both

LTC4 and MGST2 show a remarkable degree of sequence identity to the 5-lipoxygenase activating protein as well as the small degree of sequence similarity with the MGST1 noted above. Considerably less is known about structure and catalytic mechanisms of the membrane-bound GSTs compared to the cytosolic GSTs.

1.1.2 Soluble GSTs

Cytosolic GSTs are extremely diversified and are grouped into a number of classes based on their primary sequence similarity, substrate specificity, immunological properties, tertiary structure and quaternary structure, which are thought to originate from an ancient group of proteins. It is generally accepted that GSTs share greater than 40% amino acid sequence identity within a class, and those with less than 30% identity are assigned to separate classes (1,10). Each class is composed of several subunits, of which the biologically active forms are either homo- or heterodimeric proteins. The GST classes are designated as alpha, mu, pi, theta, zeta, kappa and omega in mammal (10-14), sigma class in cephalopods and arthropods (15), the phi and tau classes in plants (16), the delta and epsilon classes in insects and the beta class in bacteria (17,18). Theta and zeta classes occur in plants, insects and bacteria as well as in animals (19). A nomenclature has been agreed upon for the human cytosolic enzymes which is, in principle, applicable to all vertebrate glutathione transferases and extendible to insects, prokaryotes and other organisms (10,20). For example, the human enzymes are named with respect to the class in which they fall (A, M, P, K, or T for alpha, mu, pi, kappa, and theta) with their subunit composition or isoenzyme type represented by Arabic numerals. For example, a homodimer of type 1 mu subunits is M1-1 and the heterodimer of type 1 and 2 alpha subunits is A1-2. The existence of numerous isoenzymes is largely responsible for the broad substrate specificity of GSTs. Remarkably; additional breadth in specificity is attained by the catalytic competency of any single GST toward a number of chemically unique substrates.

A common feature of the GSTs is their ability to bind glutathione; another property is their ability to recognize and detoxify compounds with diverse chemical structures. The evolution of the GSTs in which relatively low binding affinities are offset by broad substrate specificities constitutes an energy-efficient response to toxin

exposure. Although substrate specificities are somewhat overlapping, the enzymes are critical to eukaryotic organisms in that they display unique activities toward a variety of harmful compounds (13). The heterogeneity of substrate specificity between isoforms in any given class has significant physiologic and pathophysiologic importance in detoxication of endogenous and exogenous compounds (21). The natural evolution of GSTs has occurred by both convergent and divergent pathways (15,22). The cytosolic enzymes are the best characterized examples of divergent evolution. GSTs are expressed at high levels in mammalian tissues constituting 1 to 5% of the total soluble proteins (23,24).

Most GST classes are encoded by multigene families. The alpha, mu and pi classes account for the majority of cytosolic GST activity in mammalian tissues (2). Several enzymes belonging to the alpha and mu classes have been recognized, while the pi class originally contained only one protein. These GSTs are expressed in discrete tissue and species specific patterns (25). GST P1-1 has a widespread distribution in most tumor cells and tissues but it is absent in liver. Whereas livers of some species are rich in alpha and several mu-class GSTs (24).

Insect GSTs are of interest because of their important role in conferring insecticide resistance (26) and in protecting cells against damage by oxidative stress (27,28). Elevated GST levels have been detected in pesticide-resistant strains of insects (29). Three major distinct classes, I, II and III have been classified as insect specific delta (D) (30-32), sigma (S) (33) and epsilon (E) class (28,34,35), respectively. Delta class enzymes together with epsilon GSTs are implicated in conferring resistance to insecticides (34). Sigma-class GSTs, however, are poorly characterized and their exact biological function remains elusive. Delta class is so far unique. It possesses both a cluster of intronless genes and genes with introns that undergo alternative RNA splicing. Two of the GST genes (*GSTd1* and *GSTs1*) are alternatively spliced to produce multiple transcripts with identical N-termini but differing C-termini (30,32). Alternative splicing and the formation of hetero-dimers, may add a further level of heterogeneity to this enzyme family.

1.1.3 *Anopheles dirus* GSTs

In *Anopheles dirus,* a Thai malaria vector, five delta class GSTs isoenzymes have been previously acquired and characterized for structural as well as functional roles (32,36-39). The major *adgst1AS1* gene (*Anopheles dirus* alternatively spliced GST gene) of 7.5 kb encoded four alternatively spliced products; adGSTD1-1, adGSTD2-2, adGSTD3-3 and adGSTD4-4, derived from six exons, which share the first two exons, and vary among four different exon 3 sequences (exon 3A–3D) (32). They four spliceforms share an untranslated exon 1 and a translated exon 2 that codes for 45 amino acids at the N-terminus. These two exons are spliced to one of four alternative exons 3, namely 3A, 3B, 3C or 3D. This generates four different mature transcripts coding for proteins of 209 to 219 amino acids that have been called adGSTD4-4, adGSTD3-3, adGSTD2-2, and adGSTD1-1, respectively. These four spliceforms therefore differ in their C-terminal amino acids, which possess 61-77% amino acid identity (32,37). The upstream sequence of *adgst1AS1* gene yields a mature transcript of adGSTD5-5 (40). This gene organization is highly conserved between *An. dirus* and *An. gambiae* (*aggst1*a), with .80% nucleotide identity in the coding region (30). The gene encoding adGSTD6-6 is in an unknown location. This GST isoenzymes yielded very low enzymatic activities toward classical known GST substrates, however, the putative element analysis reviewed this GST may involve in development and cell differentiation (39). These six GSTs isozymes contain a highly conserved glutathione binding region in the N-terminus, although the sequences at the C-terminus are highly variable. These six adGST enzymes therefore possess distinct enzyme kinetic properties toward substrates including insecticides and inhibitors (37,39). However, they are all highly active for conjugating GSH toward the traditional 1-chloro-2, 4-dinitrobenzene (CDNB) substrate compared to the other insect GST classes (33,41).

1.1.4 GST structure

The soluble GSTs exist as stable homo or hetero dimeric proteins of approximately 50 kDa formed by association between subunits from within a given GST class (42). The sequences and the known three-dimensional (3D) structures suggest that these proteins share a common ancestry, although the precise details of their evolution remain obscure. Three-dimensional structures of members of the different classes of GST determined by x-ray crystallography over the last decade (43-45) have provided insight into their catalytic mechanisms.

Numerous structures of mammalian GSTs have been described (3). These include pi class (46-48), mu class (49) and alpha class (43,50). Non-mammalian GST structures include ones from the bacterial beta class (51) and the plant phi and zeta classes (52). Currently, only five structures of insect GSTs are known, which all belong to the delta class. One from the Australian sheep blowfly *Lucilia cuprina* (53) and four from the mosquito *Anopheles dirus* (36,40). Despite the low sequence identity between classes (often less than 20%), crystallographic studies have indicated that the overall polypeptide folding of the different classes of soluble GST is very similar (44,54). Each GST monomer has an active site which contains two distinct functional domains; the hydrophilic G-site that binds to the physiological substrate glutathione (GSH) and an adjacent H-site which provides a hydrophobic environment for binding to a variety of electrophilic substrates (2). The N-terminal domain or G-site consists of four β-sheets with three flanking α-helices, adopting a βαβαββα topology. Helices α1 and α3 represent core secondary structural elements, whereas helix α2 is a mobile surface-exposed helix (55). The C-terminal domain or H-site is entirely α-helical, with helix α5 adopting a marked bend. There are five α-helices in the pi and mu class (49,56) and six α- helices in alpha class in total (43) **(Figure 1.1 A)**. Due to its high specificity for GSH, the G-site is highly conserved across all GSTs. In contrast, the structure of the H-site governs the substrate specificity of a particular GST, diversity in the H-site gives the GST family the ability to catalyze reactions towards an exceedingly large number of structurally diverse substrates (23).

Structural investigations have revealed many features of the subunit interface that are conserved in the members of the distinct GST classes (43) but the differences that do exist among subunits of different classes make their interfaces incompatible.

Interactions at the subunit interface contribute to the stabilization of the subunit tertiary structures of GSTs, and the dimer is required to maintain functional conformations at the active site on each subunit and the nonsubstrate ligand binding (or ligandin) site at the dimer interface (57-59). Inter-subunit contacts occur between domain I of one subunit and domain II of the other. The H-site is located in the crevice between the two domains and makes a number of contacts with residues in domain II, particularly along the face of the α4-helix and the C-terminal tail **(Figure 1.1 B)**. Thus, domain II appears to provide structural elements for the recognition of xenobiotic substrates and helps to define the substrate selectivities of the various isoenzymes. The dimer interface of the GSTs features extensive hydrophobic and hydrogen bonding interaction. The structural features at the dimer interface of the GSTs appears to have evolved relatively recently suggesting at least two major areas of interactions, a hydrophobic ball-and-socket and electrostatic interactions at the subunit interface. The ball and socket feature known as "lock-and-key motif" is highly conserved in the mammalian GST structures (54). This involves an aromatic residue (Phe-52 in alpha, Phe-56 in mu and Tyr-49 in pi) termed the "key", from the loop preceding strand α3 and a hydrophobic "lock" from helices α4 and α5 of the other monomer (60). Electrostatic interactions are formed as salt bridges by positive charged residues, arginine, and negative charged residues, glutamate from both subunits at the edge (43) as well as the top of the subunit interface (36,49).

In addition, there are many positions in GSTs that appeared to be sensitive structural regions, for example the structural conformation of α6 and the proceeding loop called the N-capping box motif (Ser/Thr-Xaa-Xaa-Asp) at Ser-150/Asp-153 (61,62) and the hydrophobic staple motif at Ile-149/Tyr-154 (63). These residues have hydrogen bonds and hydrophobic interaction that play an important role for GST folding and stability. Mutagenesis of residues in these motifs generate proteins more unstable compared to the wild type. Furthermore, several studies reviewed the importance of sensitive residues in the GST structure that modulates enzyme catalytic activity as well as stability (64-69). Therefore, the dimerization of the GSTs not only allow for the construction of a fully functional active site, part of which is situated near the subunit interface, but also contributes to the stabilization of the subunit tertiary structure.

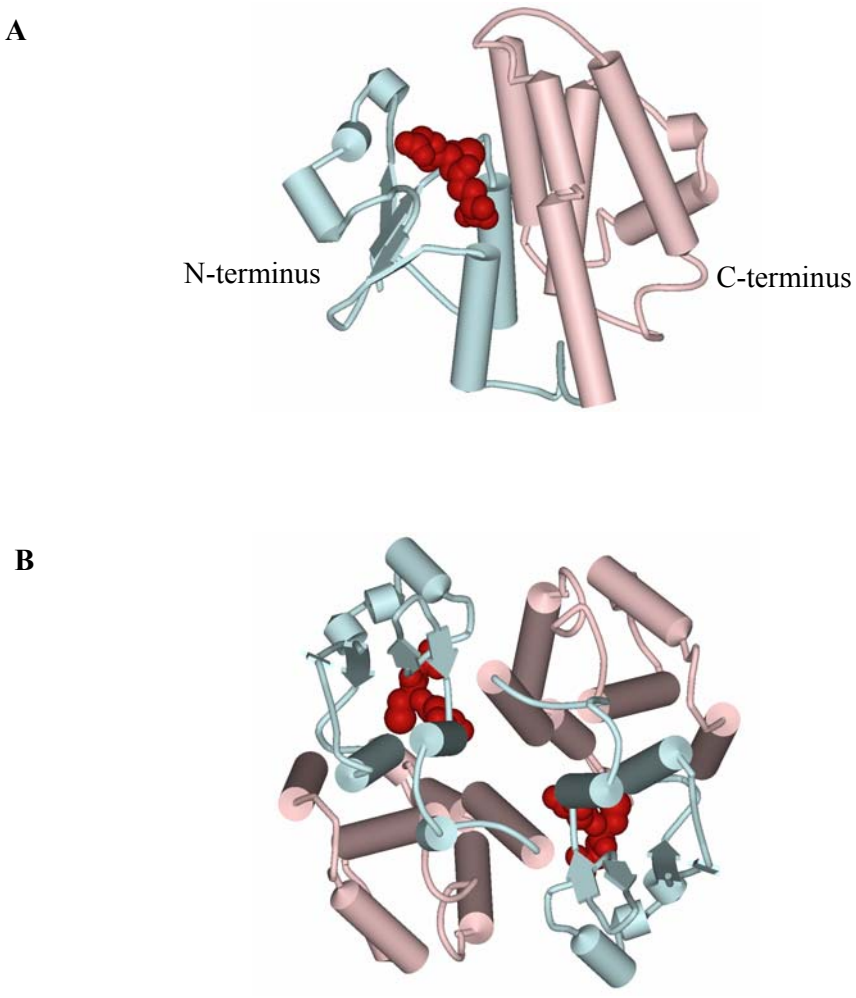

Figure 1.1 GST structure (A) Three-dimensional structures of GST subunits GST domains are distinguished by different colors (domain 1; blue, domain 2; pink). The ligands are shown in CPK form, identifying the location of the active site. **(B) Quaternary structures of dimeric GST** View of the GST dimers down the two fold axis relating the two subunits. The major intersubunit interactions occur between domain I of one subunit and domain II of the other subunit (2).

1.1.5 The enzyme mechanism

Much emphasis tends to be placed on the primary structure at the N-terminus because, within the classes, this region tends to be better conserved than others, as it includes an important part of the active site. This region contains a catalytically essential tyrosine, serine or cysteine residue that interacts with the thiol group of GSH, thus lowering its pK_a from its normal value of around 9.0 to a value of approximately 6.0 to 7.0. This is thought to be a key component of catalysis in GSTs (70,71). Enzyme catalysis scheme for GST involves GSH substrate binding to the active site, GSH ionization to form a nucleophilic thiolate anion (GS^-), substrate conjugation, product formation and product release (54,72).

GSTs are highly specific for GSH as the nucleophile but are notably nonspecific with regard to structurally diverse electrophilic second substrates (4, 17). Because the proteins are not designed to accommodate any particular substrate, and each form exhibits broad specificity for binding of substrates and nonsubstrate ligands (18), catalysis by GSTs is in many ways unique. Therefore, the activation of GSH for reaction with diverse types of electrophilic centers is important for the function of GSTs.

The function of the enzyme is to bring the substrate into close proximity with glutathione (GSH) by binding both GSH and the electrophilic substrate to the active site of the protein to activate the sulfhydryl group on GSH, thereby allowing for nucleophilic attack of GSH on the electrophilic substrate (R-X) (2). The pK_a of its sulhydryl group (-SH) is lowered from 9.0 to about 6.0 to 6.5. A general form of the reaction is expressed thus: GSH + R-X → GS-R + HX**,** where **R** is the substrate with electrophilic group **X**. The enzyme uses the binding interactions with GSH to activate sulfur for nucleophilic attack.

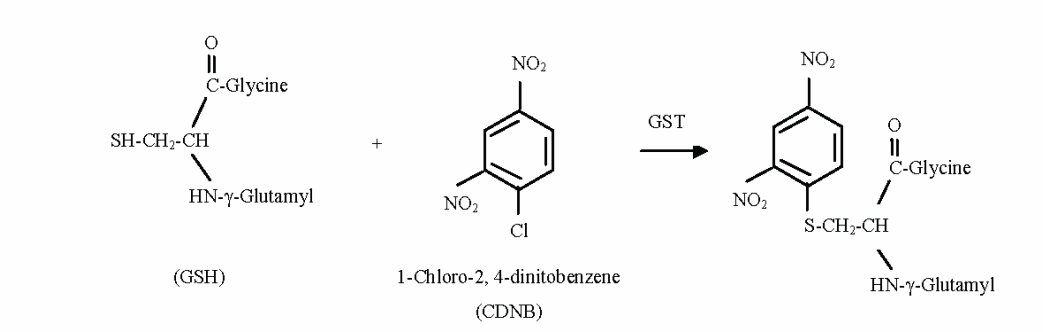

The binding of substrates by alpha, mu and pi class GSTs occurs by an accelerating, multi-step mechanism depending on an increase of flexibility in critical regions of the structure, that enables rapid access, optimal orientation for conjugation and subsequent product release (73).

GSTs normally use hydroxyl group containing residues in the N-terminal domain of the enzyme to stabilize the activated form of the co-substrate, glutathione, except beta class GSTs for which the origin of the stabilization remains a mystery. A conserved tyrosine residue near the N-terminus in Alpha, Mu, Pi and Sigma class GSTs and a similarly located serine or threonine residue in Theta class GSTs have been shown to be important in catalysis, probably by stabilizing the GSH thiolate anion (54,74). In mammalian GSTs, a conserved tyrosine hydroxyl group is responsible for promoting the formation of a thiolate anion in GSH. It has been demonstrated for alpha-, mu-, and delta-class GSTs that a proton is released by GSH upon binding to the enzyme (75). However, in the human theta class GST, it is a serine residue that provides the hydroxyl group (76), similar to that found in insect delta (36) and plant phi class GSTs. Unlike other eukaryotic GSTs, the mammalian GSTO 1-1 and the bacterial beta class GST has a molecule of GSH covalently bound to a cysteine residue (12). Nevertheless, mutational studies have demonstrated that none of the tyrosine, serine or cysteine residues located in the N-terminal domain of *Proteus mirabilis* GST (PmGST) B1-1 are directly involved in its catalytic mechanism (77).

1.1.6 GST functions

GSTs are expressed qualitatively and quantitatively at various constitutive basic levels in most mammalian tissues but are also involved in normal cellular metabolism as well as the detoxication of various hydrophobic endogenous and xenobiotic compounds (1). The central importance of GSTs in detoxication lies in their unique capacity to conjugate glutathione with a wide variety of compounds (2). This detoxification reaction is of critical importance in cell survival. In addition, several other functions of GSTs have been recently discovered; for example, they are involved in the binding and transport of non-substrate hydrophobic ligands (1) and in a range of physiological roles such as signal transduction, gene regulation and

apoptosis (23). Thus, GSTs can be considered as multi-functional enzymes devoted to various aspects of cell defense.

1.1.6.1 Role of GSTs in Glutathione conjugation and detoxification

The enzyme detoxification of xenobiotics has been classified into three distinct phases, which act in a tightly integrated manner. Phases I and II involves the conversion of a lipophilic, non-polar xenobiotic into a more water-soluble and less toxic metabolite, which is catalysed mainly by the cytochrome P450 system and GSTs respectively (3,23). GSTs catalyze the reaction of glutathione with a wide variety of organic compounds to form thioethers, a reaction that is a first step in a detoxification process leading to mercapturic acid formation, thereby decreasing the compounds' reactivity with cellular macromolecules. These conjugation products increase the compounds solubility and excretion from the cell (44).

1.1.6.2 Role of GST in binding and transport of non-substrate hydrophobic ligands.

In addition to their enzymatic roles, GSTs bind to large lipophilic molecules (molecular masses >400 Daltons). These ligands include such molecules as hemin, bilirubin, bile salts, steroids, thyroid hormones, fatty acids and a wide variety of drugs and xenobiotics, which represents a potentially important mechanism of drug resistance. GSTs are involved in the intracellular uptake and/or storage as well as rapid transport of a great variety of these hydrophobic non-substrate compounds in the aqueous phase of the cell (78,79).

1.1.6.3 Role of GST in gene regulation and apoptosis

Besides their roles in conferring insecticide resistance, GSTs can display glutathione peroxidase activity under conditions of oxidative stress and are further implicated in physiological roles such as signaling, cell proliferation, differentiation and apoptosis by protecting against oxidative damage (33,80). The expression of some mammalian GSTs increases in response to chemical and oxidative stress (12) and indeed it was also recently reported that the *Sacharomyces pombe* *gst2*$^{+}$ promoter is induced by oxidative stress (31).

Because the Bcl-2 family member Bax regulates programmed cell death by promoting apoptosis (8), a role for GST theta in regulation of apoptotic cell death has also been suggested following its identification as a Bax-interacting protein (9). It has also been reported that certain GSTs (class Theta) may inhibit the proapoptotic action of Bax (18), and the most recently discovered class omega, GST O1-1, modulates calcium channels, thus protecting mammalian cells from apoptosis induced by Ca^{2+} mobilization (19).

Other interactions of GSTs to alter intracellular signal transduction events have been reported. Most often these implicate GST in the regulation of the Jun N-terminal kinase (JNK) signal transduction pathway. JNK is a member of the MAPK family which is conserved across all eukaryotes ranging from yeast and insects to mammals (81-84). GSTs have been shown to be involved with stress kinase response in studies of the mammalian GST pi that served as a JNK (Jun N-Terminal kinase) regulatory protein through GST inhibition of JNK activity (85). A mu class GST similarly interacted and inhibited ASK1 (Apoptosis signal-regulating kinase 1) which is an upstream kinase of JNK participating in cell death (86). Moreover, a small stress response protein (p28) was identified as a GST-like protein related to theta class GSTs based on sequence homology and protein activity (87).

1.1.7 GST inhibitors

The currently existing GST inhibitors tend to fall into three classes, determined by their binding site on the protein and mechanism of inhibition. The first of these are analogues of electrophilic substrates, which bind in the hydrophobic region of the active site (H-site) and competitively inhibit the binding of hydrophobic electrophiles. Second are glutathione conjugates, which occupy both the glutathione binding site (G-site) and at least part of the H-site, and are typically competitive with respect to both glutathione and hydrophobic substrate. Third, a collection of compounds referred to as nonsubstrate ligands are noncompetitive inhibitors of the GSTs. These inhibitors are typically hydrophobic anions and include endogenous compounds such as porphyrins and bile acids and such exogenous compounds as sulfated organic dyes. The binding site of this group of inhibitors has historically been called the ligandin site, and its location remains uncertain; however, it may lie at one

edge of the H-site or within the wide cleft between the two subunits of the GST dimer. These nonsubstrate ligands are unique among the GST inhibitors in that they elicit noncompetitive inhibition with respect to both glutathione and electrophilic substrate (88).

1.2 c-Jun NH_2-Terminal Kinases Mitogen-Activated Protein Kinases (JNK MAPK)

External stimuli play a major role in regulating intracellular processes such as gene expression, cell survival, cell growth, cell differentiation and cell death. Examples of these stimuli include cell–cell and cell–extracellular matrix adhesion and mechanical forces, in addition to the exposure to soluble factors such as growth factors, hormones and cytokines. Mammalian cells respond to extracellular stimuli by activating members of the mitogen-activated protein kinase (MAPK) family, which include the extracellular signal regulated kinases (ERK), the Big MAPK (BMK/ERK5), the 38 kDa protein kinases (p38) and the c-Jun N-terminal kinases (JNK)/ Stress activated protein kinase (SAPK) (89). These different MAPKs can be activated in response to specific stimuli, define independent signaling pathways, and can subsequently regulate specific substrates. Whereas ERK is activated mainly by mitogenic stimuli in response to hormones and growth factors (90), BMK/ERK5, p38 and JNK/SAPK are activated mainly by inflammatory cytokines or stress stimuli such as lipopolysaccharide (LPS), heat shock, hyperosmolarity, and radiation (84,91,92).

The MAPKs are serine/threonine kinases that are activated by dual phosphorylation of threonine and tyrosine residues of the Thr-X-Tyr segment in a loop located adjacent to the active site (84). MAP kinases comprise a group of intracellular signal transduction enzymes that allow a cell to respond to such stimuli. The transmission of signals is achieved by sequential phosphorylation and activation of the pathway kinase components specific to a respective cascade. The MAPK cascades are typically organized in a three-kinase architecture consisting of a MAPK, a MAPK activator (MEK, MKK, or MAPK kinase), and a MEK activator (MEK kinase [MEKK] or MAPK kinase kinase). Phosphorylation of each MAP kinase is carried out by specific kinases upstream of the MAP kinase. Activated MAP kinases

then phosphorylate various substrates, including transcription factors, which in turn regulate the expression of specific sets of genes and thus mediate a specific response to the stimulus **(Figure 1.2)**.

The Jun-N-terminal protein kinase (JNK) family of enzymes is conserved across all eukaryotes ranging from yeast and insects to mammals (91). JNK has been implicated in a variety of biological processes in response to stress including inflammation, apopotosis, development and tumorigenesis (84,93). JNK is activated by treatment of cells with cytokines (e.g. TNF and IL-1) and by exposure of cells to many forms of environmental stress (e.g., osmotic stress, redox stress and radiation). JNK activation requires dual phosphorylation in the conserved motif Thr-Pro-Tyr, which is brought about by two dual specificity protein kinases, MAP kinase kinases MKK4 and MKK7 [also called JNK kinase (JNKK) 1 and 2, respectively]. The MKK4 protein kinase also functions as an activator of p38 MAP kinase *in vitro* (94). In contrast, MKK7 functions as a specific activator of JNK (95-97). The activation of JNK relays extracellular cues to transcription factors such as c-Jun (98), ATF2 (99) and Elk1 (100), thereby regulating gene expression, cellular homeostasis, differentiation, apoptosis and cell death **(Figure 1.3)**.

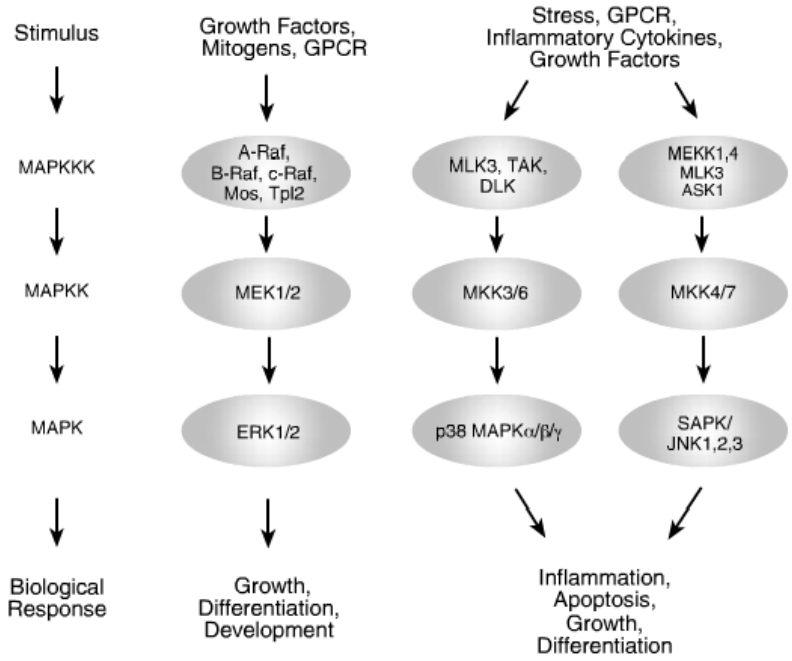

Figure 1.2 The mammalian MAPK signaling pathways Mitogen-activated protein kinases (MAPKs) are generally activated by a conserved type of signaling pathway and are involved in many cellular programs such as cell proliferation, cell differentiation, cell movement and cell death. MAPKs are activated by phosphorylation on threonine and tyrosine residues by dual specificity MAPK kinases (MAPKKs). MAPK signaling cascades are organized hierarchically into three-tiered modules. MAPKs are phosphorylated and activated by MAPK-kinases (MAPKKs), which in turn are phosphorylated and activated by MAPKK-kinases (MAPKKKs). The MAPKKK is in turn activated by interaction with a family of small GTPases and/or other protein kinases connecting the MAPK module to the cell surface receptor or external stimuli (84).

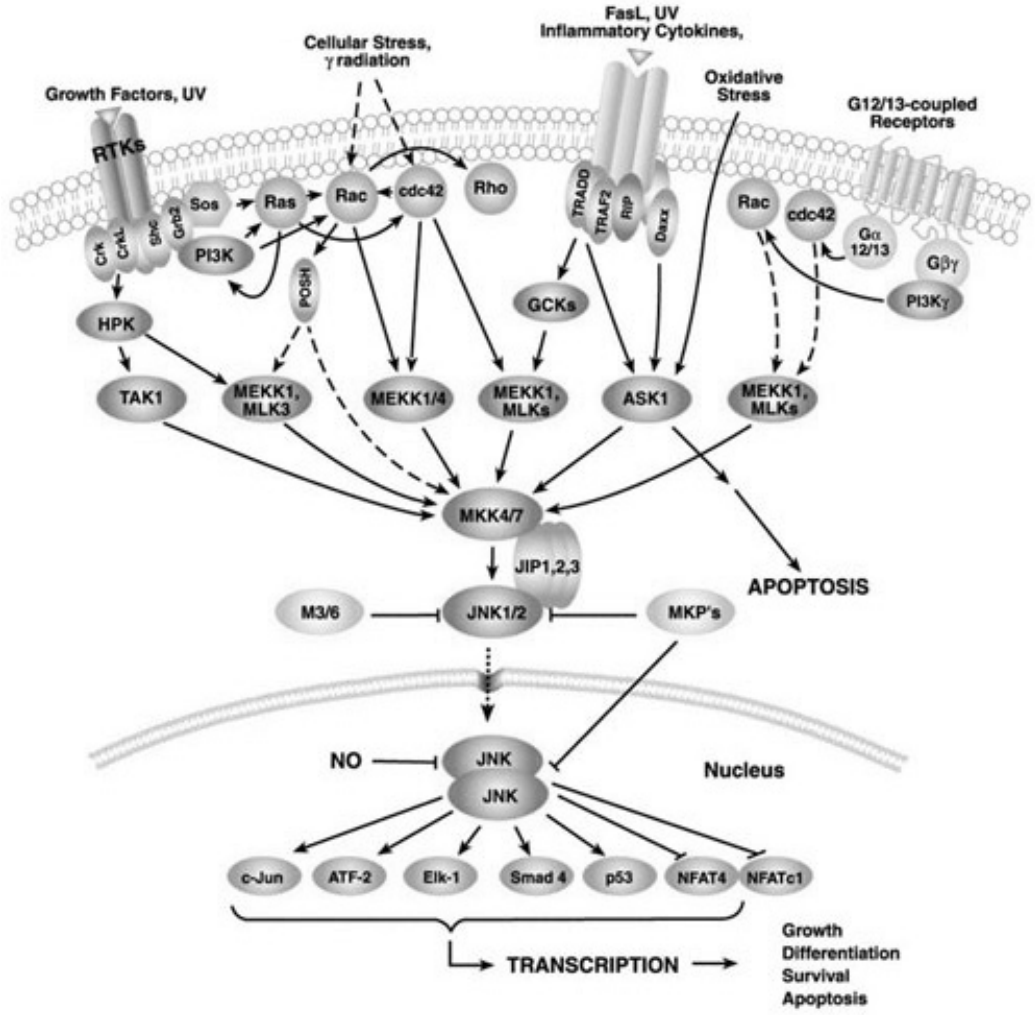

Figure 1.3 Mammalian JNK MAPK cascade JNKs are activated by a variety of environmental stresses, inflammatory cytokines, growth factors and G-protein coupled receptors (GPCR) agonists. Stress signals are delivered to this cascade by members of small GTPases of the Rho family (Rac, Rho, cdc42). As with the other MAPKs, the membrane proximal kinase is a MAPKKK, typically MEKK1/4, or a member of the mixed lineage kinases (MLK) that phosphorylates and activates MKK4 (SEK) or MKK7, the SAPK/JNK kinases. Alternatively, MKK4/7 can be activated by a member of the germinal center kinase (GCK) family in a GTPase-independent manner. SAPK/JNK translocates to the nucleus where it regulates the activity of several transcription factors such as c-Jun, ATF-2 and p53 (92,101).

In mammals, the JNK protein kinases are encoded by three genes, *jnk1*, *jnk2* and *jnk3*. The *jnk1* and *jnk2* genes are ubiquitously expressed. In contrast, the *jnk3* gene is selectively expressed in the brain, heart, and testis. These genes are alternatively spliced to create four JNK1 isoforms, four JNK2 isoforms, and two JNK3 isoforms which are expressed as 46 kDa and 54 kDa protein kinases due to the differential processing of the 3' coding region of the corresponding mRNA (102). Although, studies in *Drosophila* indicate there is only one JNK (DJNK) (103), components of the JNK signaling pathway are conserved in mammals and insects (96,104-107). MKK7 is a homolog of hemipterous (HEP), which has been defined by biochemical and genetic analysis as an activator of DJNK in *Drosophila* (96,103,105,107). Furthermore, there is conservation of at least one target of the JNK signaling pathway, the Jun transcription factor which is encoded by the c-Jun and DJun genes in mammals and insects, respectively. The identification of a JNK homolog in *Drosophila*, DJNK, has established a useful model for the genetic analysis of the JNK signal transduction pathway and has been confirmed by several recent studies including the morphogenetic process of dorsal closure (DC), the insect immune response, photoreceptor determination and the establishment of tissue polarity **(Figure 1.4)** (105,108-110).

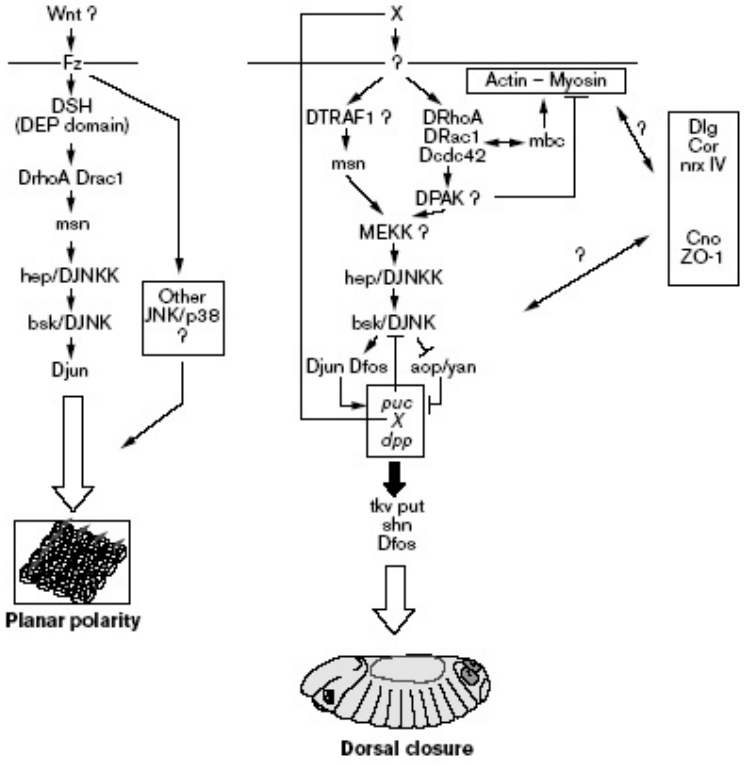

Figure 1.4 The *Drosophila* JNK pathway controls dorsal closure and planar polarity. During dorsal closure, the JNK signaling pathway is activated in the leading edge (LE) by an unknown signal, and one important outcome of this signaling activity is the induction of *dpp* (the product of which is a TGF-b homolog) expression in these cells. This coupling of JNK and *dpp* signaling pathways is proposed to control morphogenesis of the more lateral ectodermal cells by the *dpp* pathway. In addition to JNK signal transducers, membrane-associated proteins participate in the elaboration of normal JNK and cytoskeletal activities to realize a concerted movement. In planar polarity, the coupling of frizzled/disheveled and JNK activities signals the correct arrangement of cells within the plane in the eye imaginal disc. Arrows indicate activation and lines ending in a bar represent repressor functions. bsk, basket; Cno, Canoe; Cor, Coracle; Dlg, Discs large; DSH, dishevelled; Fz, Frizzled; hep, hemipterous; nrx, neurexin; msn, misshapen; *puc*, *puckered*; put, punt; shn, schnurri; tkv, thickveins (93,111).

1.2.1 JNK MAPK structure

JNK MAPKs, are serine/threonine protein kinases containing 11 protein kinase subdomains (102). These motifs comprise the conserved features of protein kinases, namely ATP as well as peptide substrate binding regions, and maintain the conserved protein kinase three-dimensional fold. The protein kinase activation loop is located between domains VII and VIII between the conserved amino acid motifs DFG and APE. Within this loop are the threonine and tyrosine that must be phosphorylated for full kinase activation. The JNK MAPKs are made complex by the alternative splicing of three JNK genes to produce ten different isoforms. There is one splicing site, between subdomain IX and X of the JNK1 and JNK2 gene, and the resulting splice forms show altered substrate specificity (102). The second alternative splicing occurs at the C-terminus of the protein, producing proteins which differ in length by 42 or 43 amino acids (i.e. the typical 46 and 55 kDa proteins originally noted, and the total number of amino acid in each isoform is indicated).

Insight into the function of JNK protein kinases has recently been achieved through the determination of the atomic structure of JNK3. The structure of the inactive JNK3 in the presence of non-hydrolyzable ATP analog is shown in **Figure 1.5**. The overall structure is typical for protein kinases and is similar to other MAPK, which consists of two domains with an active site cleft. The small N-terminal lobe (predominantly anti-parallel β-sheets; subdomains I–IV) aids in the orientation and binding of ATP. The larger C-terminal lobe (predominantly α-helices; subdomains VIA– XI) acts in peptide substrate recognition as well as anchoring the phosphate of Mg^2+ ATP (112). The defining motif of all ten JNK MAPK isoforms is the amino acid sequence Thr–Pro–Tyr (T–P–Y) within the activation loop in kinase subdomain VIII (102). One significant difference between JNK3 and other MAPK is that the ATP binding site is well-ordered in the inactive structure. The low activity appears to result from misalignment of active site residues and the location of the T-loop, which blocks access of substrates to the active site. MAPKK activates JNK by phosphorylation of the T-loop on Thr and Tyr. The mechanism of JNK activation by dual phosphorylation is unclear, but it is thought that this phosphorylation may alter the structure of the T-loop and cause realignment of the NH_2- and COOH-terminal domains to create a functional active site (112).

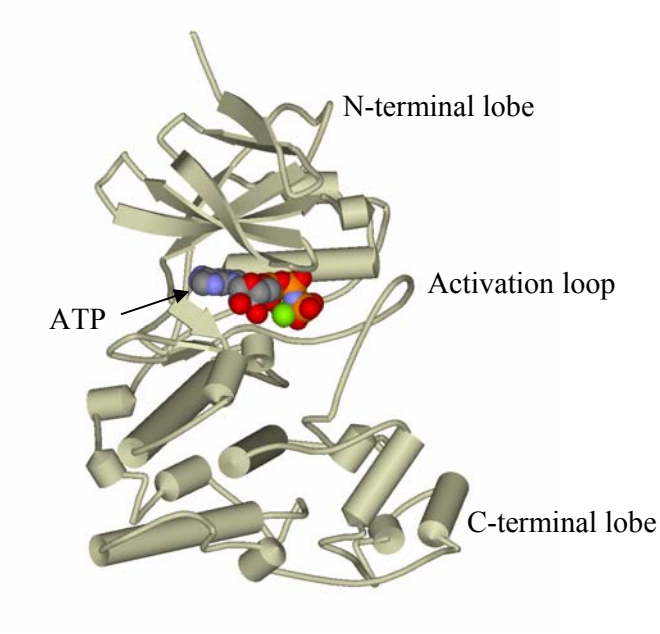

Figure 1.5 Structural features of the JNK MAPKs The crystal structure of JNK3-1 is illustrated. The JNK MAPKs are typical serine/threonine protein kinase containing all 11 protein kinase subdomains as indicated (I–XI). The N- and C-terminal lobes as well as the activation loop are indicated. The arrow shows the position of the bound Mg^{2+}AMP–PNP, indicating the ATP-binding site. The coordinates of the JNK3 structure have been deposited in the Protein Data Bank with accession code 1JNK (112).

1.2.2 JNK MAPK function

Mitogen-activated protein kinase signaling pathways relay, amplify and integrate signals from a diverse range of extracellular stimuli, thereby controlling the genomic and physiological response of a cell to changes in the environment. In mammalian systems, these responses include cellular proliferation, differentiation, development, the inflammatory response and apoptosis. JNK represents one subgroup of MAP kinases that is activated primarily by cytokines and exposure to environmental stress. A traditional biochemical approach to understanding JNK MAPK function has focused on the identification of the JNK MAPK-specific substrates (102). These substrates are predominantly transcription factors, thus

suggesting that the effects of JNK MAPKs can be mediated by changes in gene expression. The results of these types of studies taken together illustrate the complex roles that JNK MAPKs have been shown to play in cell death, cell survival and cell growth. In addition, the role of JNK in the embryonic morphogenesis as well as immune response has been reviewed (93).

1.2.2.1 Role of JNK in regulation of gene expression

An example of JNK-regulated gene expression is the phosphorylation of transcription factors within their activation domains, leading to increased transcriptional activity (94). Not only are MAP kinases capable of affecting gene expression via intermediary kinases and by phosphorylating proteins in the cytoplasm, but MAP kinases also translocate to the nucleus where they are able to phosphorylate transcription factors to regulate their activities (113). A major target of the JNK signaling pathway is the activation of the AP-1 (Activator protein-1) transcription factor that is mediated, in part, by the phosphorylation of c-Jun and related molecules. c-Jun, acting within the activator-protein-1 (AP-1) complex, has been implicated in various cellular processes, ranging from cell proliferation and differentiation to neoplastic transformation (94). The AP-1 family (activating protein-1) of transcription factors including c-Jun (98), c-Fos (114), and ATF-2 (99) are leucine zipper proteins that form homodimers and heterodimers when activated to bind to DNA (115). Activation of JNK causes phosphorylation of c-Jun on residues Ser-63 and Ser-73 within its N-terminal activation domain (94,98), whereas the phosphorylation by ERK1/2 takes place on the C-terminal inhibitory sites (98). Phosphorylation at the N-terminal sites results in increased stability of c-Jun and an increase in its transactivation potential and DNA binding affinity (98); phosphorylation of the C-terminal sites inhibits DNA binding (101). Although c-Jun is an exclusive JNK MAPK substrate, JNK MAPKs can also phosphorylate and activate other transcription factors including activating transcription factor (ATF2) (99). ATF2 is a JNK MAPK substrate that heterodimerises with c-Jun and stimulates expression of the *c-jun* gene. Therefore, through activation of both c-Jun and ATF2, JNK MAPKs can regulate the abundance and activity of c-Jun. Elk-1 is another direct JNK MAPK target (100), and it is involved in the induction of the *c-fos* gene, whose product forms

the AP-1 heterodimer with c-Jun (94). Again this shows that JNK MAPK has the potential to regulate transcriptional activity at multiple levels. However, in the cases of the transcription factors ATF2 and Elk-1, it should be noted that other protein kinases can lead to their phosphorylation and activation (92,101). Specifically, ATF2 may also be phosphorylated by p38 MAPKs whereas Elk-1 may also be phosphorylated by both ERK MAPKs and p38 MAPKs. Thus, there is the possibility of cross-talk between the MAPK pathways at the level of their transcription factor substrates.

Not only is the induction of c-*jun* and c-*fos* transcription dependent on JNK, but Jun and Fos can induce the transcription of xenobiotic-metabolizing enzymes such as GST (116). Thus, c-Jun is directly involved in GST pi expression *in vivo* (117). This suggests a role of JNK in the induction of a cellular defense program against cytotoxic xenobiotics.

1.2.2.2 Role of JNK in regulation of cell death and survival

A balance between signaling pathways was proposed to dictate the cellular decisions of death or survival. It has been reported that JNK is activated by many pro-apoptotic stimuli (94). Since apoptosis can be considered to be a form of stress, it is possible that JNK activation may occur in response to the stress of apoptosis. JNK anti-sense oligonucleotides inhibit apoptosis and JNK signaling was found to activate caspases that are known to mediate cell death (118). A more perplexing idea is JNK not only contributes to some apoptotic responses; JNK MAPK activation might enhance cell survival under some circumstances for example, JNK MAPK activation enhances cell survival in response to TNF-α (119), protects HeLa cells from apoptosis following photodynamic therapy (120), and protects myocytes from nitric oxide-induced apoptosis (121). This is partly because the JNK-dependent apoptotic signaling pathway can be blocked by activation of survival signaling pathways (122).

How can JNK mediate both pro-apoptotic and antiapoptotic signals? One possibility is that this difference simply reflects the properties of different cell types; however, JNK-dependent and JNK-independent apoptotic pathways have been defined in the same cell type (119). A second possibility is that different JNK

isoforms do not mediate the same signal. Evidence in favor of this possibility derives from the finding that, in small cell lung cancer cells, dominant negative JNK1 inhibits UV-induced apoptosis, while dominant negative JNK2 is ineffective (123). A third possibility is that the biological effects of JNK depend on the state of activation of other signaling pathways within the cell, which implies that JNK provides a permissive rather than an instructive signal.

1.2.2.3 Role of JNK in regulation of Embryonic Morphogenesis

The fruit fly *Drosophila melanogaster* has its own isoforms of Jun (D-Jun), JNK MAPK (Basket, Bsk) and direct upstream activators of JNK MAPK (Hemipterous, Hep; Misshapen, Msn) (104). These components possess sequence similarities to the mammalian homolog MAPK proteins functioning in a concerted signal transduction pathway to regulate gene expression and cytoskeletal remodeling during embryogenesis. *Drosophila* JNK MAPKs play roles in mediating immune and inflammatory responses, as well as developmental processes (124). JNK MAPK compartments regulate at least two morphogenetic processes of dorsal closure and thorax closure in the embryo, and is also activated by the insect immune response regulator, lipopolysaccharide (93). In particular, mutations in JNK pathway components disrupt a morphogenetic process referred to as dorsal closure. The sequence and pathway similarities between *Drosophila* and mammalian JNK MAPK pathways suggest that studies in *Drosophila* may provide useful clues regarding JNK MAPK regulation in mammals.

1.2.3. Mechanism of JNK MAPK regulation

In living cells, a large number of molecules should fulfill their specific mission in an appropriate time and place, independently of, or coordinated with other molecules. As all MAPKs phosphorylate very similar motifs conforming to the minimal consensus sequence Ser/Thr-Pro, and as many MAPK substrates contain this motif, the question arises as to how the reactions between MAPKs and their interacting molecules take place correctly. To avoid undesirable outcomes, each molecule must react with appropriate partners. Such a variety of molecules must transduce signals with high efficiency and specificity. Then mechanisms would be

required to arrange and maintain such complicated systems. There are two main mechanisms regulating the signal transduction in the MAP kinase cascades: the docking interaction and the scaffolding. The docking interactions achieved through specific conserved regions on MAPKs and MAPK-interaction molecules. Scaffolding generally requires a third molecule to tether enzymes and substrates.

1.2.3.1 Docking interaction of JNK MAPK

One mechanism regulates the formation of MAP kinase complexes via interactions with specific docking sites present in transcription factors, protein kinases, protein phosphatases, scaffold proteins, and substrates (125). These docking sites are evolutionarily conserved, and serve to regulate specificity and enhance signal transduction. Several docking sites on MAP kinases have been identified (CD and ED domains). The carboxy-terminal common docking (CD) motif is found in all known MAP kinase family members in a region distinct from the catalytic site (126). This motif contains acidic and hydrophobic residues that interact directly with targeting domains in MAP kinase kinases, dual specificity phosphatases and MAP kinase substrates (126,127). However, the CD domain alone does not determine docking specificity. A second conserved sequence, termed the ED site, functions together with the CD domain to regulate docking specificity (128). Like the CD motif, the ED motif is located on the opposite side of MAP kinases with respect to the active site and these motifs may form a ‘docking groove’ on their surface. It should be noted, however, that the CD motif is not essential under some conditions and that additional determinants of docking specificity exist (127). For example, the amino-terminal region of MAP kinases (129) and the carboxyl terminal helix within subdomain III can contribute to docking specificity (130).

In addition to the docking domains related to those found in transcription factors, other determinants have been identified in substrates that contribute to MAP kinase specificity (125). The most widely characterized of these is the D-domain, which is a hydrophobic Leu–Xaa–Leu (LXL) or Leu–Xaa–Leu–Xaa–Leu (LXLXL) motif separated by 2–6 residues from a cluster of at least two basic residues (Lys, Arg) (125). Leu can also be replaced by other hydrophobic residues. Recently, the basic and hydrophobic residues of the D-domain have been shown to be

important for recognition, binding, specificity, and phosphorylation (126,127,131,132). Similarly, the Phe–Xaa–Phe–Pro (FXFP motif) targeting domain, which can be critical for phosphorylation by ERK, does not appear to contribute to docking and phosphorylation by JNK. Furthermore, a recent study has demonstrated that the location of targeting domains within a substrate directs the phosphorylation of specific residues in the substrate (133).

1.2.3.2 Scaffold proteins

There are two kinds of scaffolding mechanisms; a third molecule is required and an enzyme serves as a scaffold for assembling the other enzymes. JNK-interaction protein (JIP), the mammalian well-known scaffold protein, acts as the third molecule that organizes specific members of the JNK MAPK cascade to facilitate signaling. The JIP family consists of three members, JIP-1, 2 and 3. JIP-1 associates with JNK, MKK7 and members of the mixed-lineage protein kinase (MLK) group (134). However, over expression of JIP-1 also shows the capacity to inhibit JNK MAPK signaling either by inhibiting JNK MAPK activity or by altering subcellular localization (135), which prevents the phosphorylation of transcription factors such as c-Jun and ATF2 (81).

1.2.4 JNK inhibitors

While JNK is activated by phosphorylation of specific Thr and Tyr residues by MAP kinase kinases (variously referred to as MAPKKs, MKKs of MEKs), it can be inactivated by dual specificity Ser/Thr/Tyr MAP kinase phosphatases (MKPs) (136). These MKPs are able to inactivate JNK, although their relative specificities towards the JNK, p38 and extracellular-signal-regulated kinase (ERK) MAP kinases differ between MKP isoforms (94,102). This pathway appears to be conserved in *Drosophila*, since *Drosophila* JNK (DJNK) signaling induces the expression of the MKP homolog *puckered* (*puc*) (108). It is likely that there are additional mechanisms that are able to suppress signaling by JNK protein kinases. For example, the JNK protein kinases are inhibited by interaction with the cytoplasmic protein JNK interacting protein 1 (JIP-1) (135). Overexpression of JIP-1 causes cytoplasmic retention of JNK and inhibition of the JNK signaling pathway (135). GPS2 (G-protein

pathway suppressor-2) was also recently shown to suppress JNK activation by association with HTLV-I Tax oncoprotein and suppresses Tax- and tumor necrosis factor (TNFα)-mediated activation of JNK1. (137). In addition, GSTs has also been reported to inhibit the JNK pathway (85,86).

1.3 GST and JNK interactions

JNK pathway components and GSTs are evolutionally conserved across mammals and insects. Different mammalian GST classes such as GST pi and GST mu have been reported to interact with different stress kinase proteins in the JNK pathway. For example, GST pi is a JNK regulatory protein, and its association with JNK maintains a low basal level of JNK activity in the non-stressed cell (85). GST has been linked to the regulation of stress induced cell signaling by inhibition of c-Jun N-terminal kinase (JNK) through direct protein-protein interaction of the GSTP1 monomer (85,138). Inhibition of JNK by GSTP has been demonstrated *in vitro* using embryonic fibroblasts from mice with a GSTP-null (*GstP1*/*P2*(-/-)) genotype; moreover fibroblasts from null mice exhibited a higher basal JNK activity compared with those from wild type mice (85). The lack of GST pi also increased constitutive JNK activity *in vivo* and therefore regulated the expression of genes that were specific downstream targets of the JNK pathway (139). The association between GSTP and JNK has also been demonstrated from recent studies that utilized apoptosis in cell lines as a measure of JNK activation. Ishisaki *et al.*(140) determined that the protection of dopaminergic neurons against dopamine-induced apoptosis was mediated by an increase in the expression of GSTP and the subsequent suppression of JNK activity. Conversely apoptosis was shown to increase in a human leukemia Jurkat cell line following etoposide treatment, which was attributed to the dimerization of GSTP1-1 resulting in the release of JNK from the GSTP-JNK complex and thus increased JNK activity (141). Moreover, GST pi coordinates ERK/p38/IKK activation as part of the mechanism underlying its ability to elicit protection against H_2O_2-induced cell death (142). In addition, GST mu interacts with Apoptosis Signal-regulating Kinase 1 (ASK1), an upstream activating kinase of JNK that participates in cell death (86).

1.4 Background and Objectives

In *Anopheles dirus,* two genes encoding five GST isoenzymes from Delta class have been previously acquired and characterized for structural as well as enzyme activities (32,36,37,39). New Delta class GST isoenzyme from *Anopheles dirus* species B which we named adGSTD5-5 (in insect GST nomenclature, "D" refers to the Delta class and "5-5" refers to the homodimeric isoenzyme (10,20) has been identified (40). The adGSTD5-5 was thus characterized. Moreover, we now have six adGST enzymes to characterize the non-enzymatic role involve the GST regulation of the JNK pathway.

1.4.1 Enzymatic study of adGSTD5-5

With the aid of several colleagues, the adGSTD5-5 was characterized from gene to protein function. The availability of the *An. dirus* genome sequence has enabled a putative promoter prediction. The adGSTD5-5 enzyme was expressed and studied for structural as well as functional characteristics. Moreover, an adGSTD5-5 crystal structure was also obtained.

1.4.2 GST and JNK interaction study

In mammalian systems, GST regulates JNK signal transduction by interaction with JNK itself or other proteins upstream in the JNK pathway. This study was focused on GSTs and their interaction with components of the JNK pathway from *Diptera*. The effects of six delta class *Anopheles dirus* GSTs, adGSTD1-1, D2-2, D3-3, D4-4, D5-5 and D6-6 on the activity of full-length recombinant *Drosophila* HEP (MAPKK7) and the *Drosophila* JNK as well as the reciprocal effect of these kinases on GST activity was evaluated.

CHAPTER 2
MATERIALS and METHODS

2.1 Preparation of DNA constructs

The six Delta class GSTs isoenzymes from *Anopheles dirus* GSTs (adGSTs); adGSTD1-1, D2-2, D3-3, D4-4, D5-5 and D6-6, wild type and mutant forms of D3-3 and D4-4 were cloned into a pET3a vector (32,37,65-67,143) as shown in **Figure 2.1**. The recombinant proteins in the *Drosophila* JNK pathway consisting of *Drosophila* HEP (HEP; Genbank accession number AAB63449.1), *Drosophila* JNK (JNK and also known as *basket*; Genbank accession number AAB97094.1) and the transactivation domain of *Drosophila* Jun (amino acids 1-104; Jun 1- 104; Genbank accession number P18289) were obtained by RT-PCR from adult *Drosophila melanogaster*. The PCR products were then cloned into a pET28b vector (Stratagene) as shown in **Figure 2.2**. The HEP recombinant plasmid was also used as the template for site-directed mutagenesis method to construct a constitutively-active HEP mutant (HEP_{3E}). The mammalian MKK7-β1 isoform mutant ($MKK7_{3E}$) has constitutive kinase activity following the substitutions of Ser^{271}, Thr^{275} and Ser^{277} to Glu (144), we therefore altered the three homologous residues (Ser^{348}, Thr^{352} and Ser^{354}) of *Drosophila* HEP to Glu by two step PCR using a Quik Change™ Site-Directed Mutagenesis kit (Stratagene). All recombinant clones were identified by restriction digest of the plasmids and confirmed by full-length sequencing in both directions using a BigDye™ Terminator Cycle Sequencing Kit (Perkin–Elmer).

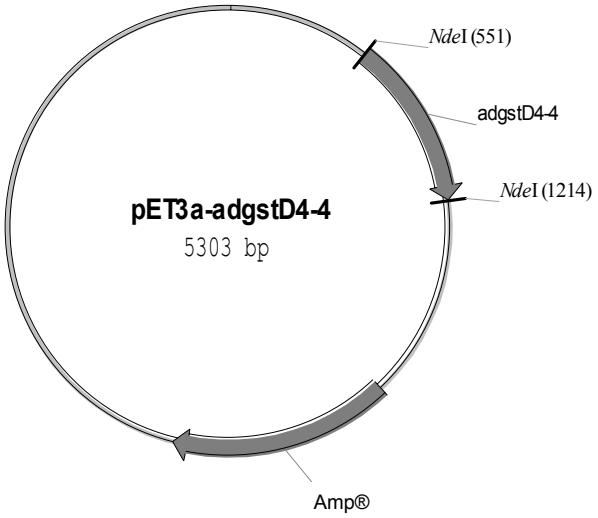

Figure 2.1 Construction of the adgstD4-4 sequence in the pET3a vector The figure illustrates the recombinant plasmid containing the adgstD4-4 gene cloned into the pET3a vector. The pET3a contains the ampicillin resistant gene for screening and T7 promoter for expression.

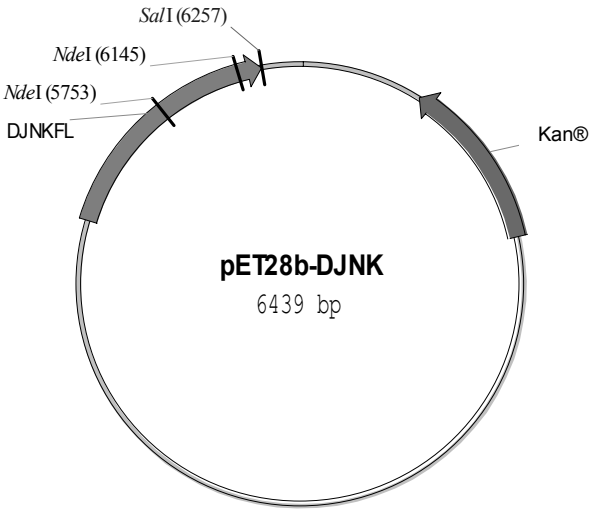

Figure 2.2 Construction of the *Drosophila* JNK sequence in the pET28b vector The figure illustrates the recombinant plasmid containing the *Drosophila* JNK gene cloned into the pET28b vector. The pET28b contains the kanamycin resistant gene for screening and T7 promoter for expression.

2.1.1. Plasmid preparation

All plasmids including pET3a, pET28b, pGL2-Basic and recombinant plasmids were extracted using a cetylmethylammonium bromide (CTAB) plasmid mini preparation method. The procedure was performed using a single colony of *E. coli* inoculated in 3 ml LB broth containing 100 µg/ml ampicillin and grown at 37 ºC with 200 rpm shaking overnight. The *E. coli* culture was transferred to a 1.5 ml microtube and the pellet was collected by centrifugation at 12,000x g for 30 sec, resuspended in 300 µl of STET buffer (8% (w/v) sucrose, 0.1% (v/v) Triton X-100, 50 mM EDTA, 50 mM Tris-HCl, pH 8.0) and mixed by vortexing. Then 5 µl of freshly prepared lysozyme solution (100 mg/ml) was added to the suspension and incubated for 10 minutes at room temperature. The mixture was boiled at 100 ºC for 45 seconds and centrifuged at 14,000x g for 15 minutes at room temperature. The cell pellet (cell debris and chromosomal DNA) was removed by using a sterile toothpick and 30 µl of 5% (w/v) CTAB was added to the supernatant, mixed by inversion and incubated for 10 minutes at room temperature. The contents were centrifuged at 12,000x g for 5 minutes at room temperature and the supernatant was discarded. The cell pellet (plasmid and low molecular weight residual DNA) was dissolved in 300 µl of 1.2 M NaCl. 10 µl of 10 mg/ml RNase A was added to the solution and incubated at 37 ºC for 30 minutes to remove RNA. An equal volume of chloroform was added, mixed by inversion and centrifuged at 12,000x g for 15 minutes. The aqueous phase was transferred to a new 1.5 ml-micro tube and 2 volumes of absolute ethanol was added. The mixture was incubated at -80 ºC for 15 minutes and centrifuged at 12,000x g for 15 minutes. The pellet of plasmid DNA was washed twice with 70% ethanol. The DNA was air-dried at room temperature and dissolved in sterile 30 µl distilled water and stored at -20 ºC.

2.1.2 DNA fragment preparation

2.1.2.1 Total RNA isolation

Approximately 200–400 mg of adult *D. melanogaster* was snap frozen in liquid nitrogen and homogenized to a powder using a mortar and pestle. The RNA was extracted by using either the GenElute™ Mammalian Total RNA Kit (Sigma) or

TRIzol™ LS reagent (Gibco BRL). The GenElute™ Mammalian Total RNA Kit was performed as described in the manufacturer's instructions.

The total RNA was isolated by The TRIzol™ LS reagent, a mono-phasic solution of phenol and guanidine isothiocyanate, was obtained by adding approximately 1 ml TRIzol™ LS reagent/50-100 mg of tissues. The homogenized sample was incubated at room temperature for 5 minutes to lyse the cells and permit the complete dissociation of nucleoprotein complexes. Then 0.2 ml of chloroform was added per 1 ml of TRIzol™ LS reagent. The sample was shaken vigorously for 15 seconds and incubated at room temperature for 2-3 minutes. Then the sample was centrifuged at 12,000x g for 15 minutes at 4 °C. Following centrifugation, the mixture was separated into a lower red, phenol-chloroform phase, an interphase, and a colorless upper aqueous phase. RNA remains exclusively in the aqueous phase. The aqueous phase was transferred to a fresh tube. RNA was precipitated by adding 0.5 ml of absolute propanol per 1 ml of TRIzol™ LS reagent and incubating at room temperature for 10 minutes, followed by centrifugation at 12,000x g for 10 minutes at 4 °C. The supernatant was discarded and the RNA pellet was washed once with 75% ethanol. The sample was mixed and centrifuged at 7,500x g for 5 minutes at 4 °C. The supernatant was then removed and the RNA pellet was briefly air dried for 10-20 minutes. The total RNA was dissolved in DEPC-treated water (RNase-free) and keep at -80 °C until used.

2.1.2.2 Determination RNA concentration and purity

The concentration and purity of RNA can be determined by measuring the absorbance at the wavelength 260 and 280 nm with a spectrophotometer. The quantity of RNA could be estimated by the calculation of nucleic acid in the sample from absorbance at 260 nm using the coefficient of an OD of 1.0 corresponds to approximately 40 μg/ml of RNA. The purity of RNA was determined from the OD_{260}/OD_{280} ratio; pure preparation of RNA has OD_{260}/OD_{280} value of 2.0. If there is significant contamination with protein or phenol, the OD_{260}/OD_{280} value will be less than 2.0 and the quantitation of the amount of nucleic acid will not be accurate.

2.1.2.3 First strand cDNA synthesis

The first strand cDNA was synthesized by using SUPERSCRIPT™ II RNase H Reverse Transcriptase (GIBCO BRL), according to the manufacturer's protocols with oligo $(dT)_{15}$ primers (GGCGGTCGACATATGTTTTTTTTTTTTTTT). For 20 µl of reaction, 250 ng of total RNA was mixed with 500 ng of oligo $(dT)_{15}$ primers, then DEPC treated water was added to give a 12 µl reaction volume. The mixture was heated to 70 °C for 10 minutes then quickly chilled on ice. The final concentration of 1X First Strand Buffer (50 mM Tris-HCl pH 8.3, 75 mM KCl and 3 mM $MgCl_2$), 10 mM DTT and 50 µM of each dATP, dGTP, dCTP and dTTP were added to the mixture. The mixture was mixed gently by pipetting and incubated at 42 °C for 2 minutes. Then 200 units of SUPERSCRIPT™ II RNase H Reverse Transcriptase was added, mixed gently and incubated at 42 °C for 50 minutes. The reaction was inactivated with heating at 70 °C for 50 minutes.

2.1.3 Primer design

All the primers (PROLIGO Primers & Probes, Singapore) were designed using Vector NTI suite 6 software.

2.1.3.1 *Drosophila* wild type MAPK proteins primer design

The sets of oligonucleotide primers for *Drosophila* proteins in the MAPK pathway were designed according to specific 5' and 3' sequences of *Drosophila* genes obtained from the Genbank database. The *Nde*I and *Sal*I restriction sites were used for cloning into the pET28b vector, except for the JNK recombinant clone obtained from 5' blunt end ligation. The recognition sites for restriction endonucleases are underlined.

***Drosophila* HEP**

HEP-F *Nde*I

5’ CGATCATATGTCCACCATTGAGTTCG 3’

*Nde*I

HEP-R *Sal*I

5’ GAAATGTATGTCGACTTAGGTAACCTC 3’

*Sal*I

***Drosophila* JNK**

JNK-F

5’ GAACAATGACGACAGCTCAGCACCAAC 3’

JNK-R *Sal*I

5’ GGAAAAAGTGTCGACCTACCGCGTTC 3’

*Sal*I

***Drosophila* Jun (Tran-activation domain)**

Jun 1-104-F *Nde*I

5’ GAGCACATATGAAAACCCCCGTTTCCG 3’

*Nde*I

Jun 1-104-R *Sal*I

5’ GCGGGTCGACTTACAGATTGTTGGATAGC 3’

*Sal*I

2.1.3.2 HEP mutagenesis primer design

The three residues of HEP (Ser^{348}, Thr^{352} and Ser^{354}) were mutated to Glu by a two step PCR using Quick Change™ Site-Directed Mutagenesis kit from Stratagene. Two sets of oligonucleotide primers were designed to introduce the residues. Both changed nucleotides and amino acid residues are shown in bold letters. The recognition sites for restriction endonucleases are underlined. Deduced amino acid sequences are shown above the reverse primer sequences.

HEP:S348D-F *Sal*I

G I S G R L V D **D** K A N T R S

5’ GGGATCAGCGGTCGCCTGGT**C**GAC**GAG**AAGGCTAACACTCGATCCG 3’

*Sal*I

HEP:S348D-R *Sal*I

5’ CGGATCGAGTGTTAGCCTT**CTC**GT**C**GACCAGGCGACCGCTGATCCC 3’

*Sal*I

HEP: T352D/S354D-F *Bgl*I

D K A N **D** R **D** A G C A A Y M A

5’ CGAGAAGGCTAAC**GAG**CGA**GAG**GCCGGCTGTGCAGC**C**TATATGGCGC 3’

*Bgl*I

HEP: T352D/S354D-R *Bgl*I

5’ GCGCCATATA**G**GCTGCACAGCCGGC**CTC**TCG**CTC**GTTAGCCTTCTCG 3’

*Bgl*I

2.1.4 Polymerase chain reaction (PCR)

The sample reactions were prepared as indicated in **Table 2.1**. The PCR amplification of *drosophila* MAPK genes were performed using a P-E Thermal Cycler 2400 (Perkin Elmer Cetus, USA) according to the conditions shown in **Table 2.2**. The annealing temperature and extension time were varied depending upon melting temperature (T_m) of the primer and size of the product. The cyclic parameters for the site-directed mutagenesis of HEP mutant were performed following conditions in **Tables 2.3**. All PCR products were analyzed by agarose gel electrophoresis and were purified before performing a ligation reaction.

Table 2.1 PCR solutions used for the *Drosophila* genes.

Reagents	Amount (µl)
10X reaction buffer (*pfu* DNA polymerase buffer)	2.5
10 pmol/µl of oligonucleotide primer 1	0.5
10 pmol/µl of oligonucleotide primer 2	0.5
10 mM dNTP mix (2.5 mM each dNTP)	0.5
cDNA template 100-200 ng of dsDNA template 100 ng of genomics DNA	X
Native *pfu* DNA polymerase (2.5 U/µl)	0.5
H_2O	20.5-X
Total volume	25

Table 2.2 Temperature cycling parameters for amplification of *Drosophila* MAPK genes.

Segments	Steps	Temperature (°C)	Time	Number of cycles
1	Initial denaturing	95	30 seconds	1
2	Denaturing Annealing Extension	95 55-60 72	30 seconds 1 minute 0.5-1.5 minutes	35
3	Final extension	72	7 minutes	1

Table 2.3 Temperature cycling parameters for amplification of HEP_{3E} mutant

Segments	Steps	Temperature (°C)	Time	Number of cycles
1	Initial denaturing	95	30 seconds	1
2	Denaturing Annealing Extension	95 55 68	30 seconds 1 minute 14 minutes	16
3	Final extension	68	7 minutes	1

The PCR products were analyzed by 1% agarose and treated with 1 µl of *Dpn*I endonuclease (Promega) which specifically digested the *in vivo* methylated parental DNA template at 37 ºC for 3 hours. The *Dpn*I-treated DNA was transformed into competent *E. coli* DH5α.

2.1.5 DNA purification

The PCR product band was separated on 1% agarose gel in 1X Tris-acetate EDTA (TAE) electrophoresis buffer (40 mM Tris-acetate, 1 mM EDTA pH 8.0) and the expected DNA band was excised from the gel and purified with GENECLEAN II™ kit (Bio 101). The gel sample was mixed with 3 volumes of sodium iodide (NaI) and incubated at 55 °C for approximately 5 minutes to melt the gel. Then the sample solution was mixed with Glassmilk suspension (1 µl of Glassmilk will bind 1-2 µg of DNA), and incubated at room temperature for 30 minutes to allow binding of the DNA to the silica matrix. The solution was mixed every 2-3 minutes to ensure that the Glassmilk stayed suspended. After that, the Glassmilk in the solution was centrifuged approximately five seconds at 12,000x g, and the supernatant was removed. The Glassmilk was washed with buffer three times, centrifuged and the supernatant discarded. The pellet was air-dried and the DNA was eluted from the Glassmilk with sterile distilled water by carefully removing the supernatant containing the eluted DNA and placing in a new tube.

2.1.6 Agarose gel electrophoresis

One percent agarose was prepared in 1X TBE buffer (0.09 M Tris-borate and 2 mM EDTA, pH 8.0). The agar was melted and poured into a gel tray and allowed to set 30 minutes. The plasmid DNA was mixed with loading buffer (0.25% (w/v) bromophenol blue and 30% (v/v) glycerol in water) before being loaded into the wells. Then the DNA was loaded on the gel along with the marker either λ/*Hind*III or λ/*BstE*II DNA. The electrophoresis was performed at 100 volt for 60 minutes then the gel was stained with 0.5 mg/ml of ethidium bromide solution in water for 10 minutes and destained with distilled water for 10 minutes. The DNA bands were visualized by ultraviolet irradiation and photographed.

2.1.7 DNA ligation

The purified *Nde*I and *Sal*I digested PCR products were ligated into *Nde*I/*Sal*I digested pET28b vector in the ratio 3:1, 5:1 and 10:1 (insert: vector) in a 20 µl reaction mixture. The reaction mixture 20 µl contained:

- 1 unit of T_4 DNA Ligase (GIBCO BRL)
- 1X DNA Ligase Reaction Buffer [50 mM Tris-HCl pH 7.6, 10 mM $MgCl_2$, 1 mM ATP, 1 mM DTT and 5% (w/v) polyethylene glycol-8000]
- Sterile distilled water to final volume of 20 µl

The ligation mixtures were incubated at 14 °C overnight and kept at 4 °C until used.

2.1.8 Subcloning insert into the vector

2.1.8.1 Preparation of *E.coli* competent cells (Calcium Chloride Method)

A single cell colony of *E. coli* DH5α was inoculated into 2 ml of LB medium and grown with 200 rpm shaking overnight (12-16 hours) at 37 ºC. The starter culture was diluted 1:100 in LB media and grown with 200 rpm shaking at 37 ºC until the bacterial growth reached the log phase (OD value at 600 nm was approximately 0.3-0.5). The culture was divided into 2 sterile disposable ice-cold polypropylene tubes and placed on ice for 10 minutes. The cells were collected by centrifugation at 4,000x g for 10 minutes at 4 ºC. The medium was decanted and drained by inverting the tubes on a pad of paper towels. The pellets were resuspended in 10 ml of ice-cold 0.1 M $CaCl_2$ solution by gently vortexing. The cells were recollected by centrifugation at 4,000x g for 10 minutes at 4 ºC and the steps of resuspension by $CaCl_2$ solution and recollecting the cells were repeated. The pellets were resuspended in 10 ml of 0.1 M $CaCl_2$ with 15% glycerol. Competent cells were aliquoted (200 µl) into chilled-microtubes and kept at -80 ºC until used.

2.1.8.2 Transformation of competent cells

For the transformation 100 ng of DNA was added to 200 µl of competent cells and placed on ice for 1 hour. The cells were heat-shocked at 42 ºC for 90 seconds and rapidly transferred to ice for 5 minutes. The transformed cells were added to 1 ml of LB broth and allowed to recover by growing for 1 hour in a 37 ºC shaking incubator. The 200 µl of transformed cells were spread onto agar medium containing an appropriate antibiotic. The plates were incubated at 37 ºC for 12-16 hours.

2.1.9 Restriction enzyme analysis

Five to ten clones of recombinant plasmids were randomly selected for restriction analysis. The reaction contained 1 µl of recombinant plasmid DNA, 1X buffer, 1 unit of restriction enzyme and sterile distilled water to the final volume of 10 µl. The reactions were incubated at an appropriate temperature depending on the enzyme used for 2-3 hours. The digested plasmids were analyzed in 1% agarose gel. The positive recombinant clone was selected for DNA sequencing and stored at -20 ºC.

2.1.10 DNA sequencing

To verify the correct DNA sequence in both directions with T7 promoter universal primers, DNA sequencing was conducted using ABI PRISM Bigdye™ Terminator or Cycle Sequencing Ready Reaction Kit (Perkin Elmer), following the manufacturer's instructions. The PCR reaction mixture was performed in a thin wall 0.5 ml PCR tube containing 4 µl of 2.5X buffer, 4 µl of Bigdye kit [A-Dye Terminator labeled with dichloro (R6G), C-dye Terminator labeled with dichloro (ROX), T-Dye Terminator labeled with dichloro (TAMRAO), G-Dye Terminator labeled with dichloro (R110), deoxynucleoside triphosphates (dATP, dCTP, dITP, dUTP), $MgCl_2$, Tris-HCL pH 9.0, Amplitaq DNA polymerase], 10-20 pmol of Universal primer (T7 promoter or T7 terminator) and 200 ng of DNA. The sequencing reactions were adjusted to 20 µl with sterile distilled water and were amplified using a Thermocycler (GeneAmp960, Perkin Elmer). The PCR cycling parameters are shown in **Table 2.4**.

Table 2.4 Temperature cycling parameters for DNA sequencing

Segments	Steps	Temperature (ºC)	Time (min:sec)	Number of cycles
1	Initial denaturing	96	3 minutes	1
2	Denaturing Annealing Extension	96 50 60	10 seconds 5 seconds 4 minutes	28
3	Final extension	60	7 minutes	1

The PCR products from thermal cycling were transferred to a sterile 1.5 ml microcentrifuge tube with 1/10 volume of 3M sodium acetate and 2.5 volumes of absolute ethanol. The mixture was incubated at room temperature for 30 minutes and centrifuged at 14,000x g for 15 minutes. The pellets were washed twice with 70% ethanol and allowed to dry. The DNA samples were analyzed by the automated DNA sequencer ABI Prism 377 (Perkin Elmer).

2.2 Recombinant protein preparation

The GST proteins were expressed and purified using either GSTrap or S-hexyl glutathione affinity chromatography (37,39,67). The five recombinant proteins HEP, HEP_{3E}, JNK and Jun were expressed as histidine fusion proteins. The JNK and Jun recombinant proteins were expressed as soluble proteins and purified according to a standard Ni^{2+}-NTA column protocol (Amersham Pharmacia Biotech). In contrast, HEP and HEP_{3E} recombinant proteins were expressed mainly in inclusion bodies. Therefore, these HEP and HEP_{3E} were purified using Ni^{2+}-NTA column chromatography under denaturing conditions and renatured by slow dialysis following the Roti®-Fold reagent protocol (Carl Roth GmbH+ Co.).

2.2.1 Protein expression

All recombinant plasmids was transformed into *E. coli* BL21(DE3)pLysS for protein expression. The starter was obtained by inoculating a single colony of *E. coli* BL21(DE3)pLysS in 3 ml LB broth supplemented with appropriated antibiotics. *E. coli* BL21(DE3)pLysS 100 µg/ml containing adGSTs recombinant plasmids were grown in LB broth supplemented with ampicillin as well as 34 µg/ml chloramphenical, whereas *Drosophila* kinase proteins plasmids were grown in LB broth supplemented with 30 µg/ml kanamycin and 34 µg/ml chloramphenical. The culture was further grown at 37 ºC with 200 rpm shaking overnight. The aliquot of culture equal to 1% of the final induction culture was transferred to a fresh LB broth containing antibiotics. The culture was grown with 200 rpm shaking at 37 ºC until the OD at 600 nm reached approximately 0.6. The IPTG induction was performed at a final concentration of 0.1 mM and incubated at 37 ºC or 25 ºC for 3 hours for adGSTs and *Drosophila* kinase proteins, respectively. The culture was placed on ice for 20 minutes before being centrifuged at 6,000x g, 4 ºC for 10 minutes. The LB broth was decanted. The collected cells were resuspended in 10 ml of LB, transferred to a new 50 ml-centrifuge tube and centrifuged at 7,000x g, 4 ºC for 10 minutes. The supernatant was discarded and the pellet was stored at -20 ºC until used.

2.2.2 Protein purification

2.2.2.1 Glutathione affinity chromatography

The pellet from 200 ml induced culture was resuspended with 14.5 ml of PBS buffer pH 7.3 (140 mM NaCl, 2.7 mM KCl, 10 mM Na_2HPO_4, 1.8 mM KH_2PO_4 pH 7.3), 600 µl of 100 mg/ml lysozyme and 10 µl of 1.4 M β-mercaptoethanol by gentle vortexing. The cell suspension was placed on ice for 20 minutes and 75 µl of 2 M DTT was added. The crude cell extract was obtained by breaking the cells twice with a French Press at 11,000 psi. The lysed cells were centrifuged at 10,000x g at 4 ºC for 20 minutes. The supernatant was collected and placed on ice for enzyme purification.

The soluble GST in the supernatant of total cell lysate was purified using GSTrap affinity chromatography (5 ml GSTrap^{TM} FF) following the manufacturer's instruction and all steps were performed at 4ºC. The column was

equilibrated with 5 column volumes of the binding buffer, PBS pH 7.3. The supernatant was passed through the column at the rate of 1-5 ml/min. The entire buffer solution passing through the column at each step was collected and placed on ice for further characterization. The non-specific binding proteins were washed out with 8 column volumes of PBS buffer. The bound GST was eluted out with 4 column volumes of elution buffer (10 mM GSH in 1.5 M Tris-HCl pH 8.0, and 10 mM DTT). To remove the bound GSH the elution fraction of purified GST was pooled in a centriprep-10 (Amicon) ultrafiltration unit and centrifuged at 2,900x g 4 ºC using Avanti™ J-25I (Beckman), JA-25.50 rotor until the final volume was less than 1.5 ml. The concentrated GST was adjusted to 1.5 ml and applied to a HiTrap desalting column (Amersham Pharmacia Biotech) equilibrated with 5 column volumes of desalting buffer (50 mM phosphate buffer pH 6.5). The GST was eluted with 2 ml of desalting buffer containing 10 mM DTT and concentrated to a final volume of less than 1 ml by using the centriprep-10 as previously described. The purified GST was stored in 50% glycerol at -20 ºC.

2.2.2.2 S-hexyl glutathione affinity chromatography

The cell pellet from 1 litre induced cell culture was resuspended with 28.8 ml of 50 mM Tris-HCl pH 7.4 containing 1 M EDTA, 1.2 ml of 100 mg/ml fresh lysozyme, 22 µl of 1.4 M β-mercaptoethanol by gentle vortexing. The cell suspension was placed on ice for 20 minutes and 150 µl of 2 M DTT was added. The crude cell extract was obtained by breaking the cells twice with a French Press at 11,000 psi. The lysed cells were centrifuged at 10,000x g at 4 ºC for 20 minutes. The supernatant was collected and placed on ice for enzyme purification.

The S-hexyl glutathione agarose media was pre-packed into 5 ml columns. Then a column was equilibrated with equilibration buffer (50mM Tris-HCl pH 7.4, 1 mM EDTA and 0.2 M NaCl). All steps of the purification were performed at 4 ºC and the entire buffer solution passing through the column at each step was collected and placed on ice for further characterization. The supernatant of soluble recombinant GST was passed through a sterile filter with 0.45 µm cut-off and applied to the column. The non specific binding proteins were washed out with 5 column volumes of washing buffer (50 mM Tris-HCl pH 7.4, 1 mM EDTA and 1 M NaCl).

The recombinant GST was eluted from the column with 5 column volumes of equilibration buffer containing 5 mM S-hexyl glutathione and 10 mM DTT. To remove S-hexyl glutathione and salts the eluted fractions of purified GST were pooled in a centriprep-10 (Amicon) ultrafiltration unit and centrifuged at 2,900x g at 4 ºC using an Avanti™ J-25I (Beckman), JA-25.50 rotor until the final volume was less than 1.5 ml. The concentrated GST was adjusted to 1.5 ml and applied to a HiTrap desalting column (Amersham Pharmacia Biotech) equilibrated with 5 column volumes of desalting buffer (50 mM phosphate buffer pH 6.5). The GST was eluted with 2 ml of desalting buffer containing 10 mM DTT and concentrated to a final volume of less than 1 ml by using a centriprep-10 as previously described. The purified recombinant GST was stored in 50% glycerol at −20 ºC.

2.2.2.3 Metal chelating chromatography

2.2.2.3.1 Native condition: JNK, Jun

The pellet from 1.5 L induced culture was resuspended with 20 ml of binding buffer pH 7.4 (0.5 M NaCl, 20 mM Sodium phosphate buffer pH 7.4), 830 µl of 100 mg/ml lysozyme and 14 µl of 1.4 M β-mercaptoethanol by gentle vortexing. The cell suspension was placed on ice for 20 minutes. The crude cell extract was obtained by breaking the cells twice with a French Press at 11,000 psi. The lysed cells were centrifuged at 10,000x g at 4 ºC for 20 minutes. The supernatant was collected and placed on ice for enzyme purification.

The soluble $(His)_6$-tagged *Drosophila* kinase proteins in the supernatant of total cell lysate was purified using Ni^{2+}-NTA column according to the manufacturer's instructions and all steps were performed at 4 ºC. The entire buffer solution passing through the column at each step was collected and placed on ice for further characterization. A Ni^{2+}-NTA column was pre-packed to 7.5 ml with Chelating Sepharose™ media. The column preparation was performed by charging with ½ column volume of 0.1 M $NiCl_2$. The excess nickel was washed out with 5-10 column volumes of distilled water. After column preparation, the column was equilibrated with 5-10 column volumes of binding buffer (0.02 M sodium phosphate, 0.5 M NaCl, pH 7.4). The supernatant was applied to the equilibrated column and the non-specific binding proteins were washed out with 10-15 column volumes of binding

buffer containing 40 mM imidazole. To increase the purity of eluted recombinant kinase proteins, a wash with 2 column volumes of binding buffer containing 60 mM imidazole was performed although kinase proteins were partially eluted with this step. The bound recombinant proteins were eluted out with 5 column volumes of binding buffer containing 200 mM imidazole. To remove imidazole, the eluted fractions of purified proteins were pooled in a centriprep-10 (Amicon) ultrafiltration unit and centrifuged at 2,900x g at 4 ºC using an Avanti™ J-25I (Beckman), JA-25.50 rotor until the final volume was less than 1.5 ml. The concentrated recombinant proteins were adjusted to 1.5 ml and applied to a HiTrap desalting column (Amersham Pharmacia Biotech) equilibrated with 5 column volumes of desalting buffer (50 mM Tris-Cl buffer pH 8.0). The recombinant proteins were eluted with 2 ml of desalting buffer containing 10 mM DTT and concentrated to a final volume of less than 1 ml by using a centriprep-10 as previously described. The purified kinase proteins were stored in 50% glycerol at -20 ºC.

2.2.2.3.2 Denaturing condition: HEPWT, $HEP_{3E}MT$

Due to insoluble expression, the recovery of active HEP protein from purified inclusion bodies required the denaturation of the polypeptide and then it's refolding to an active form.

The pellet from 3 L of induced culture was resuspended with 20 ml of binding buffer pH 7.4 (0.5 M NaCl, 20 mM Sodium phosphate buffer pH 7.4), 830 µl of 100 mg/ml lysozyme and 14 µl of 1.4 M β-mercaptoethanol by gentle vortexing. The cell suspension was placed on ice for 20 minutes. The crude cell extract was obtained by breaking the cells twice with a French Press at 11,000 psi. The lysed cells were centrifuged at 10,000x g at 4 ºC for 20 minutes. The HEP proteins were expressed as an insoluble form, therefore the pellet, the inclusion fraction, was collected and solubilized by resuspension with 3 ml of binding buffer pH 7.4 containing a denaturant (8 M urea) for protein purification under denaturing condition.

The solubilized protein was applied to the Ni-NTA column which had been equilibrated with the binding buffer containing 8 M urea. All purification steps were performed following the native conditions, except urea in the eluted fractions

needed to be removed by dialysis before the desalting step. Protein refolding was performed using Roti®-fold reagent following the manufacturing protocol. The recombinant proteins were concentrated to a final volume of less than 1 ml by using a centriprep-10. The purified HEP protein was stored in 50% glycerol at −20 ºC.

2.2.3 SDS-polyacrylamide gel electrophoresis

2.2.3.1 Protein Sample Preparation

The OD_{600} of the bacterial cell culture was measured. Then the cells corresponding to 0.1 OD were collected by centrifugation at 5,000 rpm for 2 minutes. The cell pellet was resuspended by vortexing in 60 µl sterile distilled water and 20 µl of 4X gel sample buffer (4 mM EDTA, 4% SDS, 40% glycerol, 100 mM DTT, 1.45 mM bromophenol blue, 200 mM Tris-HCl, pH 7.5) and heated at 95 ºC for 10 minutes in a heating block to denature the proteins and stored in the refrigerator until the SDS-PAGE had been set up.

2.2.3.2 Separation of Protein Samples

An SDS-PAGE gel was prepared as described in **Table 2.5.** After the gel was polymerized for approximately 30 minutes the well comb was removed. The wells were washed with water to remove unpolymerized acrylamide solution. The electrophoresis apparatus was assembled. The samples were loaded, approximately 0.05 OD, including 4 µl of a protein standard marker. The separation was started in descending direction at a constant current of 25 mA until the bromophenol marker was run to the bottom of the gel. The electrophoresis equipment was disassembled and the gel was stained in Coomassie staining solution for 2 hours at room temperature. Then the gel was destained overnight in destaining solution, dried and made a permanent record by scanning the gel.

Table 2.5 Preparation of SDS-PAGE (0.75 mm x 2 gels)

Solutions	Stacking gel (6%)	Separating gel (15%)
Acrylamide solution (ml) (30% acrylamide + 0.3% (w/v) bis-acrylamide)	0.6	5
1.5 M Tris-HCl pH 8.8 (ml)	−	2.5
0.5 M Tris-HCl pH 6.8 (ml)	0.75	−
Distilled water (ml)	1.6	2.3
10% SDS (µl)	30	100
10% (w/v) Ammonium persulphate (µl)	20	50
TEMED (µl)	10	10
Total volume (ml)	3	10

2.2.4 Protein assay

The method of Bradford (145), with BSA as a standard, was used for the determination of protein quantity. The BioRad protein reagent (Bio-Rad) was diluted 1:5 with sterile distilled water and filtered through Whatman No.1 filter paper to remove the insoluble dye. Three hundred microlitres of the reagent was added to 10 µl of sample in a microtiter plate. The mixture was incubated at room temperature and the absorbance at 595 nm was measured after 5 minutes. A protein standard curve was generated by using five different concentrations of bovine serum albumin; 0.1-0.5 mg/ml. Then the unknown protein concentration was calculated from the standard curve.

2.3 Protein characterization

2.3.1 Determination of GST activity

GST activity was measured by monitoring the formation of the conjugate between 10 mM glutathione (GSH) and 1 mM 1-chloro-2, 4-dinitrobenzene (CDNB) at 340 nm ($\Delta\varepsilon$ = 9.6 $mM^{-1}cm^{-1}$) in 0.1 M phosphate butter, pH 6.5, at 25 °C according to the method of Habig et al (146). The substrate was prepared by adding 50 µl of 42 mM CDNB in absolute ethanol and 450 µl of 21 mM GSH in 0.1 M phosphate buffer into 50 µl of 0.1 M phosphate buffer pH 6.5. The reaction was started by adding 100 µl of 0.1 M phosphate buffer with 10 µl of diluted enzyme sample to a well of a microtiter plate and then quickly adding 100 µl of the prepared substrate. The rate of conjugation between GSH and CDNB was monitored by measuring the change in absorbance at 340 nm for 1 minute using a SpectraMax 250.

2.3.2 Determination of substrate specificity

Specific activities toward different substrates were performed. Specific activity toward different substrates; 1-chloro-2,4-dinitrobenzene (CDNB), 1,2-dichloro-4-nitrobenzene (DCNB), p-nitrophenethyl bromide (PNPB), p-nitrobenzyl chloride (PNBC) and ethacrynic acid (EA) were performed as described in **Table 2.6** (143). GSH stock solution was prepared in 0.1 M phosphate buffer using the appropriate pH for each substrate. All the stock hydrophobic substrates were prepared in absolute ethanol and diluted into the assay buffer. All measurements were performed at 25-27 ºC in 0.1 M phosphate buffer. Specific activities were calculated based on the molar extinction coefficient for each substrate (146). The specific activities reported are the mean ± standard deviation from at least three independent experiments.

Table 2.6 The conditions for the determination of substrate specificities

Substrates	Concentration (mM)	pH buffer	λ max (nm)	Absorbance coefficient ($mM^{-1}cm^{-1}$)
CDNB	1 (D1-1, D3-3) 2 (D2-2) 3 (D4-4, D5-5, D6-6)	6.5	340	9.6
DCNB	1	7.5	345	8.5
EA	0.2	6.5	270	5.0
PNBC	0.1	6.5	310	1.2
PNPB	0.1	6.5	310	1.9

2.3.3 Determination of kinetic parameters

Kinetic parameters of the adGST enzymes were determined with CDNB as variable substrate and a GSH concentration at 10 mM. The electrophile concentration was varied from 0.02-3 mM. The reaction was performed in 0.1 M phosphate buffer, pH 6.5. Kinetic parameters were also established by varying the GSH at concentration of 0.008-15 mM with 1 mM CDNB. The maximal velocity (V_{max}) and the Michaelis constant (K_m) were analyzed by nonlinear regression using the software package GraphPad Prism (GraphPad Software, Inc. San Diego, CA). The catalytic constant (k_{cat}) and the catalytic efficiency (k_{cat} / K_m) were calculated on an active-site basis using the subunit molecular mass of each enzyme. The kinetic constants are the mean ± standard deviation for at least three separate experiments.

2.3.4 Inhibition study

The inhibition studies were performed using the standard GST assay conditions (10 mM GSH and 1 mM CDNB) in the presence and absence of the inhibitors. The following compounds were used as inhibitors: 0.01-0.1 mM S-hexyl glutathione, 1 mM DCNB, 0.001-0.1 mM EA, 0.1 mM PNPB, 1 mM PNBC, 2.5 mM cumene hydroperoxide, 0.01 mM permethrin, 0.01 mM deltamethrin and 0.01 mM λcyhalothrin. The inhibitors were prepared in absolute ethanol except S-hexyl GSH

which was resuspended in phosphate buffer pH 6.5. The inhibition reaction was measured by following the change in absorbance at 340 nm for 1 minute using a SpectraMax 250 at room temperature. The percent inhibition was calculated based on the activity of the enzyme with no inhibitor as 100%.

2.3.5 *In vitro* Protein Kinase assay

Constitutively active HEP_{3E} was used to activate JNK, then both HEP_{3E} and Jun were assessed as JNK substrates (103,147). HEP_{3E}, JNK and Jun in 1:2:10 molar ratio were incubated in 20 mM HEPES, 20 mM $MgCl_2$, 20 mM β-glycerophosphate, pH 7.6, containing 500 μM dithiothreitol, 100 μM sodium orthovanadate and supplemented with 20 μM ATP, 3 μCi of [γ-^{32}P] ATP. The phosphorylation reactions were performed for 25 min at room temperature and separated by SDS-PAGE. Phosphorylated proteins were visualized by autoradiography and quantitated by Cerenkov counting.

2.4 Study of the GST and JNK interaction

2.4.1 Effects of Kinase Proteins, HEP and JNK, on GST activity

The effects of HEP and JNK on GST activity were examined by incubating GSTs and kinase proteins in a 1:1 molar ratio at room temperature (27-30) ºC for 5 min. The GST activity was measured in the presence and absence of kinase proteins. The effects on GST activity were evaluated as described below.

2.4.1.1 % inhibition of GST activity

The % inhibition was determined by measuring GST activity in the presence of HEP or JNK as well as without kinase proteins as the control.

2.4.1.2 Type of inhibition and affinity binding (K_i)

GST and kinase protein interactions were performed by varying concentration of CDNB from 0.05 to 3.0 mM and measuring kinetic parameters for CDNB and GSH conjugation (148,149). The kinetic parameters and K_i were determined by both linear and non-linear regression analysis using GraphPad Prism 2.01 software.

2.4.1.3 Change of GST substrate specificity by JNK.

GST and JNK were incubated in a 1:1 molar ratio and the effects of JNK on GST activity were determined using the hydrophobic substrates for GST, as mentioned above. A positive or negative change of GST activity towards a substrate, when compared to activity in the absence of JNK, indicated a substrate selectivity change of GST.

2.4.1.4 The effect of glutathione (GSH) on GST activity in the presence of JNK.

A 1:1 molar ratio of GST: JNK was incubated at room temperature for 5 minutes in the presence and absence of 2 mM GSH. The GST activity was determined towards its hydrophobic substrates as described above.

2.4.2 Effects of GST on Protein Kinase Activity

The recombinant GSTs were incubated with kinase proteins in a 10:1 molar ratio for 10 min at room temperature. Kinase activity was then measured as described above.

CHAPTER 3
RESULTS

3.1 DNA constructs

3.1.1 *Drosophila* MAPK proteins

The *Drosophila* MAPK protein coding sequences were obtained by RT-PCR from *Drosophila* adult flies. The PCR products of full length JNK (JNK), full-length HEP (HEP) and Tran-activation domain of Jun 1-104 (Jun) were visualized by agarose gel electrophoresis with a band size of approximately 1.1, 1.5, and 0.3 kb, respectively as shown in **Figure 3.1**. These fragments were successfully cloned into a pET28b vector. The recombinant clones were screened by restriction enzyme analysis as shown in **Figure 3.2 A-C**. Positive clones from each construct were verified by full-length DNA sequencing in both directions. The correct clones were then transformed into *E. coli* BL21(DE3)pLysS for protein expression and enzyme characterization.

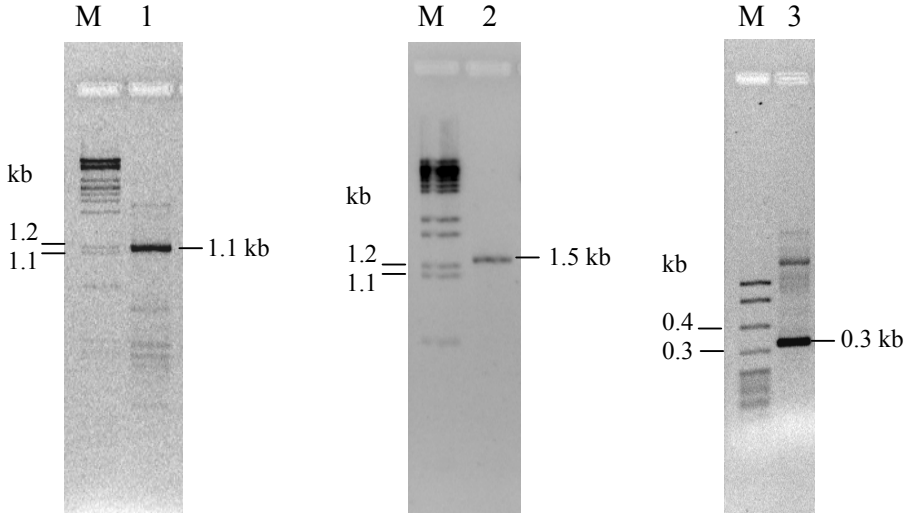

Figure 3.1 RT-PCR products of kinase proteins on an agarose gel with ethidium bromide staining. The size of JNK, HEP, and Jun are 1.1, 1.5, and 0.3 kb, respectively.

Lane M: DNA marker (200 ng)

Lane 1: JNK RT-PCR product

Lane 2: HEP RT-PCR product

Lane 3: Jun RT-PCR product

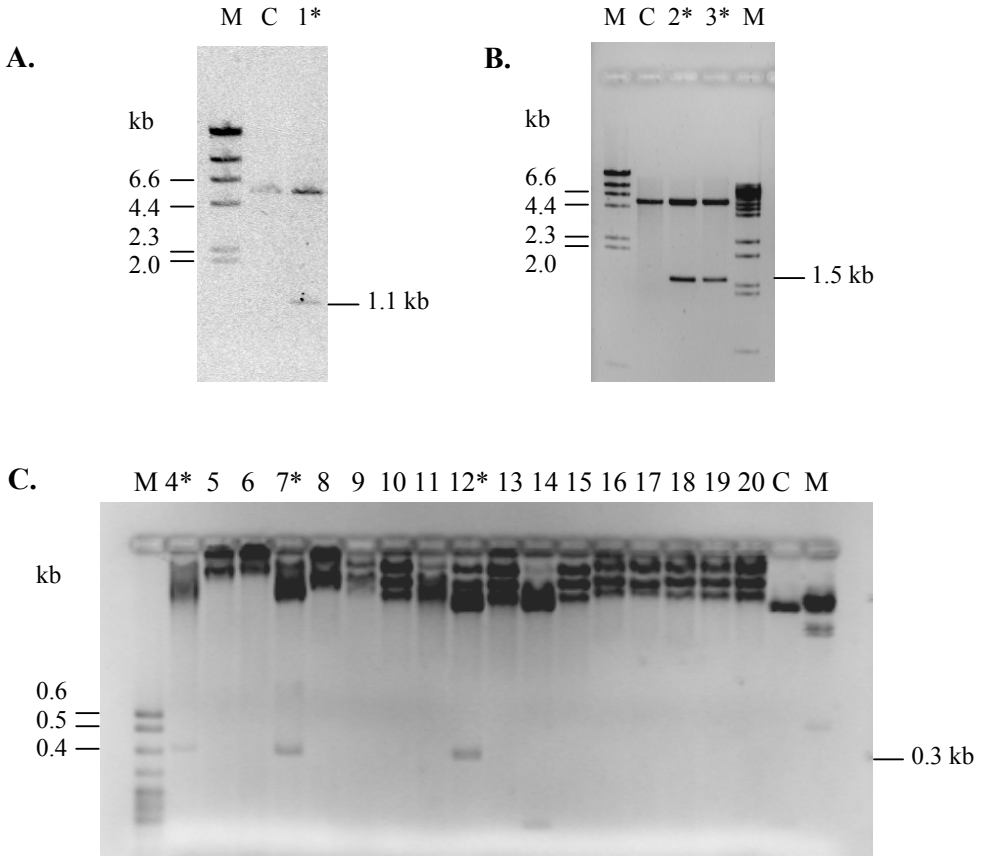

Figure 3.2 Restriction digestion analysis of MAPK protein recombinant plasmid with *Nde*I and *Sal*I. Positive clones are asterisked (*). **(A)** JNK recombinant plasmids **(B)** HEP recombinant plasmids **(C)** Jun recombinant plasmids

Lane M: DNA marker (200 ng)

Lane C: *Nde*I and *Sal*I digested pET28b vector

Lane 1: *Nde*I and *Sal*I digested JNK recombinant plasmids

Lane 2-3: *Nde*I and *Sal*I digested HEP recombinant plasmids

Lane 4-20: *Nde*I and *Sal*I digested Jun recombinant plasmids

3.1.2 *Drosophila* constitutively-active HEP_{3E} Mutant

As was recently shown that substitution to Glu of the three amino acids Ser^{271}, Thr^{275} and Ser^{277} in mammalian MKK7-β1 kinase domain successfully yielded constitutive kinase activity ($MKK7_{3E}$) (144). We therefore constructed a *Drosophila* constitutively-active MKK7 mutant (HEP_{3E}) by changing the three *Drosophila* HEP homologous residues of Ser^{348}, Thr^{352} and Ser^{354} to Glu. The two steps PCR-based site-directed mutagenesis was performed using *Drosophila* HEP wild type recombinant plasmid as the template.

The PCR products are shown in **Figure 3.3A** with a single band of 1.5 kb. After the PCR product was treated with *Dpn*I to digest out the wild type strand, the DNA was then transformed into *E.coli* DH5α. The recombinant clones were randomly screened for the desired mutations by restriction enzyme digestion as compared with the wild type DNA as shown in **Figure 3.3B**. The full-length DNA sequence was verified the in both directions. The correct clones were then transformed into *E.coli* BL21(DE3)pLysS for further expression and enzyme characterization.

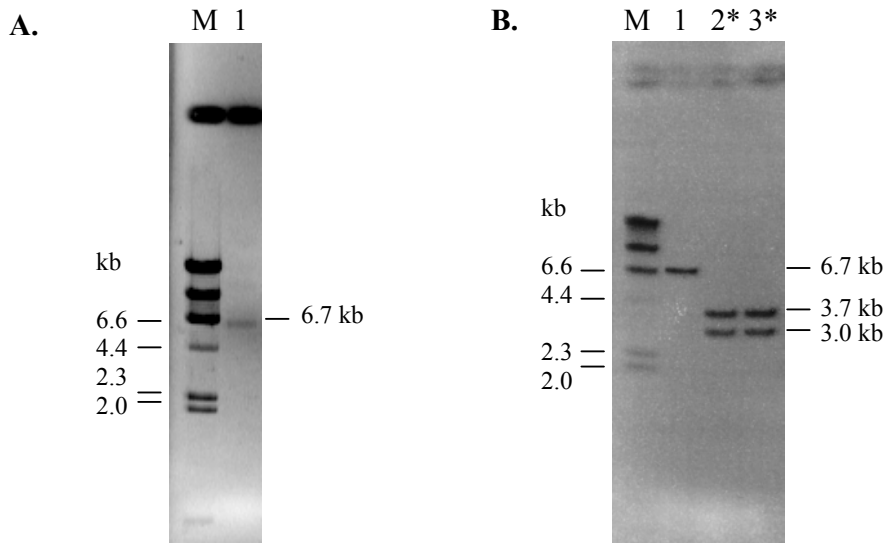

Figure 3.3 *Drosophila* constitutively-active HEP_{3E} mutant construct

(A) The 1.5 kb PCR product of site directed mutagenesis of a constitutively-active HEP mutant (HEP_{3E}) before digestion with *Dpn*I on 1% agarose gel.

Lane M: DNA marker (200 ng)

Lane 1: HEP_{3E} ($Ser^{348}/Thr^{352}/Ser^{354}$) RT-PCR product

(B) Restriction endonuclease analysis of HEP_{3E}. The figure shows 1% agarose gel electrophoresis (ethidium bromide stained) of *Bgl*I digestion patterns of wild-type and mutated plasmids. Positive clones are asterisked.

Lane M: DNA marker (200 ng)

Lane 1: *Bgl*I digested HEP wild-type plasmid

Lane 2-3: *Bgl*I digested HEP_{3E} ($Ser^{348}/Thr^{352}/Ser^{354}$Glu) recombinant plasmids

3.2 Recombinant protein preparation

3.2.1 Glutathione transferase (GST) enzymes

The recombinant GST enzymes were expressed as the soluble form at either 25 or 37 ºC under T7 promoter expression system. These GST proteins were expressed at high levels, approximately 4–300 mg from 1 L of *E. coli* culture. These enzymes were successfully purified using GSTrap or S-hexyl glutathione affinity chromatography according to the enzyme properties. GST D1-1 and D5-5 recombinant proteins were successfully purified by using an S-hexyl glutathione affinity column. The remaining enzymes of D2-2, D3-3, D4-4 and D6-6 were purified by a GSTrap column. Although GST D1-1 had the lowest expression level (4-10 mg/1 L of *E.coli* culture), it had a great affinity for binding to the S-hexyl glutathione column. The yield was roughly 2-8 mg from 1L of *E.coli* culture. In contrast, induction of the *E. coli* culture gave a high yield of recombinant D5-5 protein expression (250-300 mg/1 L of *E. coli* culture). However, D5-5 had a very weak affinity for GST affinity chromatography media compared with other GST isoenzymes from *Anopheles dirus* so the final yield of purified GST was low (10-15 mg/1 L of *E.coli* culture). D6-6 provided high induction of recombinant protein expression (50-60 mg/1 L of *E.coli* culture), nevertheless, it possessed the weak affinity binding to the matrix. The yield of purification was therefore derived in the low level of approximately 10-20 mg from 1L of *E.coli* culture. D2-2, D3-3 and D4-4 were both highly expressed and tightly bound to the GSTrap column, therefore the incredibly high yields of approximately 25-100 mg from 1 L of *E.coli* culture were obtained. The GST activities and the purification yields are shown in **Table 3.1**. These GSTs even though sharing a high homology of the glutathione binding domain, they displayed significantly different enzymatic properties as observed by the broad range of differences in specific activity. The purity of the enzyme was determined by SDS-PAGE, as shown in **Figure 3.4**. The expected bands of approximately 23-25 kDa corresponding to a GST subunit appears as a single band in the final purified protein fraction.

Table 3.1 Purification of adGST proteins

GSTs	Chromatography	Total GST (mg/1L *E.coli* culture)	Yield (%)	Specific activity (µmol/min/mg)
D1-1	S-hexyl GSH	6.73 ± 2.46	31.32 ± 12.17	6.54 ± 0.53
D2-2	GSTrap	23.37 ± 4.54	40.45 ± 3.14	45.10 ± 3.41
D3-3	GSTrap	104.17 ± 42.20	91.95 ± 7.23	67.50 ± 1.97
D4-4	GSTrap	37.56 ± 10.24	47.44 ± 11.28	41.80 ± 1.40
D5-5	S-hexyl GSH	11.68 ± 4.02	37.30 ± 13.76	13.02 ± 2.00
D6-6	GSTrap	15.40 ± 3.05	23.79 ± 0.36	0.47 ± 0.17

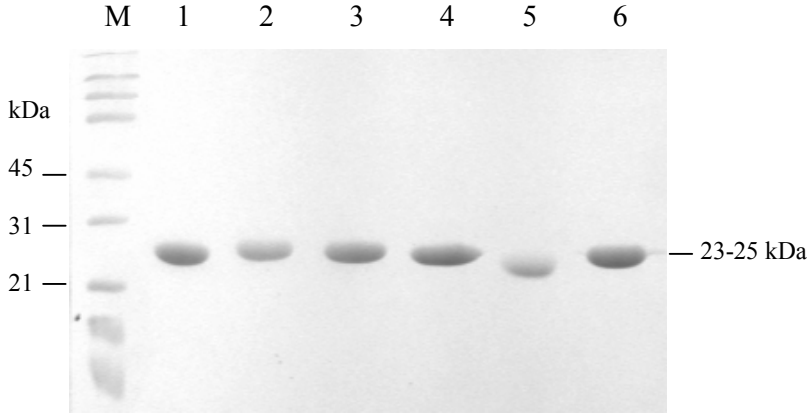

Figure 3.4 The SDS-PAGE of purified six isoenzymes of adGSTs. SDS-polyacrylamide gel demonstrated the purified GST proteins from either S-hexyl GSH or GSTrap affinity column. The 23-25 kDa bands of purified GSTs are indicated.

Lane M: Broad-range marker

Lanes 1-6: adGSTD1-1, D2-2, D3-3, D4-4, D6-6 and D5-5, respectively

3.2.2 *Drosophila* kinase proteins

The five recombinant proteins of HEP, HEP_{3E}, JNK and Jun and were highly expressed as histidine fusion proteins under the strong T7 promoter. JNK and Jun recombinant proteins were expressed as soluble proteins and purified using a standard Ni^{2+}-NTA column protocol. Whereas, HEP and HEP_{3E} recombinant proteins were mainly expressed as insoluble inclusion bodies. These HEP and HEP_{3E} were purified using Ni^{2+}-NTA column chromatography under denaturing conditions and renatured by slow dialysis. These purified proteins were shown to be homogeneous preparations that appeared as a single protein band on SDS–PAGE except Jun, where only 30% purity was obtained. The expected bands of HEP, JNK and Jun corresponding to 55, 45 and 15 kDa, respectively are shown in **Figure 3.5 A-C.** The western blot analysis using antiHis antibody was also performed in order to confirm the expression of these histidine fusion MAPK proteins (Data not shown).

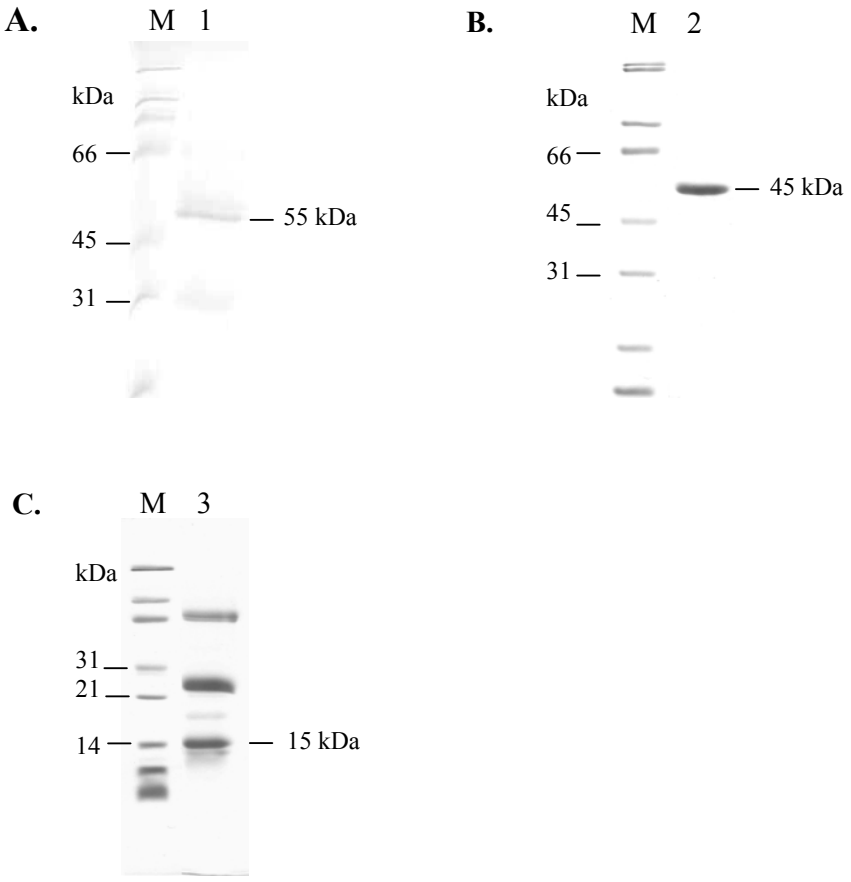

Figure 3.5 The SDS-PAGE of purified *Drosophila* kinase proteins. SDS-polyacrylamide gel demonstrated the purified *Drosophila* kinase proteins from either standard Ni^{2+}-NTA affinity column. The purified proteins are indicated. The size of JNK, HEP, and Jun are 55, 45, and 15 kDa, respectively.

Lane M: Broad-range marker

Lane 1: purified HEP

Lane 2: purified JNK

Lane 3: purified Jun

3.3 Enzyme characterization

3.3.1 GST enzymes

The enzymatic studies included 1) steady-state kinetics with respect to both GSH and CDNB, 2) the inhibition study using different hydrophobic compounds as an inhibitor in the glutathione-CDNB conjugation reaction, 3) inhibition kinetics to ethacrynic acid (EA) and 4) the substrate specificities of various hydrophobic substrates with respect to CDNB.

3.3.1.1 Kinetic constants determination

The characterization of five GSTs, the alternatively spliced products D1-1 to D4-4, and D6-6 have previously been described (32,39), therefore D5-5 was further characterized and compared the enzymatic properties with the known adGSTs. The kinetic parameters were studied by varying the concentration of both GSH and CDNB substrates and were determined from non-linear regression analysis following the Michaelis-Menten reaction. The D5-5 enzyme had an intermediate specific activity in GSH conjugation with the classical GST substrate CDNB. The K_m for GSH was the lowest observed for all six *An. dirus* GSTs **(Table 3.2)** suggesting the highest affinity binding to GSH. An estimated V_{max} of 167 μmol/min/mg and K_m of 14.9 mM are given only for purposes of comparison as the data was collected well below the K_m value due to CDNB solubility limits. The fairly high K_m for CDNB indicated low affinity binding for this substrate.

Table 3.2 Kinetic parameters of *Anopheles dirus* GSTs

GSTs	V_{max} (μmol/min/mg)	k_{cat} (s^{-1})	CDNB		GSH	
			K_m (mM)	k_{cat}/K_m ($mM^{-1}s^{-1}$)	K_m (mM)	k_{cat}/K_m ($mM^{-1}s^{-1}$)
D5-5	**167 ± 48**	**69**	**14.9 ± 4.9**	**5**	**0.21 ± 0.01**	**400**
D1-1	12.9 ± 0.6	5.03	0.10 ± 0.03	48.4	0.86 ± 0.2	5.86
D2-2	63.9 ± 3.50	25.9	0.21 ± 0.03	121	1.30 ± 0.15	20
D3-3	67.5 ± 1.97	26.9	0.10 ± 0.01	269	0.40 ± 0.05	67
D4-4	40.3 ± 1.89	16.9	0.52 ± 0.67	32	0.83 ± 0.08	20
D6-6	2.2 ± 0.3	0.9	5.3 ± 0.8	0.2	1.8 ± 0.4	0.5

The data are means ± standard error for at least three experiments. The data for D1-1, D2-2, D3-3, D4-4 and D6-6 have previously been reported (37,150,151).

3.3.1.2 Inhibition study

A range of compounds previously shown to be GST substrates as well as pyrethroid insecticides were employed as an inhibitor in a standard glutathione-CDNB conjugation assay for all six GSTs. The percent inhibition was determined by comparing between the presence and absence of these compounds. adGSTD5-5 did interact with these substrates as well as pyrethroid insecticides as shown by inhibition of CDNB activity **(Table 3.3)**. Intriguingly, only adGSTD5-5 was inhibited by dichloroacetic acid (DCA) which is the specific substrate for Zeta class GST in dechlorination of DCA to glyoxylic acid (152-156). However, no detectable of dechlorination activity was observed with adGSTD5-5.

Table 3.3 Inhibition study of CDNB activity

Compounds	mM	% Inhibition					
		GSTD5-5	**GSTD1-1**	**GSTD2-2**	**GSTD3-3**	**GSTD4-4**	**GSTD6-6**
Dichloroacetic acid	0.5	**16.84 ± 3.22**	ND	ND	ND	ND	ND
Cumene hydroperoxide	2.5	**37.17 ± 1.19**	30.36 ± 9.53	60.44 ± 2.15	28.94 ± 4.82	29.53 ± 3.77	28.27 ± 2.56
p-Nitrobenzyl chloride	1.0	**33.40 ± 6.07**	43.38 ± 5.17	37.60 ± 3.67	55.36 ± 1.84	49.77 ± 1.35	9.52 ± 1.98
p-Nitrophenyl bromide	0.1	**35.72 ± 1.50**	24.30 ± 14.52	17.28 ± 0.88	33.39 ± 3.78	31.33 ± 3.10	3.17 ± 3.85
Ethacrynic acid	0.1	**84.67 ± 0.71**	100 ± 0	99.57 ± 0.59	98.31 ± 0.10	100 ± 0	86.36 ± 1.65
	0.01	**55.22 ± 0.66**	99.46 ± 1.54	94.88 ± 1.32	81.61 ± 0.76	85.49 ± 1.58	57.73 ± 3.09
	0.001	**40.28 ± 3.16**	81.88 ± 4.14	64.16 ± 3.74	37.95 ± 1.99	46.45 ± 3.39	37.55 ± 1.40
S-hexyl glutathione	0.1	**71.98 ± 1.76**	94.93 ± 0.65	97.08 ± 0.92	67.84 ± 1.10	76.91 ± 0.26	64.14 ± 3.58
	0.01	**24.87 ± 3.93**	63.18 ± 3.21	75.44 ± 0.61	32.07 ± 1.58	20.09 ± 1.24	35.03 ± 2.46
Permethrin	0.01	**35.56 ± 1.68**	20.37 ± 1.90	27.36 ± 5.45	35.87 ± 1.87	47.73 ± 3.08	11.70 ± 1.87
Deltamethrin	0.01	**40.15 ± 2.17**	11.01 ± 7.51	30.72 ± 3.53	35.28 ± 3.05	49.30 ± 2.37	15.87 ± 5.29
λcyhalothrin	0.01	**39.96 ± 1.19**	21.88 ± 10.66	29.11± 2.88	26.38 ± 1.73	40.50 ± 1.40	23.26 ± 5.58

The data are mean ± standard deviation for at least 3 independent experiments. Inhibition assay were performed using a standard GST assay in the presence of 4-NBC, 4-nitrobenzyl chloride; CuCOOH, cumene hydroperoxide; DCNB, 1,2-dichloro-nitrobenzene; 4-NPB, 4-4-nitrophenethyl bromide; deltametrin; permetrin; EA, Ethacrynic acid; S-hexyl glutathione and DCA, dichloroacetic acid. ND is not detectable.

3.3.1.3 Inhibition kinetics study of ethacrynic acid (EA)

Since all six GSTs were strongly inhibited by ethacrynic acid (EA) **(Table 3.3)**, it was thus employed to characterize the mechanism of interaction and the affinity binding (K_i) to these GST enzymes. The GST activities were measured by varying CDNB concentration (0.05-3.0 mM) at a constant saturating concentration of GSH in the absence and presence of a constant concentration of EA at 0.001 mM. The initial rate of reaction was used to construct a double reciprocal plot, $1/V$ versus $1/S$, and the inhibition constant (K_i) was determined from the values of the appropriate intercepts on the axes (157).

The six different isoforms of GSTs displayed various mechanisms of interaction with EA **(Table 3.4)**. A double reciprocal plot, 1/V versus 1/[S] and 1/V versus [I] indicate that all adGST isoenzymes ,except adGSTD3-3, shared the same general mechanism of interaction with EA which are mixed and non-competitive inhibition **(Figure 3.6 and 3.7)**. While adGSTD3-3 selectively displayed a competitive inhibition type **(Figure 3.8)**

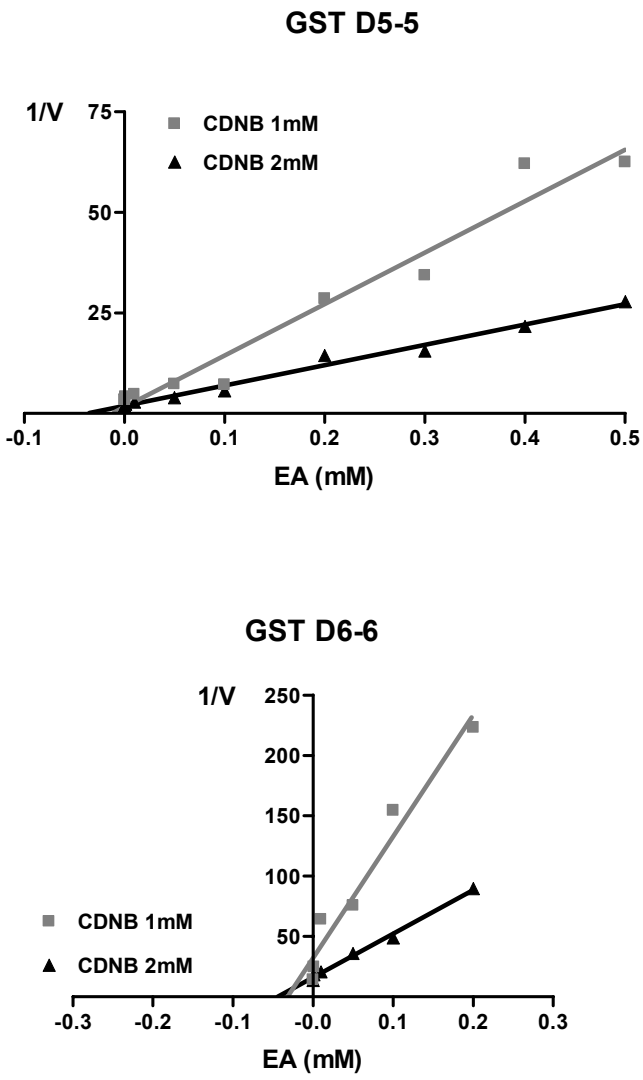

Figure 3.6 Inhibition kinetics of D5-5 and D6-6 with EA. The 1/V versus [I] plot was employed to determined the inhibition type. EA is a mixed inhibitor of GST activity toward CDNB. The experiments were carried out at least three times but the plots are shown from one representative experiment.

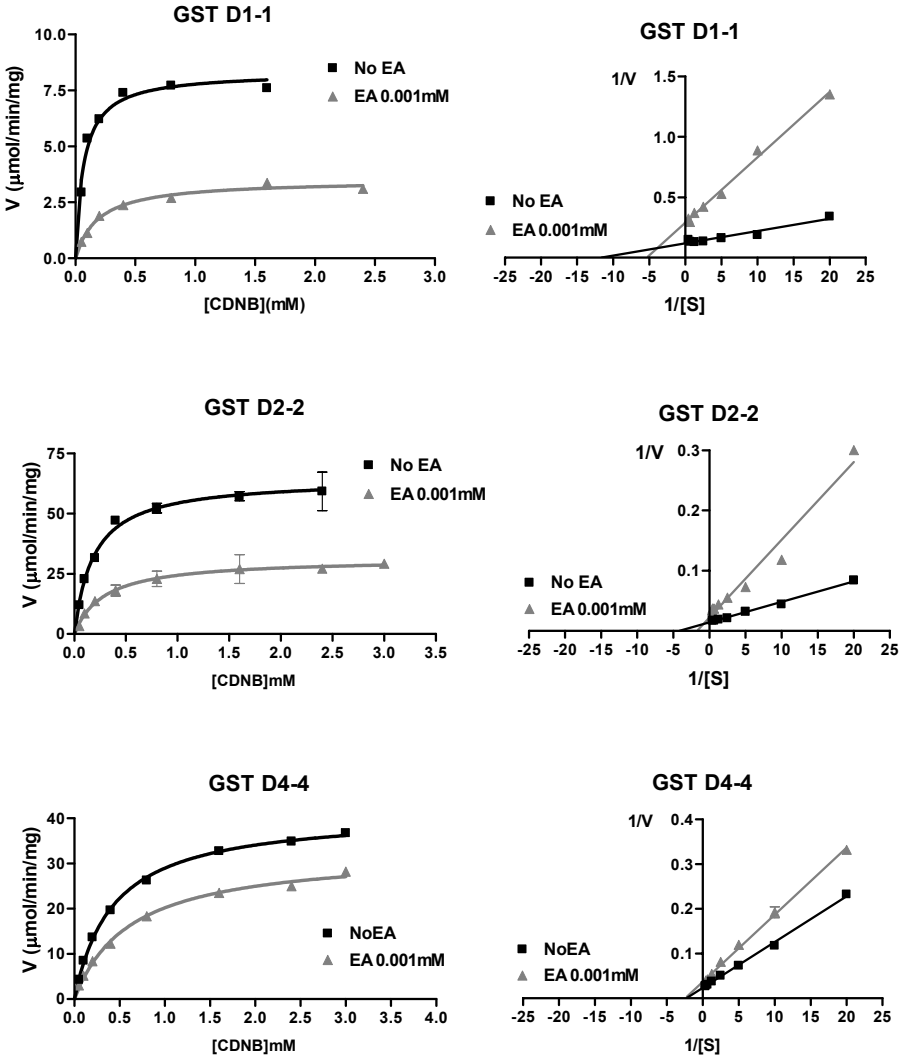

Figure 3.7 Non-competitive inhibition kinetics of GST D1-1, D2-2 and D4-4 with EA. The graph represents Lineweaver-Burk plots of purified D1-1, D2-2 and D4-4 in the absence and presence of EA. The data demonstrate EA as a non-competitive inhibitor of GST activity towards CDNB. The inhibition kinetics was performed in at least three independent experiments.

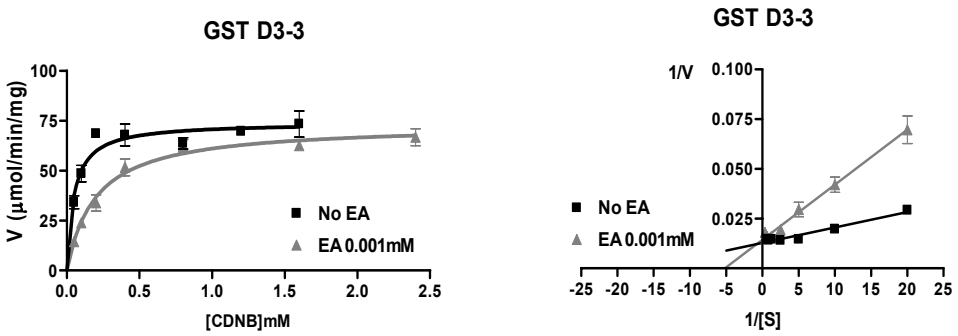

Figure 3.8 Competitive inhibition kinetics of GST D3-3 with EA. The 1/V versus 1/S plot was constructed to determine the inhibition type and affinity binding to EA (K_i). Inhibition kinetics was performed in at least three independent experiments. EA was determined as a competitive inhibitor of GST activity toward CDNB.

Mixed and Non-competitive inhibition

The mixed and non-competitive inhibition indicated that EA binds outside the active site of the GSTs **(Figure 3.6 and 3.7)** reducing enzyme efficiency.

Figure 3.9 The mixed and non-competitive inhibition demonstrated EA principally binds out side the active site.

The distinction can be determined by plotting enzyme activity with and without the inhibitor present. E and EI bind S with different affinities in mixed inhibition, whereas the substrate binding affinity of E and EI remains the same in non-competitive inhibition as described by the following schemes.

Mixed inhibition

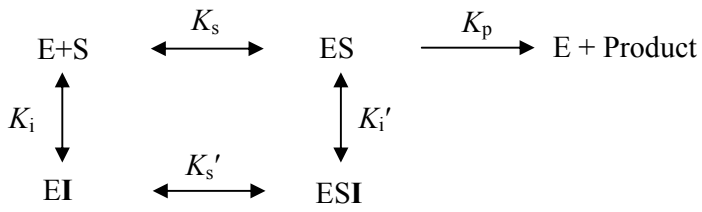

EA (I) can interact with both the enzyme-substrate complex and the free enzyme which affects both V_{max} and K_m of the reaction. According to the 1/V versus 1/S plot, the inhibitor constant (K_i) is calculated from the following equation

$$\text{Y intercept} = \frac{(1 + [I]/K_i')}{V_{max}}$$

$$\text{Slope} = \frac{K_s (1 + [I]/K_i)}{V_{max}}$$

$$K_s = \text{Slope} \times V_{max}$$

Non-competitive Inhibition

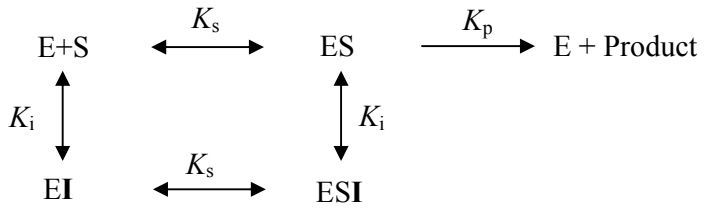

The EA (I) can interact with both the enzyme-substrate complex and the free enzyme but it affects only V_{max} of the reaction, while the same K_m is acquired. According to the 1/V versus 1/S plot, the inhibitor constant (K_i) is calculated from the following equation

$$\text{Y intercept} = \frac{(1 + [I]/K_i)}{V_{max}}$$

$$\text{Slope} = \frac{K_m (1 + [I]/K_i)}{V_{max}}$$

As adGSTD5-5 and adGSTD6-6 possess a high K_m toward CDNB **(Table 3.1)**, the kinetic experiments therefore were performed below substrate saturation of the reaction as a result of the limitation of CDNB solubility, EA kinetics to D5-5 and D6-6 were obtained by varying EA concentration (0.0-0.2 mM) in large excess of the GSH (16 mM) concentration as well as fixing the CDNB concentration at 1 and 2 mM, respectively. The initial rate of reaction was determined to initiate a plot of $1/V$ versus [I] (EA). The inhibition type was evaluated from the appropriate intercepts on the axis (157) as shown by **Figure 3.6**. However, K_i could not be determined by this manner.

Competitive inhibition

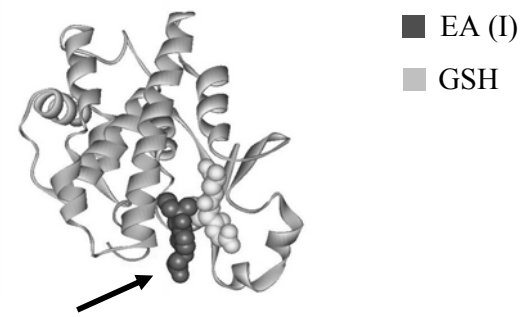

Figure 3.10 The competitive inhibition demonstrated EA principally binds to the active site as shown by the scheme.

$$E+S \rightleftharpoons ES \longrightarrow E+P$$
$$E+\mathbf{I} \rightleftharpoons E\mathbf{I}$$

As shown in the upper scheme, EA (I) and substrate can bind to the active site of the free enzyme **(Figure 3.10)**. In the presence of EA, the higher concentration of the substrates is required in order to achieve the same velocities (V_{max}). Therefore, the higher K_m, while the same value of V_{max} is obtained from this type of inhibition. According to the 1/V versus 1/S plot, the inhibitor constant (K_i) is calculated from the following equation

$$\text{Y intercept} = \frac{1}{V_{max}}$$

$$\text{Slope} = \frac{K_m (1 + [I]/K_i)}{V_{max}}$$

Table 3.4 Mechanism of ethacrynic acid and adGSTs interaction

GSTs	Inhibition type	K_i (μM)
D5-5	**Mixed**	**Not determined**
D1-1	Non-Competitive	0.607 ± 0.09
D2-2	Non-Competitive	0.567 ± 0.32
D3-3	Competitive	0.266 ± 0.04
D4-4	Non-competitive	1.690 ± 0.47
D6-6	Mixed	Not determined

The data are means ± standard deviation from at least three experiments. The affinity binding (K_i) of EA for adGSTD5-5 and adGSTD6-6 could not be determined, because the GSH-CDNB conjugating assay could not reach the maximum velocity or V_{max} of the reaction owing to the limitation of CDNB solubility.

The K_i values of the four alternatives splice GST enzymes for EA with respect to CDNB indicates a very high affinity binding in the micromolar range. Especially, the spliceforms of adGSTD3-3 and adGSTD4-4 which possess differences in affinity binding up to 6 fold as well as in the mechanism of interaction to EA. These data suggest the amino acid contribution at the C-terminus affects the binding site topology which is directly involved in the binding of EA compounds.

3.3.1.4 Specific activity using various hydrophobic substrates

The specific activities of each delta GST spliceform adGSTD1-1 to D4-4 were determined for the substrates CDNB, DCNB, PNBC and PNPB. The results are presented in **Table 3.5**. The data illustrate the striking differences in enzymatic properties among these four GSTs. For example, 10-fold differences in specific activity are noted for the CDNB substrate. Likewise 8-fold differences for DCNB, 17-fold differences for PNBC substrate, and greater than 20-fold differences for PNPB are noted. These differences must arise from the differences in amino acids at the C-terminus. These C-terminal residues contribute to the H-site and have been shown to determine substrate specificity for different compounds within each class and amongst different classes (148,149,158). However, our study of a range of these compounds revealed that there was no detectable activity of adGSTD5-5 as well as adGSTD6-6 with these known GST substrates even at 10-fold the enzyme concentration used in the CDNB assay.

Table 3.5 Specific activity of GST spliceforms using various hydrophobic substrates

GSTs	Specific activity (μmol/min/mg of protein)			
	CDNB	**DCNB**	**PNBC**	**PNPB**
D1-1	6.54 ± 0.53	0.070 ± 0.002	1.049 ± 0.191	0.002 ± 0.002
D2-2	45.14 ± 3.41	0.177 ± 0.006	17.07 ± 1.088	0.047 ± 0.010
D3-3	67.5±1.97	0.312 ± 0.023	2.963 ± 0.292	0.002 ± 0.007
D4-4	41.84 ± 1.40	0.042 ± 0.011	2.726 ± 0.105	0.023 ± 0.002

The data are means ± standard error for at least five separate assays. The substrate concentrations used were: CDNB 1 mM; DCNB 1 mM; *p*-nitrobenzyl chloride (PNBC) 1.2 mM and *p*-nitrophenyl bromide (PNPB) 0.1 mM.

3.3.2 JNK enzyme

The *Drosophila* JNK pathway commonly contains HEP, JNK and Jun (124). Activation of JNK can be achieved by phosphorylation of HEP, which further phosphorylated the downstream target, Jun (104). The *in vitro* kinase assay contained constitutively active HEP (HEP_{3E}), JNK and Jun. Therefore, the reaction was prompted by HEP phosphorylation of JNK and activated JNK phosphorylation of Jun, respectively. The time course of HEP and JNK phosphorylation was performed in order to optimize the kinase condition at a physiological condition where the substrate concentration is in large excess of the enzyme concentration, i.e. **[S] » [E]**. Experiments were therefore performed using HEP_{3E}: JNK: Jun in the molar ratio of 1: 10: 40. **Figure 3.11** depicts the curves of product formation as a function of time. At 25 minutes is the optimal time for the HEP and JNK assay as indicated by JNK and Jun phosphorylation.

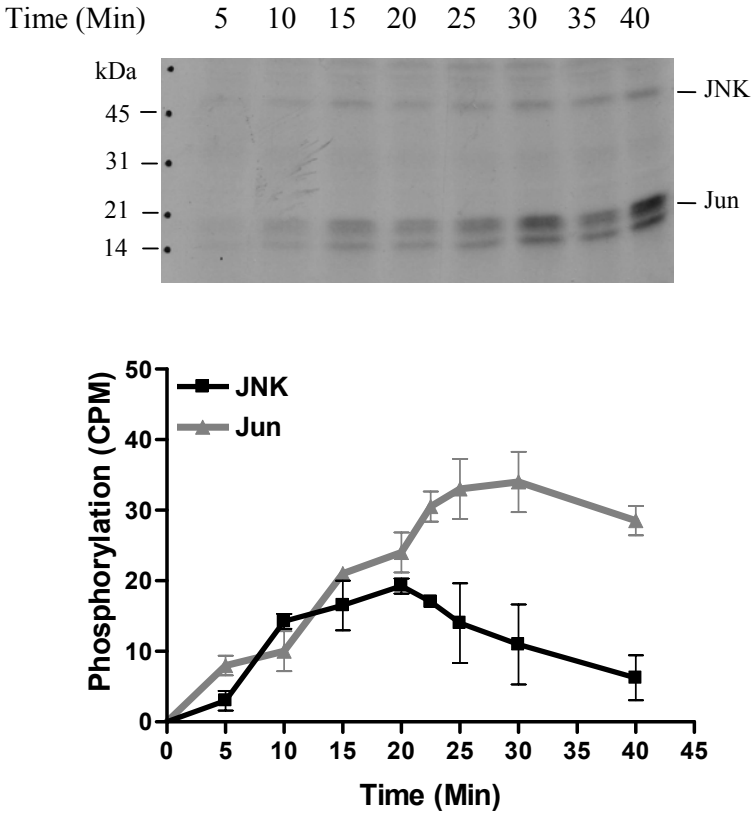

Figure 3.11 Time course of kinase phosphorylation. The experiment was performed by incubating HEP_{3E}: JNK: Jun in the molar ratio of 1:10:40 with 3 μCi of [γ-^{32}P] ATP and phosphorylation time varied from 0-40 minutes at room temperature. Proteins were then separated by SDS-PAGE, and kinase activity was visualized by autoradiography of the ^{32}P-labeled substrates. The Jun protein was a substrate for JNK as well as JNK was a substrate for HEP (103). **(A)** The autoradiograph of JNK and Jun phosphorylation. **(B)** The graph shows JNK and Jun phosphorylation at different time points. The figures shown are representative of at least three independent experiments.

3.4 Characterization of the GST and Kinase proteins interaction

3.4.1 JNK and HEP can inhibit the activity of delta GSTs

Previous studies have shown that GSTs of the mammalian pi and mu classes are capable of modulating the JNK pathway through their inhibition of JNK and interaction with ASK, respectively (86). This study has evaluated whether GSTs of the *Dipteran* delta class can interact with two kinases from *Drosophila,* either JNK or its upstream activating kinase HEP, by measuring both the effects of the kinases on GST activity and the effects of the GSTs on kinase activity. Previously a comprehensive study of six GST isoforms yielded estimates of total GST concentrations in eukaryotic cells, depending on tissue type, ranging from 0.1 to 1.4 nmol GST per mg of total soluble protein (24). From our laboratory data, *Drosophila* SL2 cells were estimated to contain 66 pg soluble protein/cell. Assuming a tissue culture cell volume of 1 pL (159), a total GST cell concentration of 7 to 90 μM can be estimated. A single MAPK protein has been estimated to have cellular concentrations of 1 to 3 μM (159). In *Anopheles gambiae* it has been reported that there are a possible 32 different soluble GST encoding transcripts with 31 being found in the adult mosquito (34). This is similar to the number of 37 putative GST genes identified in *Drosophila* (34). It was also shown that depending on specific tissue/cell type a single GST isoform could vary between 0.15 to 45 μM (24). However, these concentration determinations do not address the issue of compartmental localization known to be important in controlling message propagation in signal transduction pathways. We therefore chose an intermediate concentration range and used a 1:1 ratio for the GST: JNK experiments. We began with an evaluation of the effects of JNK and HEP on the activity of six delta GSTs. As shown in **Table 3.6**, GST activities as assessed using the standard CDNB assay were decreased in the presence of a 1:1 molar concentration of HEP. The activities of the GST spliceforms D1-1 and D2-2 were the greatest affected, but even the inhibition of GST D3-3 and D4-4 were greater than 20%. A parallel series of experiments in which JNK was incubated with each delta GST also showed that JNK could inhibit the activity of GST D2-2, D3-3, D4-4, D5-5 and D6-6 towards CDNB. However, under these assay conditions, no inhibition of GST D1-1 activity could be observed **(Table 3.6)**. The differences in the

effects of the HEP and JNK on the activities of the GST would appear to be the result of different interactions with the different amino acids in the C-terminus of each GST particularly GST spliceforms that contain the same 45 amino acids at the N-terminal region.

TABLE 3.6 The HEP and JNK proteins effect on the GST activity

GSTs	Inhibition of GSTs by HEP (%)	Inhibition of GSTs by JNK (%)
D1-1	54.64 ± 3.83	No inhibition detected
D2-2	53.29 ± 7.71	85.35 ± 6.72
D3-3	23.71 ± 1.88	44.64 ± 6.92
D4-4	29.27 ± 2.99	68.45 ± 4.00
D5-5	22.85 ± 1.26	16.75 ± 1.49
D6-6	21.62 ± 3.67	19.07 ± 1.81

The recombinant proteins of HEP and JNK were incubated with the different GST spliceforms in 1:1 molar ratio for 5 min at room temperature. The % inhibition of GST activity was calculated using reaction that contained no kinase proteins as the control. No inhibition of GST activity of GST D1-1 by JNK protein was detected. The data are mean ± standard deviation from at least four independent experiments

3.4.2 The mechanism of GST inhibition by HEP and JNK

A more detailed kinetics study of inhibition was undertaken to yield data on the affinity of binding (K_i) and the mechanism of interaction for the four GST spliceforms and the kinases HEP and JNK **(Table 3.7)**. With the exception of the JNK and GST D1-1 which showed no inhibition of GST activity, the inhibition of the GST spliceforms by JNK or by HEP was non-competitive with respect to its substrate CDNB. This indicated the interaction with each kinase did not block the GST active site despite inhibiting its transferase activity. The inhibition type for the four GSTs and the kinases HEP and JNK was evaluated from the appropriate intercepts on the axis (157) as shown by **Figure 3.12** and **3.13**, respectively. This interaction was also of high affinity with estimates of K_i in the range of 20-70 nM for GST D1-1, D2-2 and D3-3 **(Table 3.7)**. For GST D4-4, the K_i values were higher, being in the range of 100-200 nM, however all of these interactions were approximately three to four orders of magnitude greater affinity than the interactions of GSTs with glutathione (37). Furthermore, this data shows that HEP interacts with all GST delta spliceforms tested. JNK also interacts with GST D2-2, D3-3 and D4-4, but it was not possible to observe an interaction of JNK with GST D1-1 in this experiment.

TABLE 3.7 Mechanism of GST and kinase proteins interaction

GSTs	Inhibition Type	K_i (nM) HEP-GST	K_i (nM) JNK-GST
D1-1	Non-competitive	49.993 ± 2.844	Not determined
D2-2	Non-competitive	21.338 ± 5.180	73.918 ± 20.116
D3-3	Non-competitive	43.642 ± 7.188	76.777 ± 15.443
D4-4	Non-competitive	125.204 ± 45.152	218.114 ± 86.287

The type of inhibition and affinity binding (K_i) of GST and kinase proteins interaction were performed by varying concentration of CDNB from 0.05 to 3.0 and measuring kinetic parameters under the standard assay of each GSTs enzyme The data are means ± standard error for at least four independent experiments.

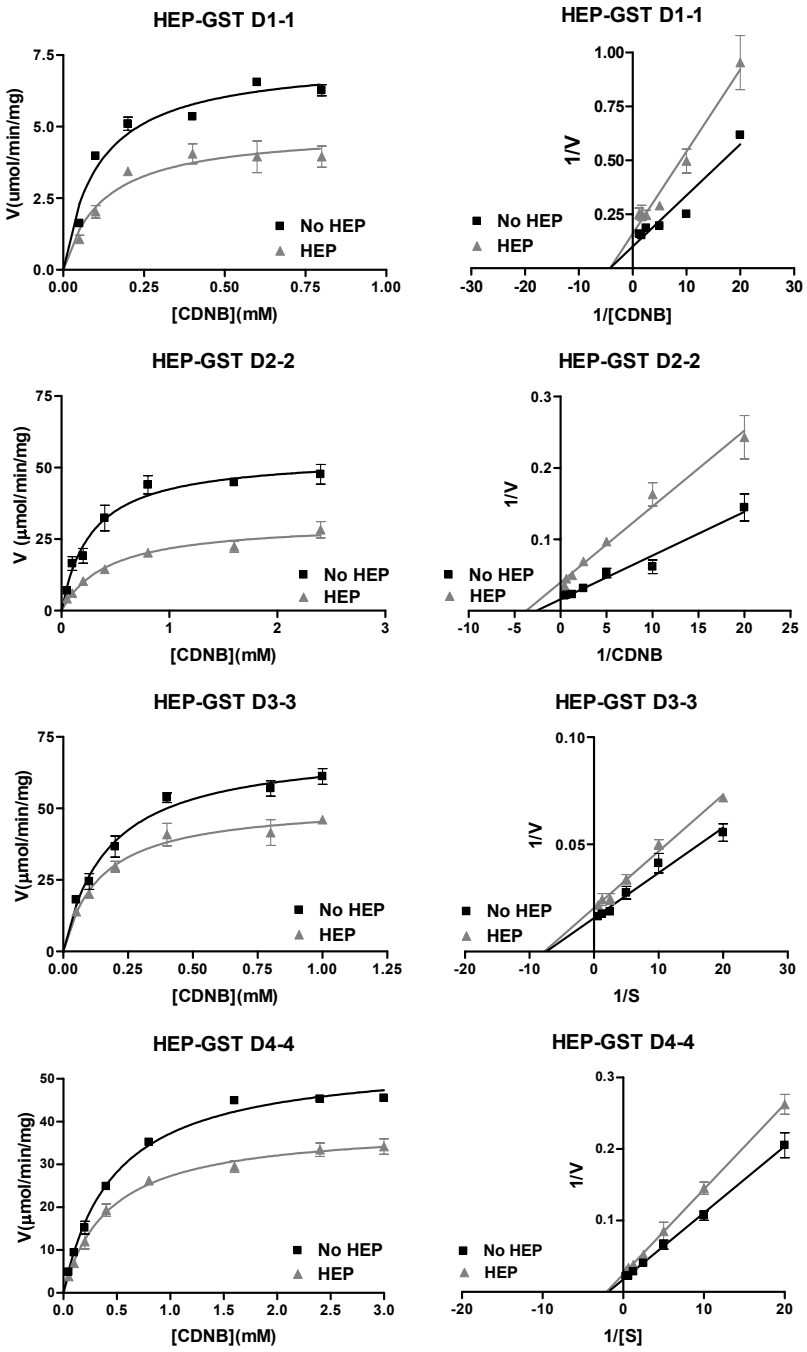

Figure 3.12 The mechanism of HEP interaction with GST. The V versus S and Lineweaver-Burk plots of purified four GST spliceforms in the absence and presence of the kinase HEP protein indicated HEP is a non-competitive inhibitor of GST activity towards CDNB. The experiments were performed at least three times.

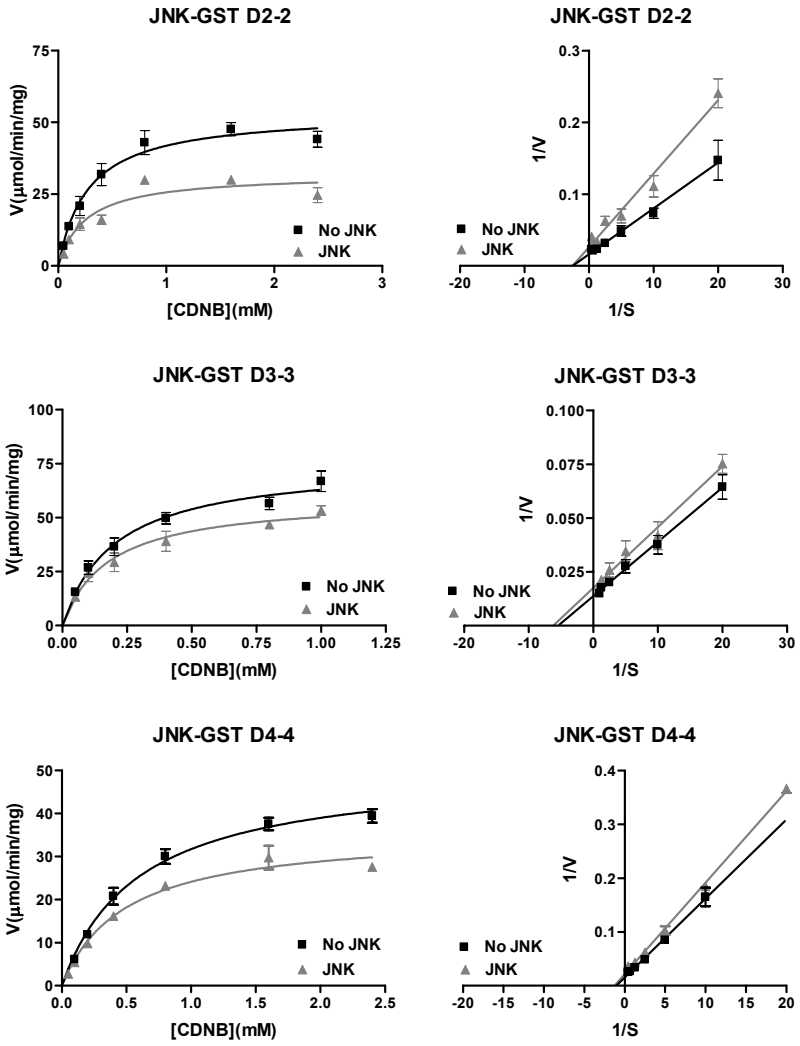

Figure 3.13 The mechanism of JNK interaction with GST. The V versus S and Lineweaver-Burk plots of purified four GST spliceforms in the absence and presence of the kinase JNK protein indicated JNK is a non-competitive inhibitor of GST activity towards CDNB. The experiments were performed at least three times.

3.4.3 The JNK affected GST substrate specificity

The study next evaluated whether JNK changed the substrate specificity of the delta GST spliceforms. The changes in GST substrate specificity upon incubation with JNK are shown in **Figure 3.14**. Some striking differences were observed. For example, GST D1-1 activity toward CDNB was not influenced when incubated in the presence of JNK, nonetheless it was dramatically increased (approximately 3,000 folds increase of GST activity) towards PNPB. Likewise, incubation with JNK increased GST D2-2 activity using PNBC and PNPB whereas it was decreased using other substrates. Both D3-3 and D4-4 displayed an increase in activity towards PNPB, however the activities were decreased toward other substrates. These data suggest the JNK interaction provokes a set of different conformational changes in each GST, thus affecting the active site topologies by changes in hydrophobicity and size through residue movement (160), in a dissimilar manner.

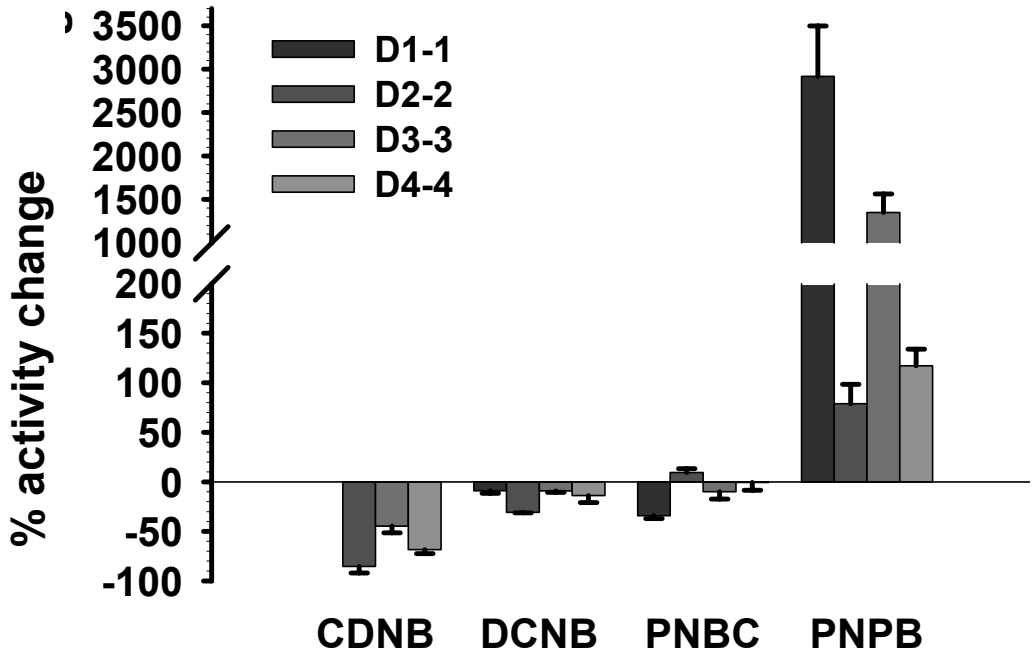

Figure 3.14 The JNK changes substrate specificity of GSTs. GST and JNK were incubated in 1:1 molar ratio for 5 min at room temperature. The GST activity was measured using various hydrophobic co-substrates. The % activity changes of GSTs were determined comparing between reactions in the presence and absence of JNK which is represented in the histogram graph. The zero line represents the reaction without JNK incubation. The positive and negative data determine the increase and decrease of GSTs activity in the presence of JNK. The specific activity of GSTs in the absence of JNK was shown in **Table 3.5**. There was no % activity change in adGSTD1-1 using CDNB as the co-substrate due to a lack of JNK affect **(Table 3.6)**. The data shown are the result of at least four independent experiments.

3.4.4 Modulation of Protein Kinase Activity in the Presence of GSTs

The next study tested the reciprocal regulation of six delta GSTs on protein kinase activity by assessing JNK activity towards its physiological substrate Jun. As shown in Figure 3.15, adGSTD1-1 inhibited the ability of JNK to phosphorylate Jun by approximately 50%. In contrast the inclusion of adGSTD2-2, D3-3, or D4-4 increased JNK activity by up to 170%. Thus, despite JNK not inhibiting adGSTD1-1 activity towards CDNB **(Table 3.6)**, adGSTD1-1 was able to inhibit JNK activity towards Jun **(Figure 3.15)**. We next repeated these protein kinase assays, but without the inclusion of the Jun substrate protein. In this way, we could assess the actions of the GST delta spliceforms on both HEP_{3E} and JNK activity using the ability of HEP_{3E} to phosphorylate JNK as well as the ability of JNK to phosphorylate HEP_{3E} (104). As shown in **Figure 3.16**, the incubation of JNK alone did not result in its significant autophosphorylation. Similarly prolonged incubation of HEP_{3E} alone did not result in its significant autophosphorylation (data not shown). The inclusion of HEP_{3E} with JNK resulted in weak phosphorylation of both HEP_{3E} and JNK proteins. When the GST delta spliceforms were also included, the most striking differences were noted with GST D2-2 and GST D3-3 which increased the phosphorylation of both HEP_{3E} and JNK proteins up to 6-fold. Furthermore, GST D1-1 and D4-4 appeared to inhibit the phosphorylation of HEP_{3E} whilst not inhibiting the phosphorylation of JNK. These results therefore show that GSTs can affect the activities of both JNK towards HEP_{3E} and HEP_{3E} towards JNK. As a result of the different effects of GSTD4-4 on JNK activity using different substrates of HEP and Jun as shown by an increased phosphorylation of Jun **(Figure 3.15)** and a decreased phosphorylation of HEP **(Figure 3.16)**, we suggest the GSTs such as D4-4 may contribute to a change of JNK substrate selectivity. They also show that GSTs were not JNK substrates because no phosphorylated GST protein was observed even upon prolonged exposure of the autoradiographs. This is consistent with these GST proteins lacking a consensus phosphorylation site for MAPKs, namely S/TP or PXS/TP (113).

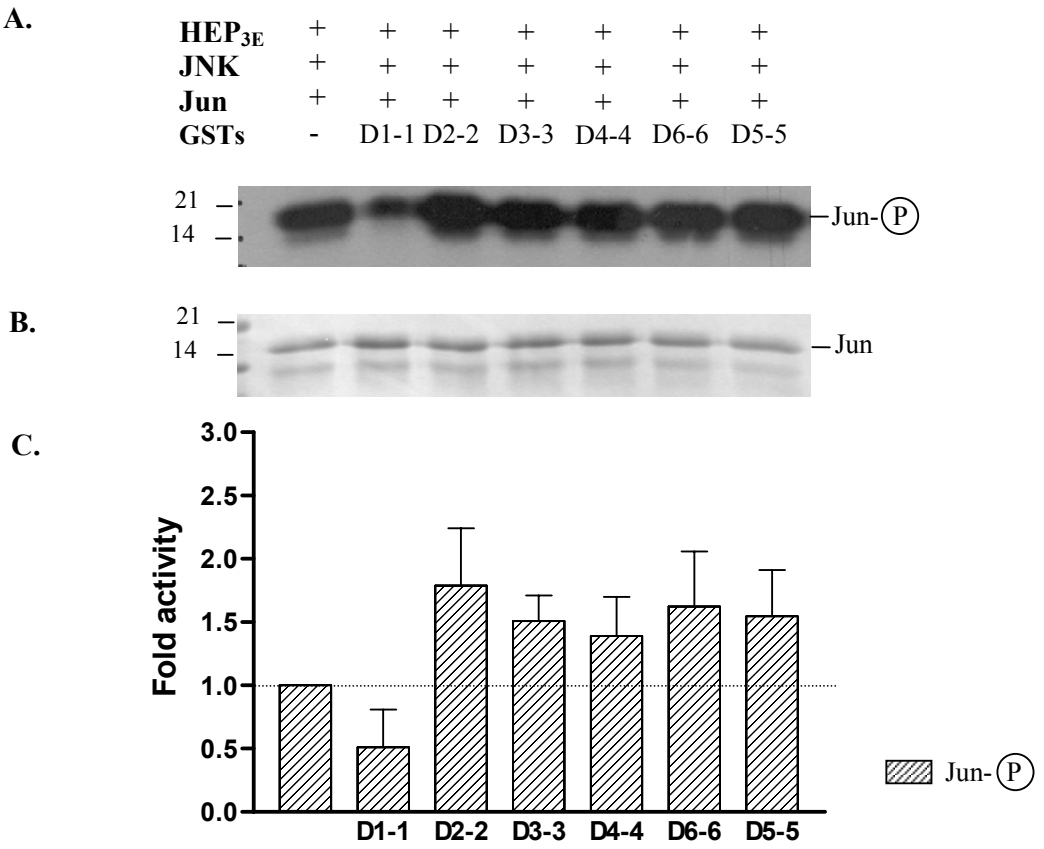

Figure 3.15 The GSTs modulated JNK activity. The GSTs modulated JNK phosphorylation of Jun. The experiment was performed using GST: HEP_{3E}: JNK: Jun in 10:1:2:10 molar ratio. GST was incubated with constitutively active HEP_{3E} for 10 min at room temperature before adding JNK and Jun with 3 μCi of [γ-^{32}P] ATP for 25 min of phosphorylation time at room temperature. Proteins were then separated by SDS-PAGE **(B)**, and JNK activity was visualized by autoradiography of the ^{32}P-labeled Jun **(A)**. The autoradiograph represented Jun phosphorylation in the presence and absence of different GST isoforms. The histogram quantitates in fold activity the GSTs effect on Jun phosphorylation compared to the reaction without GSTs **(C)**. The experiment was repeated at least three times with similar results.

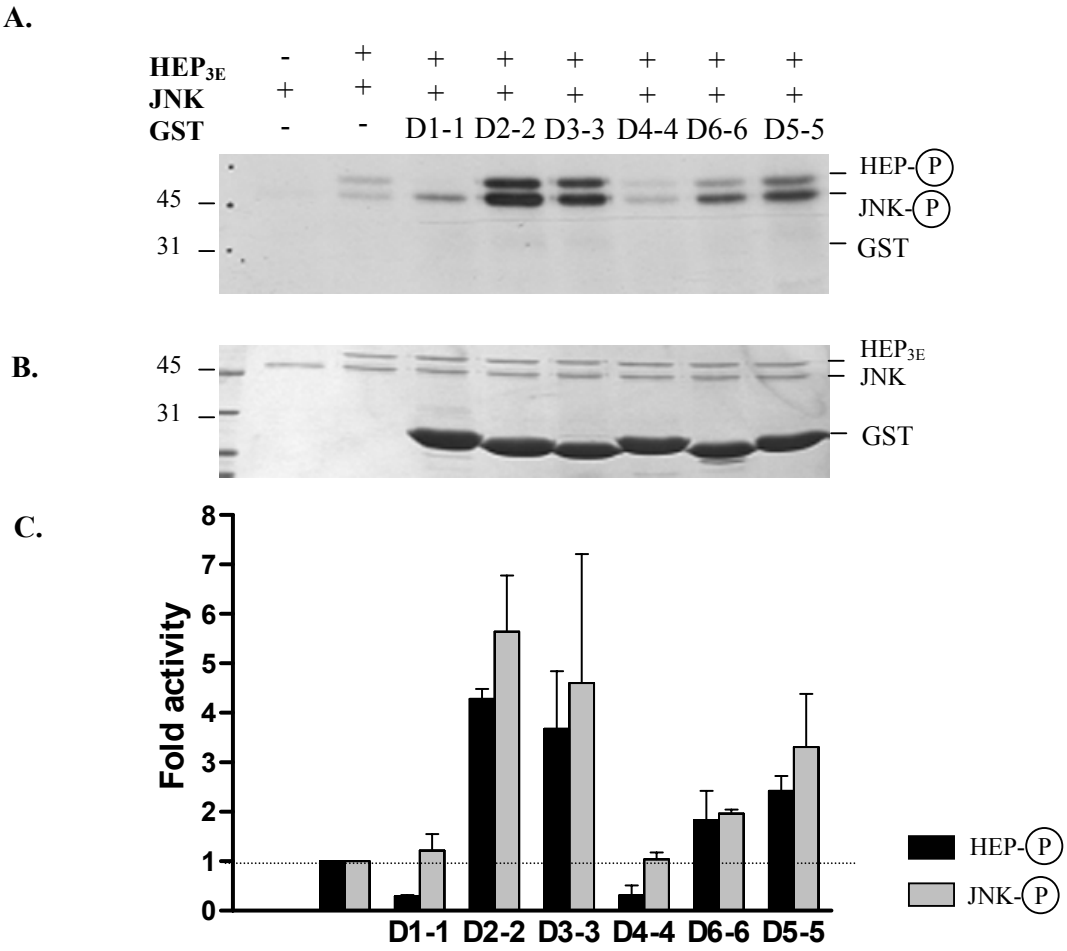

Figure 3.16 The GSTs distinctly modulated kinase activity. The experiment was performed using GST: HEP_{3E}: JNK in 10:1:2 molar ratio. GST was incubated with constitutively active HEP_{3E} for 10 min at room temperature before adding JNK with 3 μCi of [γ-^{32}P] ATP for 25 min of phosphorylation time at room temperature. Proteins were then separated by SDS-PAGE **(B)**, and kinase activity was visualized by autoradiography of the ^{32}P-labeled substrates. The JNK protein was a substrate for HEP as well as HEP was a substrate for JNK (103). The autoradiograph shows HEP and JNK phosphorylation in the presence and absence of different GST isoforms **(A)**. The histogram quantitates in fold activity the GSTs effect on HEP and JNK phosphorylation **(C)**. The figures shown are representative of at least three independent experiments.

3.4.5 The JNK interaction affected GST structure

One key mechanism for regulating a protein function is tight control of its stability. JNK association with its downstream targets (e.g., c-Jun, ATF2, p53) plays an important role in stabilizing these proteins by protecting them from ubiquitination and degradation after phosphorylation by JNK (161-163). Therefore, we have elucidated the effects of JNK-GST interaction on GST stability and activity. It appeared that adGSTD1-1 activity, even though, was not inhibited by JNK, it was stabilized by JNK **(Figure 3.17 A)** suggesting there was interaction between adGSTD1-1 and JNK. In contrast, adGSTD2-2 activity was not shown significantly stabilized by JNK **(Figure 3.17 B)**. These data indicated the interaction with JNK induced GST conformational changes variously, which have an effect on both GST structural and catalytic properties. As adGSTD1-1 and D2-2 are alternative splice products sharing the first 45 amino acids of the N-terminus, the differences in GST-JNK interaction is therefore modulated through the variation of the C-terminal amino acid sequences.

A.

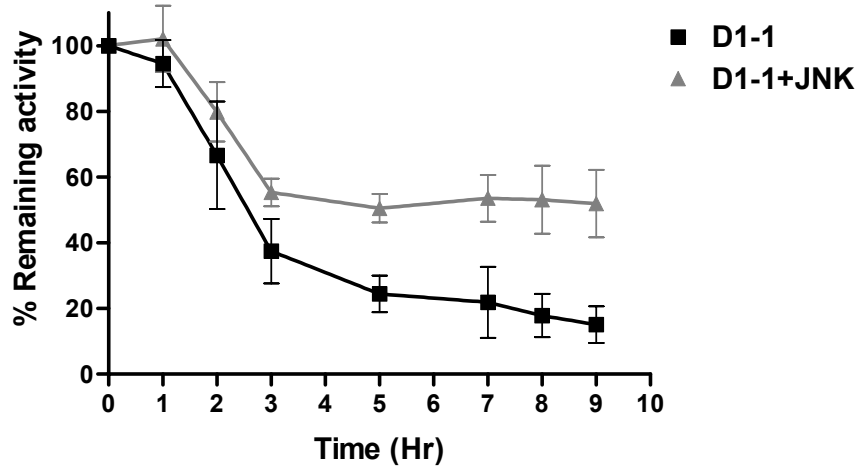

B.

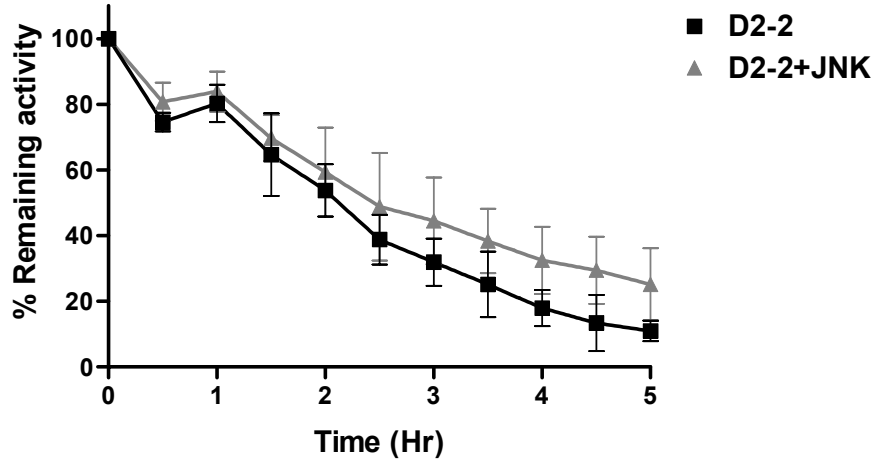

Figure 3.17 The GST stabilized by JNK protein. (A) adGSTD1-1 **(B)** adGSTD2-2 The JNK stabilization of GST was performed by incubating GST and JNK in 1:1 molar ratio and measuring the % remaining GST activity for the time course of incubation for 0-9 hrs at room temperature. The reactions in the absence of JNK were utilized as the control. The experiments were performed at least three times.

3.4.6 GST structure affects on the GST-JNK interaction

To elucidate the importance of GST residues that effect the interaction with JNK, several amino acid positions from adGSTD3-3 and D4-4 were changed to alanine. These included G-site residues (Leu-33, His-38, His-50, Ser-65, Arg-66, Met-101 and Val-107), H-site residues (Tyr-111, Tyr-119 and Phe-123) as well as a non-active site residue (Leu-103) **(Figure 3.18)**. Leu-33, His-38 and His-50 interact with glycine while Ser-65, Arg-66 and Met-101 (D3-3), corresponding to Val-107 (D4-4), interact with the carboxylic group of glutamic acid of GSH in the G-site. In addition, Met-101 (D3-3) or Val-107 (D4-4) contributes to the hydrophobic substrate binding in the H-site. Leu-103, although located outside the active site, significantly affects the GST active site through H-bond and Val der Waal contacts with six residues in the G-site (65). Previous work illustrated that changing amino acids in adGSTD3-3 as well as adGSTD4-4 at these residue positions affect both catalytic and structural properties of GST as demonstrated by altering enzyme kinetic parameters, for example V_{max}, K_m as well as enzyme half-life ($T_{1/2}$) (65,66,143). These positions were therefore of interest for further studies to determine whether they are involved in the interaction with JNK. adGSTD3-3 and D4-4 were employed for these studies, because their crystal structures are available (36). In addition, their properties of high enzymatic activities and great purification yields were exceedingly perfect for performing experiments.

Figure 3.19 demonstrated that the Arg-66-Ala mutant was not inhibited by JNK whereas Ser-65-Ala and Met-101-Ala mutants had nearly the same % JNK inhibition of GST activity as the adGSTD3-3 wild type. All adGSTD4-4 mutants, except Leu-103-Ala, were inhibited by JNK differently compared to the wild type enzyme. Interestingly, the Leu-103-Ala mutant was not inhibited by JNK. This data suggests many GST residues, in particular Arg-66 and Leu-103, impacted on the interaction with JNK. The differences of the enzyme half-life ($T_{1/2}$) between Arg-66-Ala (145.7 ± 10.5 min) and adGSTD3-3 (2.33 ± 0.12 min) (66) as well as Leu-103-Ala (0.25 ± 0.01) and adGSTD4-4 (12.9 ± 1.5 min) (65) was 60-70 fold compared to the respective wild type enzyme. This data revealed that a GST structural alteration occurred. These data suggest a structural change in GST induced by an amino acid

replacement at position 66 (D3-3) or position 103 (D4-4) impacts on the interaction with JNK.

To confirm whether GST residues can have a structural effect on GST and JNK interaction, several mutants of Arg-66-Ala, Leu-103-Ala, Met-101-Ala (D3-3); Val-107-Ala (D4-4) were reciprocally employed to study the effect of GST mutants on JNK activity. The result showed substitution at residue Leu-103 significantly decreased JNK activity to 50% whereas the remaining GST mutants of Arg-66-Ala and Met-101-Ala (D3-3); Val-107-Ala (D4-4) had nearly no effect compared to the GST wild type **(Figure 3.20)**. This data suggests structural changes induced by amino acid substitution at Leu-103 position disturbed the GST and JNK interaction. Moreover, similar effects between the equivalent residues of Met-101-Ala (D3-3) and Val-107-Ala (D4-4) in reciprocal studies of GST-JNK interaction **(Figure 3.19 and 3.20)** demonstrated a close relationship between these two GST spliceforms.

A.

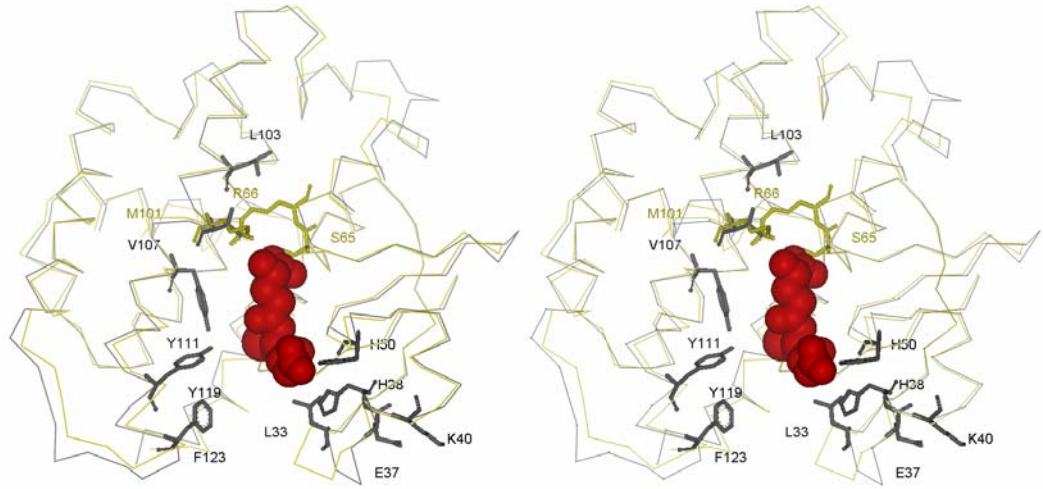

B.

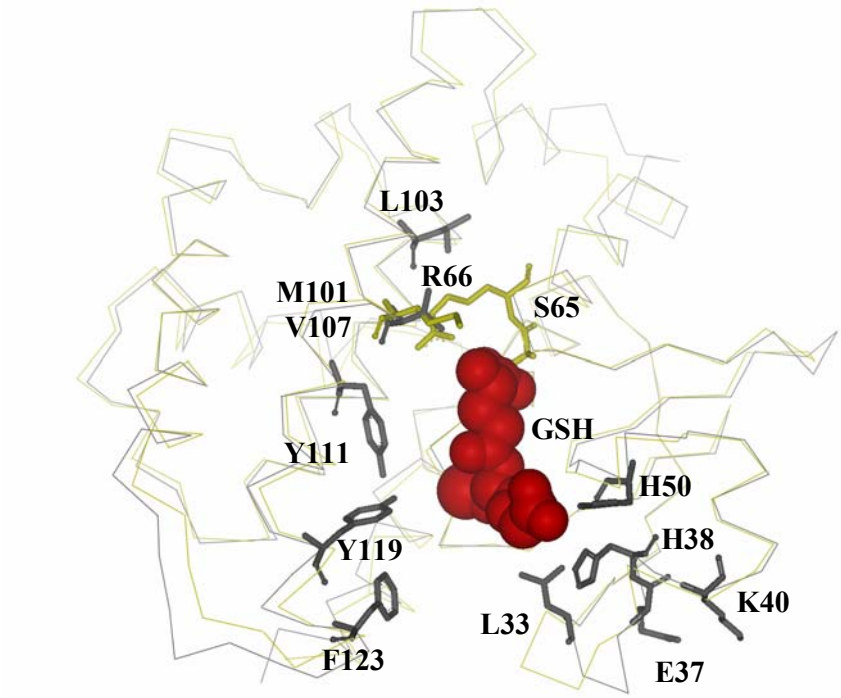

Figure 3.18 The GST residues surrounding Glutathione. (A) Stereo view and **(B)** the front view of the adGSTD3-3 and D4-4 mutant positions. All mutated residues are shown in stick form. The green color represents adGSTD3-3 and the gray color represents adGSTD4-4. The red CPK module represents the glutathione molecule.

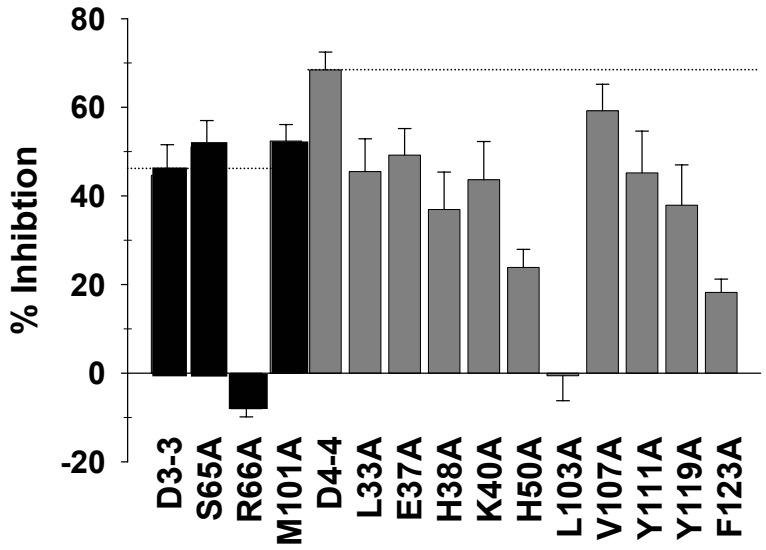

Figure 3.19 Study of the GST structure impacts on JNK interaction as shown by JNK affects on GST activity. Alanine mutants of active site residues were utilized to study the GST activity affected by JNK. The experiments was performed using GST and JNK in 1:1 molar ratio incubated for 5 min at room temperature and measure the % JNK inhibition of GST compared to adGSTD3-3 and D4-4 wild type. The % JNK inhibition of GST was represented by histogram with experiments repeated at least three times.

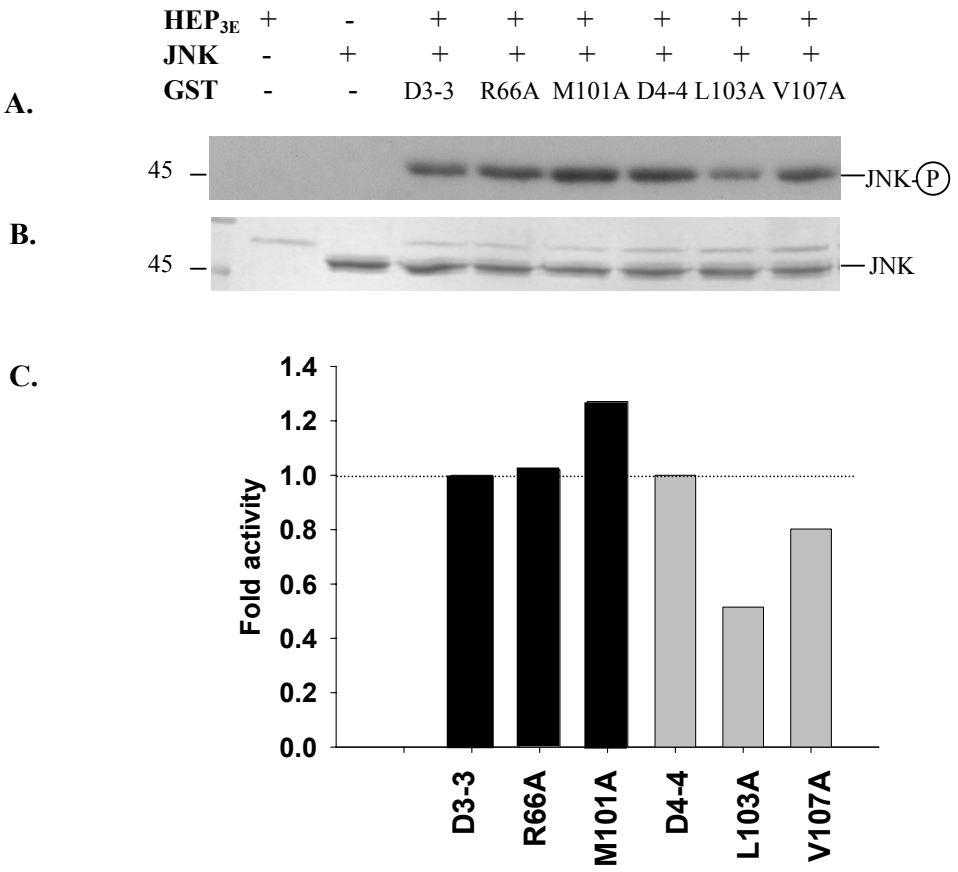

Figure 3.20 Study of the GST structure impacting on JNK interaction as shown by GST affects on JNK activity. The experiments were performed using GST mutant: HEP_{3E}: JNK: Jun in 10:1:2:10 molar ratio with 3 μCi of [γ-^{32}P] ATP for 25 min of phosphorylation time at room temperature. **(A)** The autoradiograph shows JNK phosphorylation in the presence and absence of GST enzymes including GST wild type and mutants. **(B)** The SDS-PAGE represents the equal amount of JNK protein in each lane. **(C)** The histogram quantitated in fold activity the effect of GSTs on JNK phosphorylation compared to the reaction without GSTs. Each experiment was repeated at least three times with similar results.

3.4.7 The effect of glutathione on GST and JNK interaction

Under normal cellular conditions, intracellular GSH concentrations are thought to be in the range 1-10 mM. At these concentrations, GSH would usually be bound in the GST active site (46), and therefore we evaluated whether the presence of GSH would alter the effects of GSTs on JNK activities. In the presence of 2 mM GSH, JNK had different effects on the Delta GST spliceforms, adGSTD1-1 and adGSTD2-2, for the GST substrates, CDNB, DCNB, PNBC and PNPB **(Figure 3.21)**. Specifically, when activities of the adGSTD1-1 and adGSTD2-2 spliceforms were assessed following preincubation in the absence **(Figure 3.21 A)** and presence **(Figure 3.21 B)** of glutathione, the most striking differences were noted for activities towards the CDNB substrate. adGSTD1-1 was now activated by JNK and adGSTD2-2 was also activated rather than inhibited **(Figure 3.21 B)**. Furthermore, GSH also affected JNK activity by inducing a 3.5-fold increase in JNK autophosphorylation **(Figure 3.22)** whilst attenuating Jun phosphorylation **(Figure 3.23)**. These data suggests the GSH binding in the active site of GST allow GST induce-fit conformational changes that directly effect on GST-JNK interaction.

A.

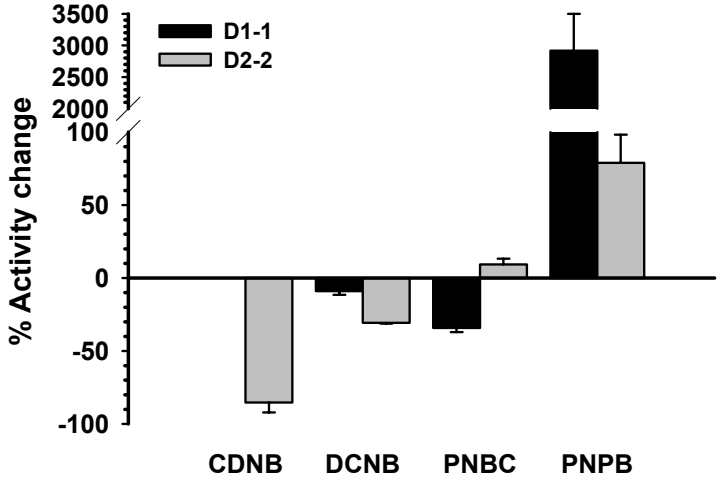

B.

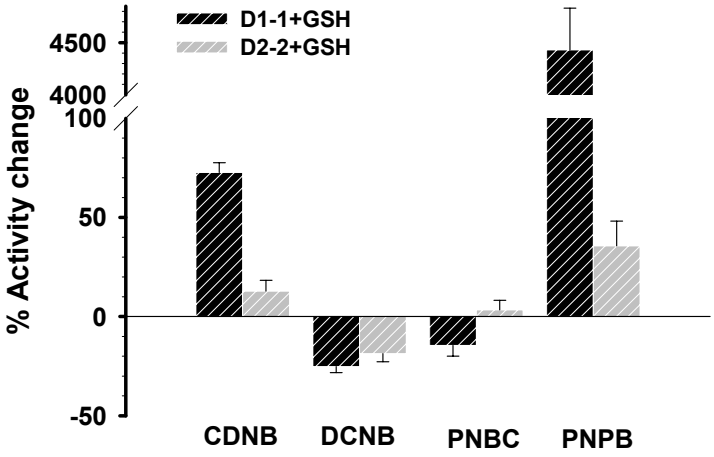

Figure 3.21 The impact of GSH on JNK affects on GST activity. The % activity change of GST affected by JNK was determined compared between reactions in the presence and absence of GSH. **(A)** The upper panel represents the specific activity of GSTD1-1 and D2-2 affected by JNK and was employed for comparison with the reaction containing GSH, shown in **(B)** the lower panel**.** GST and JNK were incubated in 1:1 molar ratio in the presence and absence of 2 mM GSH for 5 min at room temperature. The GST activity was measured using various hydrophobic co-substrates.

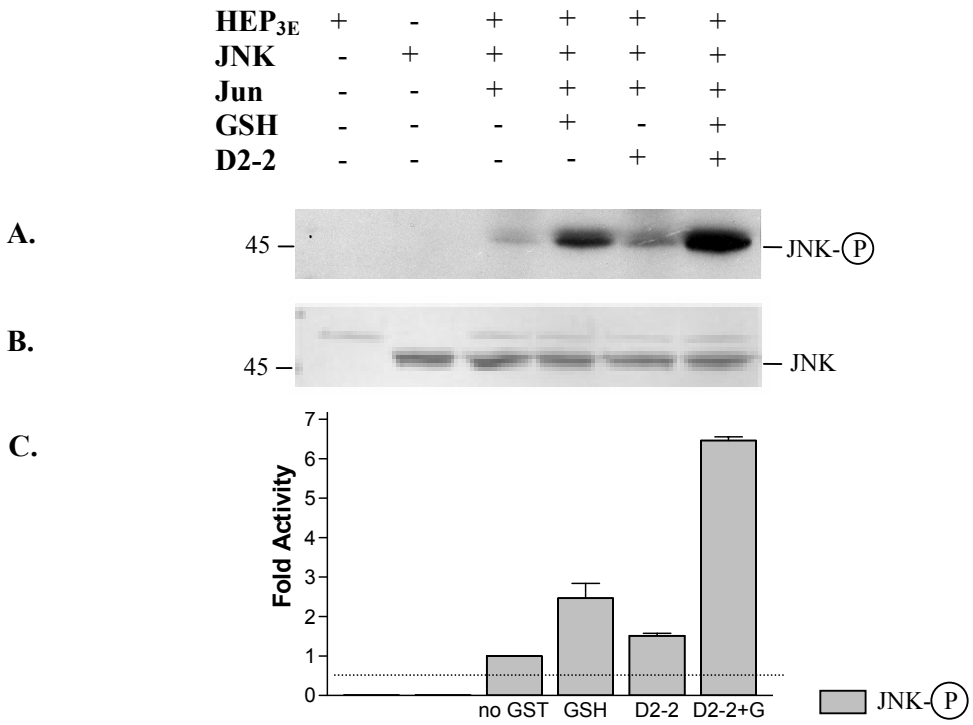

Figure 3.22 The effect of GSH on GST affected JNK activity by determining JNK phosphorylation. The experiments were performed using GST: HEP_{3E}: JNK: Jun in 10:1:2:10 molar ratio in the presence and absence of 10 mM GSH with 3 μCi of [γ-^{32}P] ATP for 25 min of phosphorylation time at room temperature. **(A)** The autoradiograph shows JNK phosphorylation in the presence and absence of GSH. **(B)** The SDS-PAGE illustrates the same loading amount of protein in each lane. **(C)** The histogram quantitates in fold activity the GSTs effect on JNK phosphorylation. The figures shown are representative of at least three independent experiments.

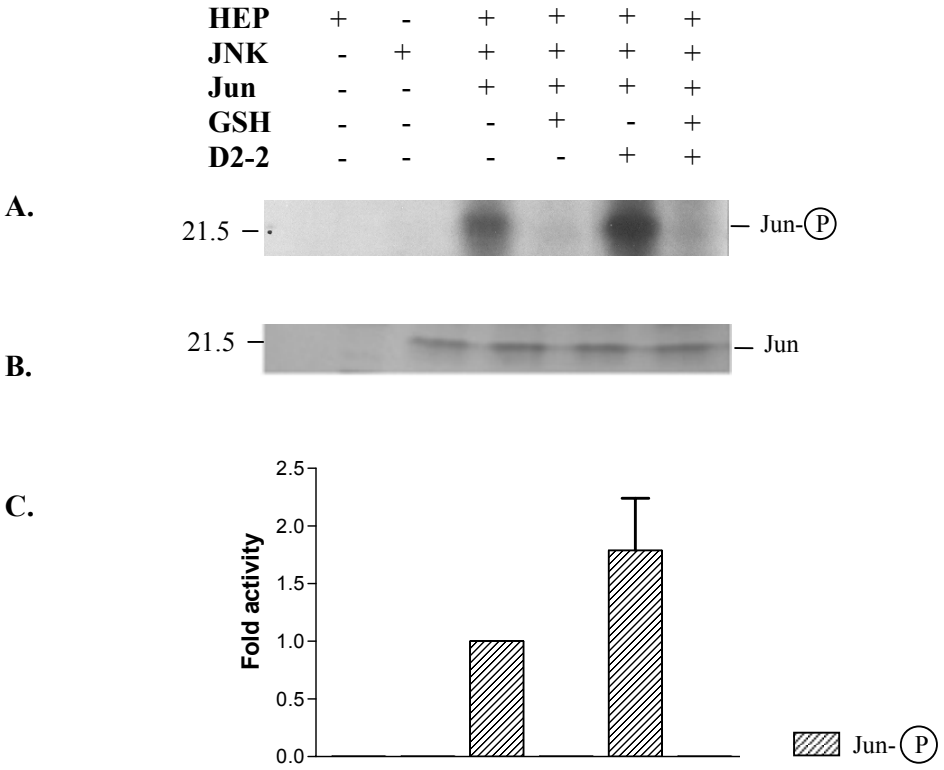

Figure 3.23 The effect of GSH on GST affected JNK activity by determining Jun phosphorylation. (A) The autoradiograph shows Jun phosphorylation in the presence and absence of GSH. **(B)** The SDS-PAGE illustrates the same loading amount of protein in each lane. **(C)** The histogram quantitates in fold activity the GSTs effect on Jun phosphorylation. The figures shown are representative of at least three independent experiments.

CHAPTER 4
DISCUSSION

The six Delta GSTs isoenzymes from Thai malaria vector, *Anopheles dirus*, consisting of the alternative spliceforms of adGSTD1-1, D2-2, D3-3 and D4-4 (32), as well as the two elucidated isoenzymes of adGSTD5-5 (40) and adGSTD6-6 (39) were characterized for enzymatic and non-enzymatic properties.

4.1 Enzymatic study of GST

We have revealed an overview of an evolutionary conserved adGSTD5-5 enzyme from gene to protein function.

4.1.1 Genome organization and putative promoter analysis

A BLAST analysis of the 15,694 bp complete sequence of phage clone 8A.2 contained a new GST gene, *adgstD5*, from the malaria vector *Anopheles dirus*. This gene was named *adgstD5* for *Anopheles dirus* GST class Delta protein coding sequence 5. The *adgstD5* gene is located upstream and in reverse orientation to the *adgst1AS1* gene **(Figure 4.1)**. Previously we had a partial sequence for the phage insert, which suggested the second gene was downstream, as well as possibly of the same Delta class GST as *adgst1AS1* and therefore was called *gst1-5* for insect GST class one enzyme five (32). The BLAST analysis yielded the highest identity to aggst1-7 (now referred to as gstD7), the product of the *aggst1* β gene of *An. gambiae* (164). The percent amino acid identity for these two enzymes is 95% and the percent similarity is 98%. The two mosquito malaria vectors *Anopheles dirus* and *An. gambiae* have been diverged for several million years, the first in Southeast Asia and the second in Africa. The high degree of sequence conservation between the two *Anopheles* species suggests that this GST isoenzyme has a role in the metabolism of a compound that is a common metabolic product or a significant component in the

environment in many living cells. A comparison with the available *An. gambiae* genome data shows the adGSTD5-5 protein has 29%-45% amino acid identity with other Delta GSTs and 9%-36% with GSTs from the remaining classes. The percent amino acid similarity to the Delta GSTs is 49%-66%. Therefore this GST is most like the Delta class GSTs; however, this gene encodes a singular GST protein with marginal amino acid identity to other Delta class GSTs.

Analysis also revealed two putative promoters, Ad5-923 and Ad5-3429, which may be defined as regulatory promoters of *adgstD5* and are required to fulfill the core promoter activity in specific physiological circumstances **(Figure 4.2)**. Ad5-923 contains several putative binding sites for developmentally regulated transcription factors such as hunchback, *Dfd*, AP-1 and GATA-1 **(Figure 4.2)**. Also of interest are several potential binding sites of estrogen receptor and estrogen-dependent protein (ER and vitillogenin binding protein) and maternal effect protein in Ad5-923 (40). It has been reported that there is an estrogen-like compound in another arthropod, the ovary of shrimp (*Parapenaeus fissurus*) (165). Searching the *Drosophila* genome database for an estrogen receptor sequence yielded one sequence (CG 7404 gene product) on chromosome 3 that was distinct from the ecdysone receptor (EcR) gene which is located on chromosome 2. BLAST analysis of the CG 7404 gene product provided the highest score to an estrogen-related receptor β (41% identity and 53% similarity). These data imply that estrogen-like compounds in insects may function in a similar way to the vertebrate estrogen. It is possible that the type of transcription factor binding sites detected in Ad5-923 may have contributed to the specific expression of Adgst5 mRNA in adult female mosquitoes. Oocyte development in female mosquitoes involves lipid synthesis at extra-ovarian sites, such as the fat body, transfer and then incorporation into oocytes (166,167). In *Aedes aegypti* the dry weight of oocytes consists of 35% lipids, 80% of which has been transported from fat body (166,167). The accumulation and transport of the lipid reserves in adult female mosquitoes would create an oxidative stress burden that could be alleviated by increased GST expression. The presence of an estrogen response element upstream of the *GSTA* gene was proposed to have a possible role in sexually maturing female plaice oocyte development (168). The authors suggested that the enormous mobilization of lipids during lipovitellin synthesis in females presents a specific

requirement of a GST-mediated detoxication mechanism to deal with lipid peroxidation, since up to 50% of total fish egg lipid is composed of polyunsaturated fatty acids originating from the mother (168). Ad5-923 contained both the estrogen response element and a vitellogenin binding protein element, which suggests that *adgstD5* might be involved in oogenesis as was proposed for the fish GST. Currently the number of genes known to be regulated by elements outside the 5' flanking region is constantly increasing. These intronic regulators often direct cell type- specific or developmentally regulated gene expression (169). The Ad5-3429 is located within the intron and contains several binding sites that are reported to be involved in embryo or tissue development; that is, bicoid, HFH8, Elf, oct, *dfd* and AP-1 **(Figure 4.2)**. This putative promoter therefore may be involved in developmental stage regulation.

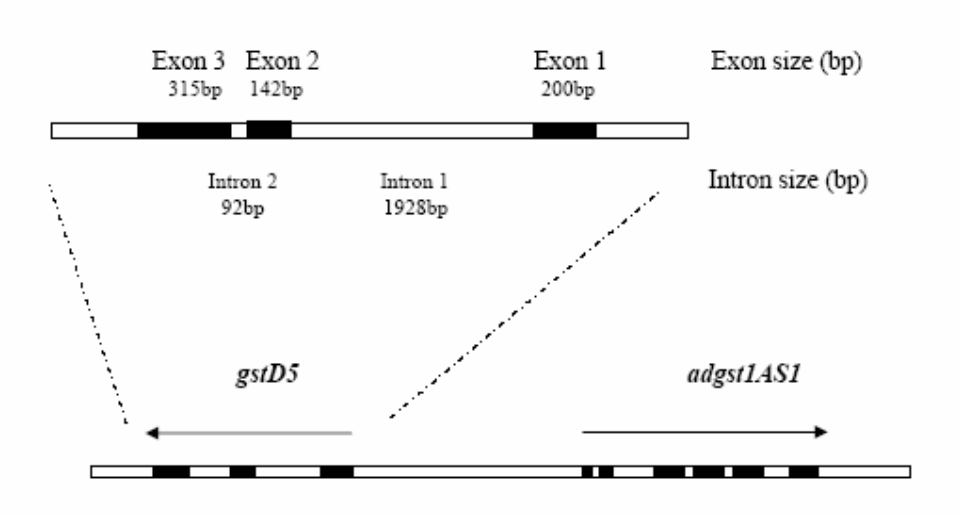

Figure 4.1 The *adgst1AS1* and *gstD5* gene organization of 8A.2 clone. The *gstD5* gene is located 4620 bp upstream with the opposite orientation of *adgst1AS1*. The 15,694 bp genomic sequence has GenBank accession number AF251478.

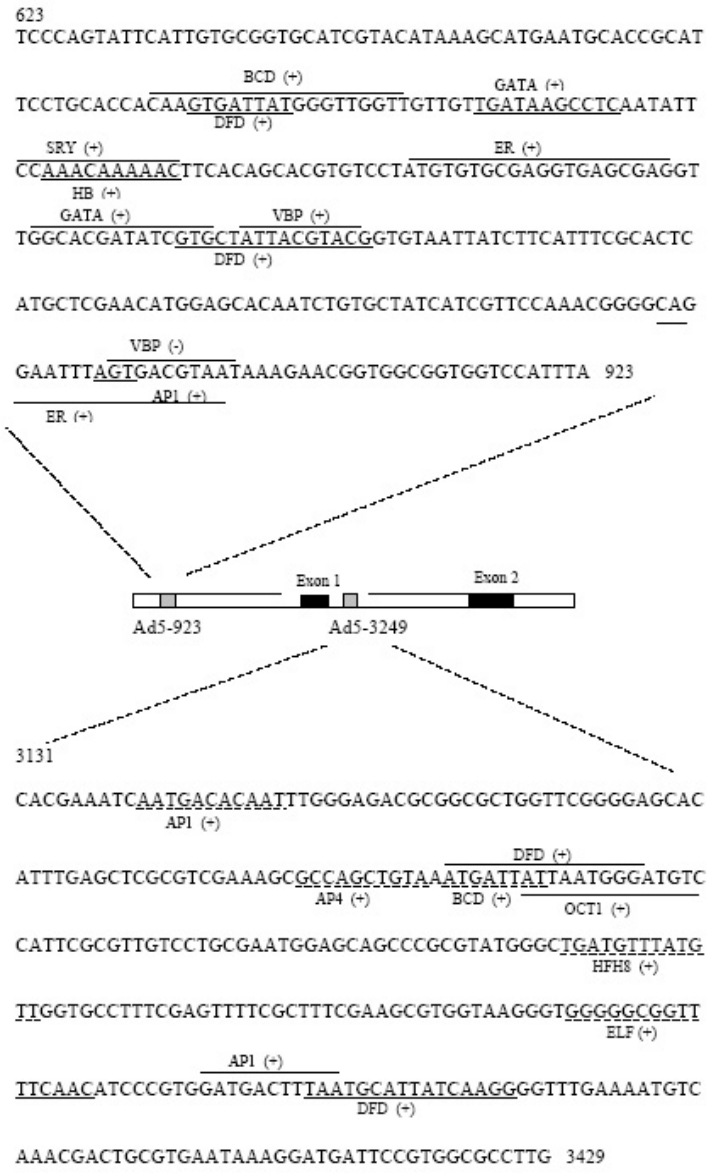

Figure 4.2 Sequence of two putative promoters of *gstD5* (Ad5-923 and Ad5-3429). Potential transcription binding sites were mapped on the region of these two putative promoters by the MatInspector program. Some abbreviations of binding sites are BCD- bicoid; SRY- sex-determining region Y; VBP- vitellogenin binding protein; ER- estrogen receptor; ELF- grainyhead protein of *Drosophila* and HFH8- fork head domain protein. The binding site of each potential transcription factor is underlined or overlined. The (+) indicates the binding site on the sense strand while (-) indicates the binding site on the antisense strand.

4.1.2 Enzymatic characterization

The characterization of the recombinant adGSTD5-5 was intrinsically problematic as the enzyme possessed low detectable activities **(Table 3.2)**, suggesting this enzyme owned very different substrate specificities compared to the other *An. dirus* GSTs. Despite low GSH conjugating activity, adGSTD5-5 possessed the greatest DDT dehydrochlorination activity of the six recombinant GSTs we have currently obtained (40). The DDTase activity was 11- to 62-fold different among the five *An. dirus* GSTs and adGSTD1-1 had no detectable activity. DDTase/CDNB activity showed that the adGSTD5-5 enzyme possessed a 4- to 100-fold greater DDT substrate preference compared to the other GSTs. Altogether, these data illustrate the adGSTD5-5 displays distinct catalytic properties from the previously defined insect GST isoenzymes. Two additional classes of soluble GSTs, Omega and Zeta, were also described with unusual enzymatic activities recently in a variety of organisms, including mammals (12,13,170). These data suggest that gene rearrangement in combination with structural evolution presumably constitutes an evolutionary function of the GST enzymes operating in nature (51). The mechanism of catalysis and the residues involved are yet to be investigated for adGSTD5-5. Various mammalian GST isoforms have been shown to be highly active in conjugating toxic lipid alkenals and purine and pyrimidine alkenals, all of which are believed to arise in cells as a consequence of oxidative processes (171,172). Interestingly, adGSTD5-5 contained the putative regulatory elements involved in detoxication of lipid peroxidation. Therefore, we investigated the role of heterologously expressed adGSTD5-5 involved in detoxication of potentially deleterious fatty acid metabolites by assaying the effect of polyunsaturated fatty acids on GSH conjugation with CDNB. Our data demonstrated adGSTD5-5 interaction with several fatty acids (40). An interesting observation was that although several fatty acids appeared to have little effect on CDNB activity the remaining tested either inhibited activity 72%-94% or enhanced activity by 104%-219%. This fatty acid interaction yielding varying effects on adGSTD5-5 implies adGSTD5-5 may have a physiological role in protection against oxidative stress as previously reported for GST Alpha class isoenzymes that appear to be involved in the signaling mechanisms of apoptosis (173).

4.1.3 Structural determination

The adGSTD5-5 structure obtained for this study is shown in **Figure 4.3** (Protein Data Bank accession number 1R5A). The tertiary structure obtained from crystallographic analysis showed the adGSTD5-5 protein to possess the canonical GST structure **(Figure 4.4)**. The physiologically relevant state of the protein is a dimer, which is present in the crystal due to a two-fold symmetry operation. The overall structure is broadly similar to that of previously determined delta-class GST structures (36). The G-site is formed mostly by residues from the N-terminal thioredoxin domain. Like other delta class GSTs, a serine residue (Ser11) appears to be responsible for activating the GSH sulfhydryl residue in catalysis. However, in the absence of direct evidence such as site-directed mutagenesis, it is possible that a nearby Ser, Cys or Tyr residue may be the major catalytic residue. adGSTD5-5 possessed an r.m.s. of 1.42 Å and 1.25 Å for the α-carbon alignment with adGSTD3-3 and adGSTD4-4, respectively. There are significant differences between the packing of helix α8 of adGSTD5-5 with the rest of the protein. As a result this helix is closer to the C-terminal domain compared with other insect GST isoenzymes **(Figure 4.4)**. This can be attributed to the substitution of packing residues in adGSTD5-5 to smaller amino acids. As such the overall shape of the H-site is different in adGSTD5-5 compared with the adGSTD3-3 and adGSTD4-4 isoenzymes. A comparison of adGSTD5-5 and adGSTD3-3 showed 47% identity in the 43 amino acids that make up the active site pocket with an average r.m.s. of 0.616 Å for the identical amino acid residues. However, the shape of the two active site pockets seems to be quite distinct with the adGSTD5-5 pocket appearing to be elongated **(Figure 4.5)**. In comparison, the adGSTD5-5 pocket also appears to be more polar with an increase in both positive and negative charges that contributes to distinct orientations of GSH and substrate binding. These structurally unique features of adGSTD5-5 especially in the vicinity of the active site and the C terminus may define the substrate repertoire for this particular GST whereby it displays an unusual enzymatic property. These results suggest that there is considerable structural plasticity in the active site of delta-class GSTs and that their catalytic activities may not be restricted to hydrophobic cosubstrates.

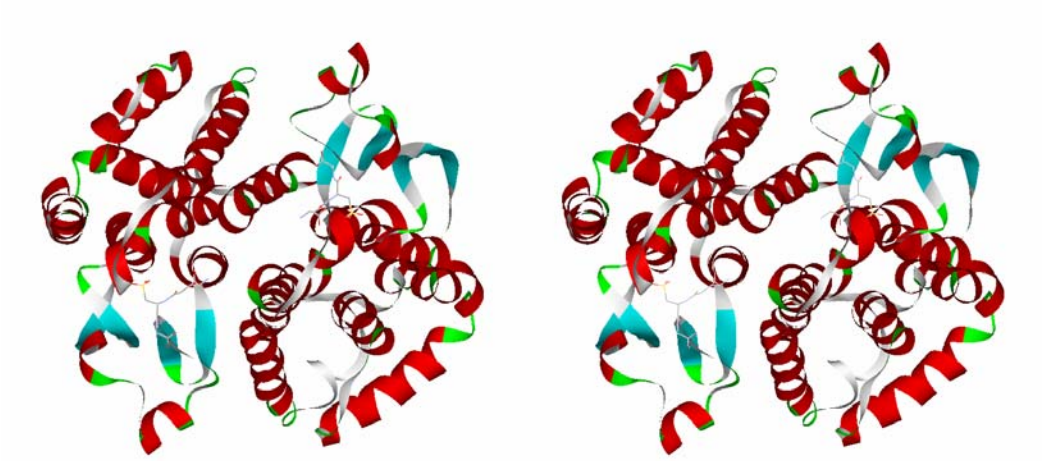

Figure 4.3 Stereo view of adGSTD5-5. The view is looking down on the two fold axis into the active site with the glutathione-sulfonic acid shown as a ball-and-stick figure. The coordinates for the tertiary structure have been deposited in the Protein Data Bank with the accession number 1R5A**.**

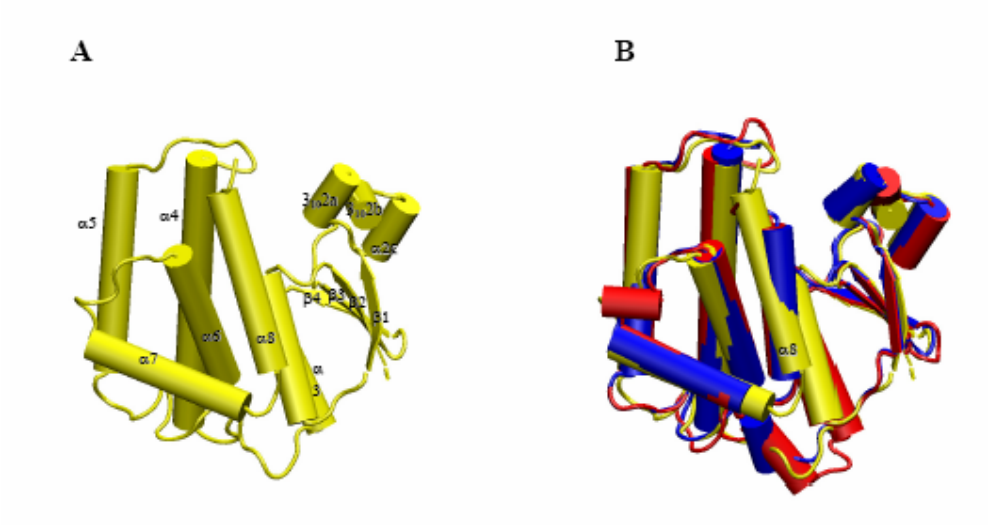

Figure 4.4 Cartoon representation of adGSTD5-5. Cylinders represent helices, arrows represent strands, lines represent random coil. **(A)** adGSTD5-5 with secondary structure elements labeled. **(B)** Aligned *Anopheles* GSTs. adGSTD3-3; blue, adGSTD4; red and adGSTD5-5; yellow.

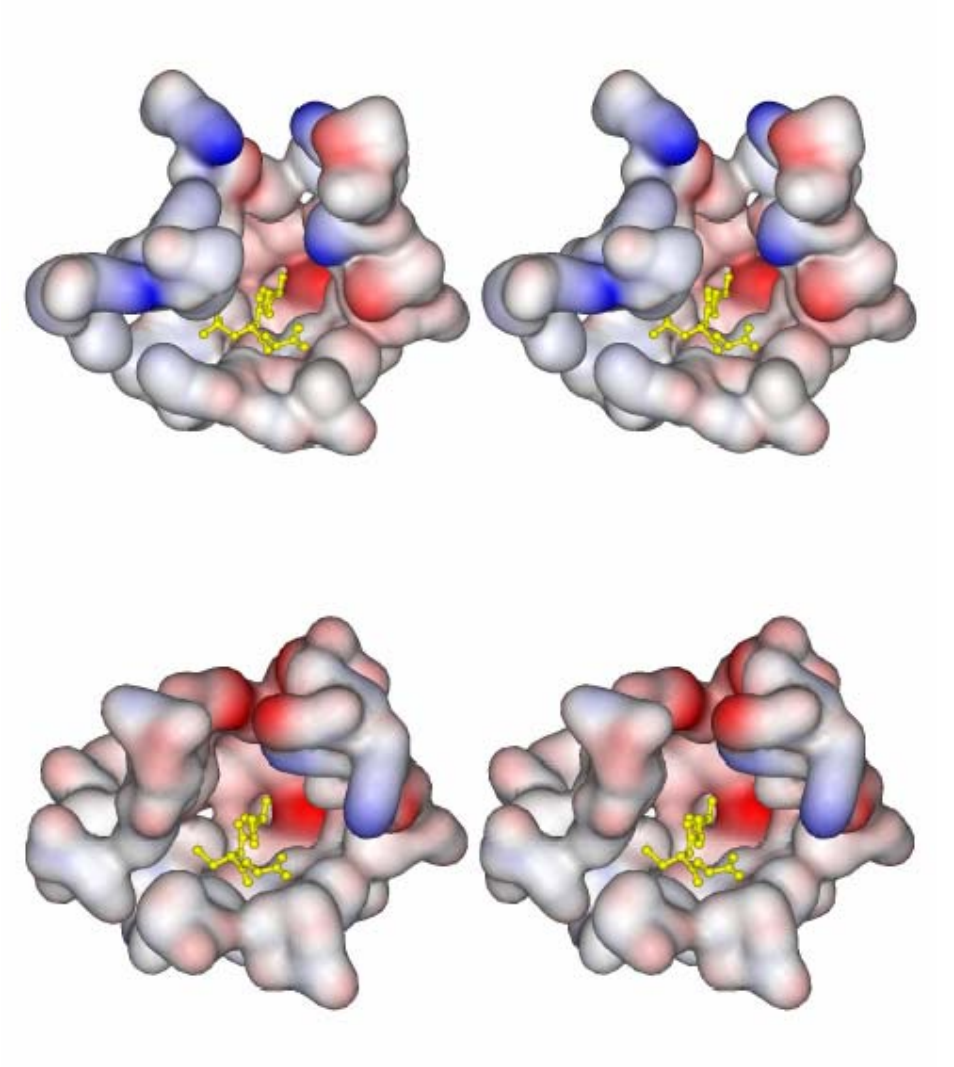

Figure 4.5 Stereo views of the electrostatic potential surface of the active site pockets of adGSTD5-5 and adGSTD3-3. The two tertiary structures were aligned to illustrate the same view of the active site. The top panel shows adGSTD5-5 and the bottom panel shows adGSTD3-3. A yellow ball and stick representation shows the GSH in the pocket.

4.2 Non-Enzymatic study of GST and Kinase proteins interaction

In the present study, we characterized the non-enzymatic function of GST in the regulation of stress-activated kinase proteins of the JNK pathway as well as the reciprocal regulation of GST by proteins of the JNK pathway. In insects, HEP or hemipterous is a homolog to mammalian MAPKK7 (MKK7) whereas the single *Drosophila* JNK or basket protein corresponds to the ten human JNK isoforms with a 61-75% amino acid identity (104). Furthermore, GSTs in insects currently fall into 6 classes, with the delta class being the best studied (34,174,175). The amino acid identities between the two delta class GSTs from *Anopheles dirus* and *Drosophila* are in range of 51-63%. Here we have concentrated on the study of six delta class GSTs from *An. dirus* including 4 spliceforms of a single delta class GST, GSTs D1-1, D2-2, D3-3 and D4-4 as well as the other two single encoded GST D5-5 and D6-6. Interestingly, the splicing of these GSTs generates products that share the same N-terminal 45 amino acids of the conserved glutathione binding region (37). The amino acid comparison among these spliceforms, D5-5 and D6-6 also indicated the high sequence similarity at the N-terminus. Any differences in the actions in these spliceforms and in the other two GSTs of D5-5 and D6-6 must therefore arise from the C-terminal regions of these proteins and we have previously shown that their substrate specificities, steady-state kinetics with respect to both GSH and CDNB, and inhibition kinetics to the pyrethroid insecticide permethrin are very different (37,39,40).

4.2.1 GSTs as a JNK regulator

Results of the present study have extended our previous studies by demonstrating an interaction between the *Dipteran* GSTs D1-1, D2-2, D3-3, D4-4, D5-5, D6-6 and the JNK pathway components, JNK and HEP. Our inhibition study showed different interactions of these kinases with the GST splice products, particularly as seen with the inhibition of several of the GST spliceforms by JNK **(Table 3.5)**. We observed, using the standard CDNB assay, that GSTD1-1 showed no inhibition whereas the remaining GSTs were inhibited by their preincubation with JNK protein. We suggest that the interaction with the kinase could change the GST conformation and result in different GST enzymatic activity.

This is also the first report of the activation of JNK activity by their preincubation with GST. Previously, GSTs have been reported to serve as negative regulators in the JNK pathway, acting either on JNK or ASK1 (85,86). Here we report that although some alternatively spliced GSTs inhibit JNK activity, other spliceforms also may function as JNK activator proteins. This data again highlights the functional diversity of the GST spliceforms in addition to their catalytic properties in kinetic studies, substrate specificity as well as inhibition studies (37). Moreover, our study shows the GSTs can associate with the immediate JNK upstream activator kinase in *Drosophila*, HEP. Hence, GST may play additional roles in regulation of kinase proteins in the JNK pathway through an, as yet, unknown mechanism.

As a consequence of the different effects of GSTD4-4 on JNK activity as shown by an increased phosphorylation of Jun **(Figure 3.15)** and a decreased phosphorylation of HEP **(Figure 3.16)**, we suggest the GSTs such as D4-4 may contribute to a change of JNK substrate selectivity. Intriguingly, GST could be a pivotal molecule to switch the JNK downstream cascade direction by changing activation of transcriptional machinery components and thereby gene expression. Similar to GSTs, JIPs (JNK-interaction proteins) occur in multiple forms including spliced isoforms as well as function in the same manner by regulating the JNK pathway (176). JIP appears to serve as both a positive (134,177) and negative (81,135) regulator of JNK activity. These data suggest the JIP-JNK interaction induced structural alterations and that these conformational changes are crucial for arrangement of the substrate binding site in JNK, which results in a change of JNK substrate specificity. One critical determinant of MAP kinase specificity and efficacy is the docking motif on the kinase surface which interacts with the substrate target site. A structural change of JNK upon interaction with GST may impact on this region critical for specificity determination (125,128). Nonetheless, JNK has many functions in controlling cell stress responses, and it is possible that the GST-JNK interaction changes substrate specificities of JNK for other JNK substrates such as ATF2 (99), Elk-1 (100) or p53 (178). The GST and JNK interaction would therefore function as switches or modulators for the various JNK processes upon stimulation by cellular stresses **(Figure 4.6)**. Due to the nature of the signaling process, there must be other molecules participating in regulation of the GST-JNK interaction. Since there are

various classes and isoforms of GSTs (1,2) and JNKs (91) that are widely distributed in different tissues, the signaling specificity of GST and JNK interactions may be also controlled by the specific classes and isoforms present in any particular cell type. Previously it was shown that distinct classes of GSTs played particular roles by interacting with different kinase proteins (85,86). Here we report that different isoforms of the same class of GST interact with JNK and modulate JNK activity in different ways. The variety of GST isoforms may be one of the keys determining signal specificity and controlling a particular cell's biological response.

The GST and JNK interaction may occur through the C-terminus of JNK which has been reported as being important for providing direct protein-protein interaction with GSTP1-1 (138). JNK has also been shown to interact electrostatically with other signaling molecules via a conserved docking motif called the CD (common docking) domain (126). The conserved polar residues within the CD domain may serve as energetic hot spots which increase the specific protein-protein interaction (179,180). In addition, hydrogen bonding and molecular surface shape complementarity are vital criteria as a basis for protein docking (181). Thus the variation in surface residues of a GST interacting with a particular JNK may induce distinct conformational changes yielding functional changes in both proteins. A shift in substrate specificity arising from this association of GST and JNK, in addition to the presence of different GST isoforms generated in the course of natural molecular evolution (182), would be a useful feature for a detoxication mechanism already well known for recognizing diverse substrate compounds.

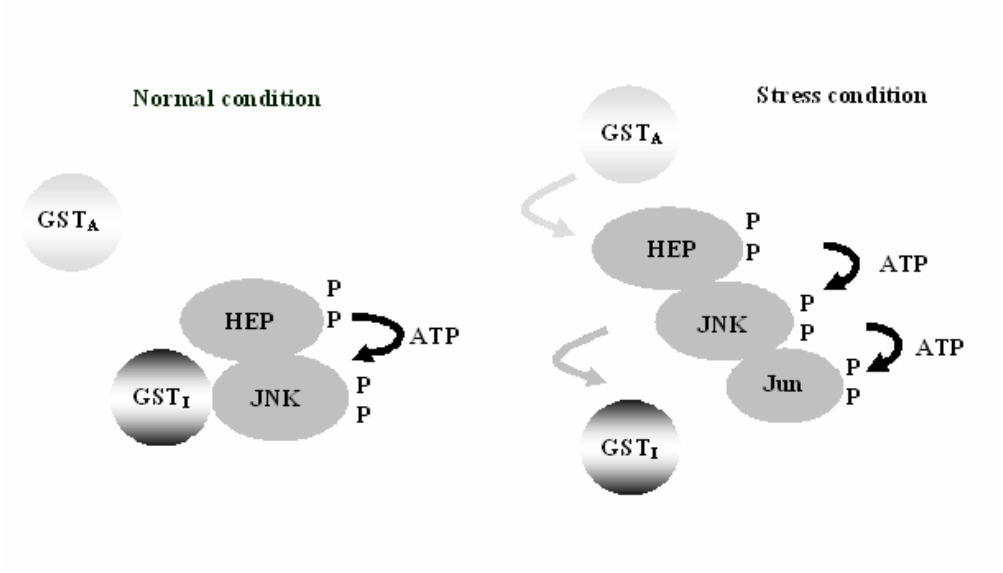

Figure 4.6 A proposed mechanism of GST regulation of stress kinase proteins through a dissociation/association process. The different isoforms of GSTs possess different JNK effector properties. GSTI refers to a JNK inhibitor and GSTA represents a JNK activator. The JNK regulation occurs on stress. Left panel: under normal conditions, GSTI inhibits JNK and maintains JNK at basal level activity (85). Right panel: once stress occurs, a mechanism to dissociate GSTI from JNK comes into effect. GSTA may now associate with JNK or an upstream activating kinase and increase or modulate the kinase cascade response.

4.2.2 Structural effect on GST and JNK interaction

Although adGSTD1-1 and adGSTD2-2 share 61% of amino acid identity, the experiment of JNK stabilization of GST demonstrated that JNK has ability to stabilize adGSTD1-1, but not D2-2 **(Figure 3.17)**. Moreover, these two GSTs were modulated by JNK differently. D1-1 was inhibited, whereas D2-2 was activated by JNK **(Figure 3.15 and 3.16)**. These data suggest the difference in amino acid composition between these two GSTs at the C-terminus confers differences in both structural and physiological functions. Many factors are involved in these GST-JNK interactions, for example interface size, the number and the type of amino acids involved in the interface, structural motif and secondary structure at an interface, hydrogen bonding and electrostatic interaction, packing, cavities, shape complementarities, as well as backbone and side-chain rearrangements (183). In addition, the induction of protein backbone flexibility can occur through high affinity protein-protein interaction, and may induce a disordering of the protein structure (184). The JNK stabilized GSTD1-1 may occur because the dynamics of the JNK-GST complex changes the flexing of GST and generates an induced-fit mechanism similar to that observed upon glutathione binding (36,185,186).

The single point mutations of the active site residues, G and H site, from adGSTD3-3 and adGSTD4-4 illustrated that the 103 position (D4-4) is important for interaction with JNK **(Figure 3.19 and 3.20)**. Substitution of Leu to Ala at this position affected the GST interaction with JNK as well as the reciprocal JNK effect on GST. This data suggests structural changes as a result of the amino acid replacement at Leu-103 position critically disturbed the GST and JNK interaction. The enzymatic studies demonstrated these residues governed both the catalytic function and the structural integrity of the GST enzymes as shown by changes in K_m, V_{max} and half-life **(Table 3.7)**. These amino acid replacements induce differing conformations that shift amino acid orientations involved in binding or catalysis and thereby affect kinetic properties (187,188). Furthermore, the subtle cumulative changes in residue interactions may influence the enzyme structure by affecting the subunit interaction (189,190), the characteristic hydrogen bonding network (68) and thus influence the packaging of the hydrophobic core (61,62) which contributes toward to protein stability. It is possible that changes in intra-molecular interactions

and side-chain conformations at the protein-protein interface may affect the JNK binding reaction (191). The GST structure shows Leu-103 directly interacts with His-100 which is located beneath the putative JNK docking residue Arg-96 **(Figure 4.7)**. The accumulated changes of a number of atom-atom interactions in the surrounding amino acids most likely exert a domino effect that effectively disturbs the GST and JNK docking region.

To elucidate the effect of surrounding residues, the equivalent residues of Met-101-Ala from D3-3 and Val-107-Ala from D4-4 were applied for this study. Despite being designated as equivalent residues, Met-101 (D3-3) and Val-107 (D4-4) provided a significant difference in stability effect (66). The adGSTD4-4 mutant, Val-107-Ala half-life (254.43 ± 9.85 min) demonstrated a striking effect with an increase of approximately 17-fold in the half-life when compared to the wild type (14.01 ± 1.70 min) while the adGSTD3-3 mutant, Met-101-Ala half-life (4.13 ± 0.41 min) showed only a slight effect compared to the wild type half-life (2.71 ± 0.35 min). This data demonstrates the milieu of these amino acids contribute to different intra-molecular interactions in which are isoform specific (192). We further show the correspondence of these equivalent residues conferred a distinct response in GST affecting JNK activity **(Figure 3.18)** as demonstrated by Met-101-Ala increased while Val-107-Ala decreased JNK phosphorylation. This data suggests the importance of neighboring residues involved in determining functional diversity.

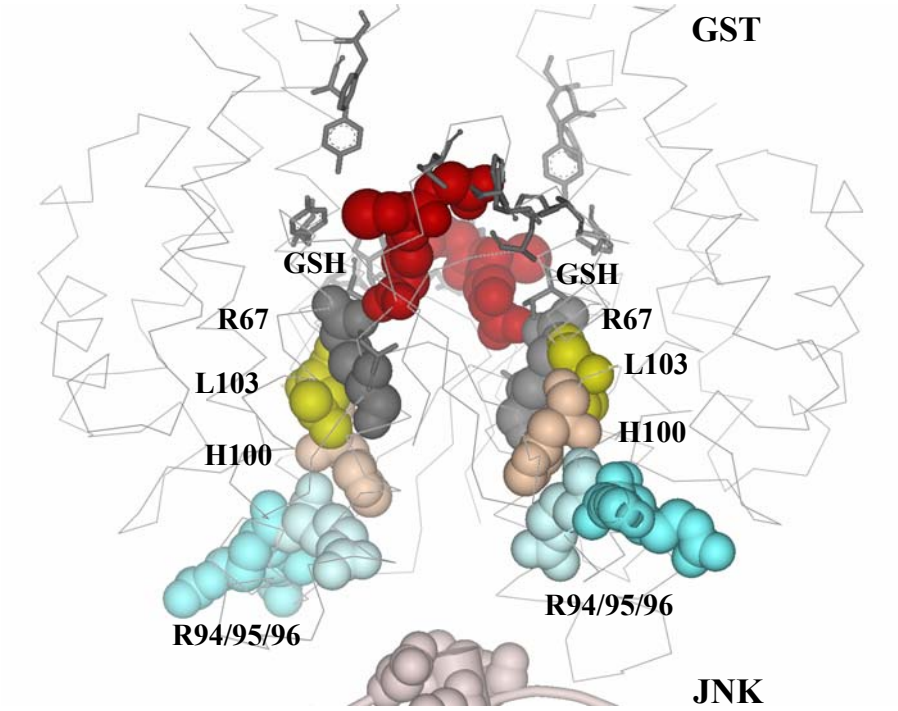

Figure 4.7 A proposed pathway of GST structural effect on JNK interaction. The surface interaction of GST and JNK is located on the opposite side of the active site of both molecules. adGSTD4-4 and JNK protein represented in gray and magenta, respectively. The pink and blue CPK modules represent the negative and positive charge-charge interaction taking place on the surface of the molecules. The red and grey CPK modules represent glutathione and Arg-67, respectively in the active site of GST. Leu-103 (yellow) directly interacts with His-100 which is located beneath the putative JNK docking residue Arg-96.

4.2.3 The effect of glutathione on GST and JNK interaction

Our data demonstrated that GSH changes the effect of JNK on adGSTD1-1 and D2-2 activity by altering the GST conformation **(Figure 3.21A and 3.21B)**. We suggest the known changes of GSH binding that result in GST induced-fit conformational changes (36) could contribute to the changes noted in the GST-JNK interaction. These changes will be observed differently depending on the GST specific isoforms and substrate employed. We further investigated the presence of GSH resulting in an increase of JNK autophosphorylation **(Figure 3.22)**, while attenuating Jun phosphorylation **(Figure 3.23)**. This study suggests glutathione may serve as a critical molecule that is directly involved in JNK regulation by controlling JNK substrate selectivity and specificity of interaction. Changes in glutathione levels have also been associated with the activation of a stress response (193) and GSTs can protect against electrophiles and oxidative stress by altering cellular glutathione levels (1). Direct interaction of GSH and kinases has been reported previously for several isoforms of PKC that were shown to be inhibited by GSH (194). High GSH concentrations have been shown to inhibit the sphingomyelin/ceramide cycle where generation of ceramide leads to cell cycle arrest and apoptosis (195). In addition, the depletion of GSH in the cell during oxidative stress exerted negative regulation over protein kinase C (PKC) isozymes (194) as well as JNK/p38 pathway (193). GSH has been shown to be a potent inhibitor of JNK activation suggesting the existence of specific cellular components involved in JNK activation in response to different forms of cellular stress (193). We suggest GSTs may be one of these components.

.

CHAPTER 5
CONCLUSIONS

In this thesis project, we have identified a new Delta class GST, which we named adGSTD5-5. This isoenzyme was only detectably expressed in *Anopheles dirus* adult female. A high degree of sequence conservation of this gene across several million years of divergent evolution between two *Anopheline* malaria vector species suggests that this GST isoenzyme performs an important function. A putative promoter analysis suggests this GST has an involvement in oogenesis and in developmental stage regulation. The enzyme displayed little activity for classical GST substrates although it possessed the greatest activity for DDT, 10-fold, observed for Delta GSTs. A tertiary structure comparison revealed differences in active site composition with an elongated and more polar active site topology.

In addition, all six adGST isoenzymes, adGSTD1-1 to D6-6, were available to study as a kinase regulator protein in the JNK pathway. The data show that distinct isoforms of GSTs specifically interact with JNK with different effects. Intriguingly, even though several of the studied GST isoforms are alternatively spliced products sharing greater than 60% amino acid identity, these GST proteins displayed contrary roles in regulation of JNK. It suggests the specific isoforms of GSTs present may be important in controlling the final cellular response. The present study provides new insight into the mechanism of GSTs in regulating and conferring specificity of stress kinase proteins in the JNK pathway.

REFERENCES

1. Hayes,J.D., Pulford,D.J. (1995) The glutathione S-transferase supergene family: Regulation of GST and the contribution of the isoenzymes to cancer chemoprotection and drug resistance. *CRC Crit.Rev.Biochem.Molec.Biol.*, 30, 445-600.

2. Armstrong,R.N. (1997) Structure, catalytic mechanism, and evolution of the glutathione transferases. *Chem.Res.Toxicol.*, 10, 2-18.

3. Sheehan,D., Meade,G., Foley,V.M., and Dowd,C.A. (2001) Structure, function and evolution of glutathione transferases : implications for classification of non-mammalian members of an ancient enzyme superfamily. *Biochem.J.*, 360, 1-16.

4. Ketterer,B. (2001) A bird's eye view of the glutathione transferase field. *Chem Biol Interact*, 138, 27-42.

5. DeJong,J.L., Morgenstern,R., Jornvall,H., DePierre,J.W., and Tu,C.P.D. (1988) Gene expression of rat and human microsomal glutathione S-transferases. *J.Biol.Chem.*, 263, 8430-8436.

6. Schmidt-Krey,I., Mitsuoka,K., Hirai,T., Murata,K., Cheng,Y., Fujiyoshi,Y., Morgenstern,R., and Hebert,H. (2000) The three-dimentional map of microsomal glutathione transferase 1 at 6 Å resolution. *EMBO J.*, 19, 6311-6316.

7. Toba,G., Aigaki,T. (2000) Disruption of the microsomal glutathione S-transferase-like gene reduces life span of *Drosophila melanogaster*. *Gene*, 253, 179-187.

8. Jakobsson,P.-J., Mancini,J.A., and Ford-Hutchinson,A.W. (1996) Identification and characterization of a novel human microsomal glutathione S-transferase with leukotriene C_4 synthase activity and significant sequence identity to 5-Lipoxygenase-activating protein and Leukotriene C_4 synthase. *J.Biol.Chem.*, 271, 22203-22210.

9. Andersson,C., Mosialou,E., Adang,A.E.P., Mulder,G.J., van der Gen,A., and Morgenstern,R. (1991) Studies on the activity and activation of rat liver microsomal glutathione transferase with a series of glutathione analogues. *J.Biol.Chem.*, 266, 2076-2079.

10. Mannervik,B., Awasthi,Y.C., Board,P.G., Hayes,J.D., Di Ilio,C., Ketterer,B., Listowsky,I., Morgenstern,R., Muramatsu,M., Pearson,W.R., Pickett,C.B., Sato,K., Widersten,M., and Wolf,C.R. (1992) Nomenclature for human glutathione transferases. *Biochem.J.*, 282, 305-306.

11. Rouimi,P., Anglade,P., Benzekri,A., Costet,P., Debrauwer,L., Pineau,T., and Tulliez,J. (2001) Purification and characterization of a glutathione S-transferase Omega in pig : evidence for two distinct organ-specific transcripts. *Biochem.J.*, 358, 257-262.

12. Board,P.G., Coggan,M., Chelvanayagam,G., Easteal,S., Jermiin,L.S., Schulte,G.K., Danley,D.E., Hoth,L.R., Griffor,M.C., Kamath,A.V., Rosner,M.H., Chrunyk,B.A., Perregaux,D.E., Gabel,C.A., Geoghegan,K.F., and Pandit,J. (2000) Identification, characterization, and crystal structure of the omega class glutathione transferases. *J.Biol.Chem.*, 275, 24798-24806.

13. Board,P., Baker,R.T., Chelvanayagam,G., and Jermiin,L.S. (1997) Zeta, a novel class of glutathione transferases in a range of species from plants to humans. *Biochem.J.*, 328, 929-935.

14. Pemble,S.E., Wardle,A.F., and Taylor,J.B. (1996) Glutathione S-transferase class kappa: characterization by the cloning of rat mitochondria GST and identification of a human homologue. *Biochem.J.*, 319, 749-754.

15. Ji,X., Von Rosenvinge,E.C., Johnson,W.W., Tomarev,S.I., Paitigorsky,J., Armstrong,R.N., and Gilliland,G.L. (1995) Three-dimensional structure, catalytic properties, and evolution of a sigma class glutathione transferase from squid, a progenitor of the lens S-crystallins of cephalopods. *Biochemistry*, 34, 5317-5328.

16. Marrs,K.A. (1996) The functions and regulation of glutathione *S*-transferases in plants. *Ann.Rev.Plant Physiol.Plant Mol.Biol.*, 47, 127-158.

17. Allocati,N., Casalone,E., Masulli,M., Polekhina,G., Rossjohn,J., Parker,M.W., and Di Ilio,C. (2000) Evaluation of the role of two conserved active-site residues in Beta class glutathione S-transferases. *Biochem.J.*, 351, 346.

18. Caccuri,A.M., Antonini,G., Allocati,N., Di Ilio,C., De Maria,F., Innocenti,F., Parker,M.W., Masulli,M., Lo Bello,M., Turella,P., and Federici,G. (2002) GSTB1-1 from *Proteus mirabilis*. A snapshot of an enzyme in the evolutionary pathway from a redox enzyme to a conjugating enzyme. *J.Biol.Chem.*, 277, 18777-18784.

19. Thom,R., Dixon,D.P., Edwards,R., Cole,D.J., and Lapthorn,A.J. (2001) The structure of a Zeta class glutathione S-transferase from *Arabidopsis thaliana*: Characterisation of a GST with novel active-site architecture and a putative role in tyrosine catabolism. *J.Mol.Biol.*, 308, 949-962.

20. Chelvanayagam,G., Parker,M.W., and Board,P.G. (2001) Fly fishing for GSTs: a unified nomenclature for mammalian and insect glutathione transferases. *Chem Biol Interact*, 133, 256-260.

21. Beckett,G.J., Hayes,J.D. (1993) Glutathione S-transferases: Biomedical applications. *Adv.Clin.Chem.*, 30, 281-380.

22. Pemble,S.E., Taylor,J.B. (1992) An evolutionary perspective on glutathione transferases inferred from class-Theta glutathione transferase cDNA sequences. *Biochem.J.*, 287, 957-963.

23. Eaton,D.L., Bammler,T.K. (1999) Concise review of the glutathione S-transferases and their significance to toxicology. *Toxicological Science*, 49, 156-164.

24. Rowe,J.D., Nieves,E., and Listowsky,I. (1997) Subunit diversity and tissue distribution of human glutathione S-transferase: interpretations based on electrospray ionization-MS and peptide sequence-specific antisera. *Biochem.J.*, 325, 481-486.

25. Perrett,S., Freeman,S.J., Butler,P.J.G., and Fersht,A.R. (1999) Equilibrium folding properties of the yeast prion protein determinant Ure2. *J.Mol.Biol.*, 290, 331-345.

26. Kostaropoulos,I., Papadopoulos,A.I., Metaxakis,A., Boukouvala,E., and Papadopoulou-Mourkidou,E. (2001) Glutathione S-transferase in the defence against pyrethroids in insects. *Insect Biochem.Molec.Biol.*, 31, 313-319.

27. Zou,S., Meadows,S., Sharp,L., Jan,L.Y., and Jan,Y.N. (2000) Genome-wide study of aging and oxidative stress response in *Drosophila melanogaster*. *Proc.Natl.Acad.Sci.USA*, 97, 13726-13731.

28. Sawicki,R., Singh,S.P., Mondal,A.K., Beneš,H., and Zimniak,P. (2003) Cloning, expression and biochemical characterization of one Epsilon-class (GST-3) and ten Delta-class (GST-1) glutathione S-transferases from *Drosophila melanogaster*, and identification of additional nine members of the Epsilon class. *Biochem.J.*, 370, 661-669.

29. Prapanthadara,L., Koottathep,S., Promtet,N., Suwonkerd,W., Ketterman,A.J., and Somboon,P. (2000) Correlation of glutathione S-transferase and DDT dehydrochlorinase activities with DDT susceptibility in *Anopheles* and

Culex mosquitos from northern Thailand. *Southeast Asian J.Trop.Med.Public Health*, 31(Suppl 1), 111-118.

30. Ranson,H., Collins,F., and Hemingway,J. (1998) The role of alternative mRNA splicing in generating heterogeneity within the *Anopheles gambiae* class I glutathione S-transferase family. *Proc.Natl.Acad.Sci.USA*, 95, 14284-14289.

31. Toung,Y.P.S., Hsieh,T.-S., and Tu,C.P.D. (1993) The glutathione *S*-transferase D genes. A divergently organized, intronless gene family in *Drosophila melanogaster*. *J.Biol.Chem.*, 268, 9737-9746.

32. Pongjaroenkit,S., Jirajaroenrat,K., Boonchauy,C., Chanama,U., Leetachewa,S., Prapanthadara,L., and Ketterman,A.J. (2001) Genomic organization and putative promotors of highly conserved glutathione S-transferases originating by alternative splicing in *Anopheles dirus*. *Insect Biochem.Molec.Biol.*, 31, 75-85.

33. Agianian,B., Tucker,P.A., Schouten,A., Leonard,K., Bullard,B., and Gros,P. (2003) Structure of a *Drosophila* sigma class glutathione S-transferase reveals a novel active site topography suited for lipid peroxidation products. *J.Mol.Biol.*, 326, 151-165.

34. Ding,Y., Ortelli,F., Rossiter,L.C., Hemingway,J., and Ranson,H. (2003) The *Anopheles gambiae* glutathione transferase supergene family: annotation, phylogeny and expression profiles. *BMC Genomics*, 4, 35-50.

35. Ranson,H., Rossiter,L., Ortelli,F., Jensen,B., Wang,X., Roth,C.W., Collins,F.H., and Hemingway,J. (2001) Identification of a novel class of insect glutathione S-transferases involved in resistance to DDT in the malaria vector *Anopheles gambiae*. *Biochem.J.*, 359, 295-304.

36. Oakley,A.J., Harnnoi,T., Udomsinprasert,R., Jirajaroenrat,K., Ketterman,A.J., and Wilce,M.C.J. (2001) The crystal structures of glutathione S-transferases

isozymes 1–3 and 1–4 from *Anopheles dirus* species B. *Protein Science*, 10, 2176-2185.

37. Jirajaroenrat,K., Pongjaroenkit,S., Krittanai,C., Prapanthadara,L., and Ketterman,A.J. (2001) Heterologous expression and characterization of alternatively spliced glutathione *S*-transferases from a single *Anopheles* gene. *Insect Biochem.Molec.Biol.*, 31, 867-875.

38. Prapanthadara,L., Koottathep,S., Promtet,N., Hemingway,J., and Ketterman,A.J. (1996) Purification and characterization of a major glutathione S-transferase from the mosquito *Anopheles dirus* (species B). *Insect Biochem.Molec.Biol.*, 26, 277-285.

39. Udomsinprasert,R., Ketterman,A.J. (2002) Expression and characterization of a novel class of glutathione S-transferase from *Anopheles dirus*. *Insect Biochem.Molec.Biol.*, 32, 425-433.

40. Udomsinprasert,R., Pongjaroenkit,S., Wongsantichon,J., Oakley,A.J., Prapanthadara,L., Wilce,M.C.J., and Ketterman,A.J. (2005) Identification, characterization and structure of a new delta class glutathione transferase isoenzyme. *Biochem.J.*.

41. Ortelli,F., Rossiter,L.C., Vontas,J., Ranson,H., and Hemingway,J. (2003) Heterologous expression of four glutathione transferase genes genetically linked to a major insecticide-resistance locus from the malaria vector *Anopheles gambiae*. *Biochem.J.*, 373, 957-963.

42. Mannervik,B., Jensson,H. (1982) Binary combinations of four protein subunits with different catalytic specificities explain the relationship between six basic glutathione S-transferases in rat liver cytosol. *J.Biol.Chem.*, 257, 9909-9912.

43. Sinning,I., Kleywegt,G.J., Cowan,S.W., Reinemer,P., Dirr,H.W., Huber,R., Gilliland,G.L., Armstrong,R.N., Ji,X., Board,P.G., Olin,B., Mannervik,B., and Jones,T.A. (1993) Structure determination and

refinement of human Alpha class glutathione transferase A1-1, and a comparison with the Mu and Pi class enzymes. *J.Mol.Biol.*, 232, 192-212.

44. Dirr,H., Reinemer,P., and Huber,R. (1994) X-ray crystal structures of cytosolic glutathione S-transferases. Implications for protein architecture, substrate recognition and catalytic function. *Eur.J.Biochem.*, 220, 645-661.

45. Dirr,H., Reinemer,P., and Huber,R. (1994) Refined crystal structure of porcine class pi glutathione S-transferase (pGSTP1-1) at 2.1 Å resolution. *J.Mol.Biol.*, 243, 72-92.

46. Oakley,A.J., Rossjohn,J., Lo Bello,M., Caccuri,A.M., Federici,G., and Parker,M.W. (1997) The three-dimensional structure of the human pi class glutathione S-transferase P1-1 in complex with the inhibitor ethacrynic acid and its glutathione conjugate. *Biochemistry*, 36, 576-585.

47. Oakley,A.J., Lo Bello,M., Battistoni,A., Ricci,G., Rossjohn,J., Villar,H.O., and Parker,M.W. (1997) The structures of human glutathione transferase P1-1 in complex with glutathione and various inhibitors at high resolution. *J.Mol.Biol.*, 274, 84-100.

48. Ji,X., Blaszczyk,J., Xiao,B., O'Donnell,R., Hu,X., Herzog,C., Singh,S.V., and Zimniak,P. (1999) Structure and function of residue 104 and water molecules in the xenobiotic substrate-binding site in human glutathione *S*-transferase P1-1. *Biochemistry*, 38, 10231-10238.

49. Ji,X., Zhang,P., Armstrong,R.N., and Gilliland,G.L. (1992) The three-dimensional structure of a glutathione S-transferase from the Mu gene class. Structural analysis of the binary complex of isoenzyme 3-3 and glutathione at 2.2- Å resolution. *Biochemistry*, 31, 10169-10184.

50. Xiao,B., Singh,S.P., Nanduri,B., Awasthi,Y.C., Zimniak,P., and Ji,X. (1999) Crystal structure of a murine glutathione S-transferase in complex with a glutathione conjugate of 4-hydroxynon-2-enal in one subunit and

glutathione in the other: evidence of signaling across the dimer interface. *Biochemistry*, 38, 11887-11894.

51. Parker,M.W., McKinstry,W.J., Oakley,A.J., Polekhina,G., Rossjohn,J., Chelvanayagam,G., Board,P.G., Di Ilio,C., Caccuri,A.M., Ricci,G., and Lo Bello,M. (2001) Evolution of functional diversity as observed through structural studies of glutathione transferases. *Chem Biol Interact*, 133, 8-12.

52. Reinemer,P., Prade,L., Hof,P., Neuefeind,T., Huber,R., Zettl,R., Palme,K., Schell,J., Koelln,I., Barrunik,H.D., and Bieseler,B. (1996) Three-dimenstional structure of glutathione S-transferase from *Arabidopsis thaliana* at 2.2 Å resolution: structural characterization of herbicide-conjugating plant glutathione S-transferases and a novel active site architecture. *J.Mol.Biol.*, 255, 289-309.

53. Wilce,M.C.J., Feil,S.C., Board,P.G., and Parker,M.W. (1994) Crystallization and preliminary x-ray diffraction studies of a glutathione S-transferase from the australian sheep blowfly, *Lucilia cuprina*. *J.Mol.Biol.*, 236, 1407-1409.

54. Armstrong,R.N., Rife,C., and Wang,Z. (2001) Structure, mechanism and evolution of thiol transferases. *Chem Biol Interact*, 133, 167-169.

55. Wilce,M.C.J., Parker,M.W. (1994) Structure and function of glutathione S-transferases. *Biochim.Biophys.Acta*, 1205, 1-18.

56. Reinemer,P., Dirr,H.W., Ladenstein,R., Huber,R., Lo Bello,M., Federici,G., and Parker,M.W. (1992) Three-dimensional structure of class π glutathione S-transferase from human placenta in complex with S-hexylglutathione at 2.8 Å resolution. *J.Mol.Biol.*, 227, 214-226.

57. Sayed,Y., Wallace,L.A., and Dirr,H.W. (2000) The hydrophobic lock-and-key intersubunit motif of glutathione transferase A1-1: implications for catalysis, ligandin function and stability. *FEBS Lett.*, 465, 169-172.

58. Hornby,J.A.T., Codreanu,S.G., Armstrong,R.N., and Dirr,H.W. (2002) Molecular recognition at the dimer interface of a class Mu glutathione transferase: Role of a hydrophobic interaction motif in dimer stability and protein function. *Biochemistry*, 41, 14238-14247.

59. Dirr,H. (2001) Folding and assembly of glutathione transferases. *Chem Biol Interact*, 133, 19-23.

60. Vargo,M.A., Colman,R.F. (2004) Heterodimers of wild-type and subunit interface mutant enzymes of glutathione S-transferase A1-1: Interactive or independent active sites? *Protein Science*, 13, 1586-1593.

61. Cocco,R., Stenberg,G., Dragani,B., Principe,D.R., Paludi,D., Mannervik,B., and Aceto,A. (2001) The folding and stability of human Alpha class glutathione transferase A1-1 depend on distinct roles of a conserved N-capping box and hydrophobic staple motif. *J.Biol.Chem.*, 276, 32177-32183.

62. Dragani,B., Stenberg,G., Melino,S., Petruzzelli,R., Mannervik,B., and Aceto,A. (1997) The conserved N-capping box in the hydrophobic core of glutathione S-transferase P1–1 is essential for refolding. Identification of a buried and conserved hydrogen bond important for protein stability. *J.Biol.Chem.*, 272, 25518-25523.

63. Stenberg,G., Dragani,B., Cocco,R., Mannervik,B., and Aceto,A. (2000) A conserved "hydrophobic staple motif" plays a crucial role in the refolding of human glutathione transferase P1-1. *J.Biol.Chem.*, 275, 10421-10428.

64. Wongtrakul,J., Sramala,I., and Ketterman,A. (2003) A non-active site residue, cysteine 69, of glutathione S-transferase adGSTD3-3 has a role in stability and catalytic function. *Protein and Peptide Letters*, 10, 375-385.

65. Wongsantichon,J., Harnnoi,T., and Ketterman,A.J. (2003) A sensitive core region in the structure of glutathione S-transferases. *Biochem.J.*, 373, 759-765.

66. Winayanuwattikun,P., Ketterman,A.J. (2004) Catalytic and structural contributions for glutathione binding residues in a delta class glutathione S-transferase. *Biochem.J.*, 382, 751-757.

67. Ketterman,A.J., Prommeenate,P., Boonchauy,C., Chanama,U., Leetachewa,S., Promtet,N., and Prapanthadara,L. (2001) Single amino acid changes outside the active site significantly affect activity of glutathione S-transferases. *Insect Biochem.Molec.Biol.*, 31, 65-74.

68. Kong,G.K.W., Polekhina,G., McKinstry,W.J., Parker,M.W., Dragani,B., Aceto,A., Paludi,D., Principe,D.R., Mannervik,B., and Stenberg,G. (2003) Contribution of glycine 146 to a conserved folding module affecting stability and refolding of human glutathione transferase P1-1. *J.Biol.Chem.*, 278, 1291-1302.

69. Wallace,L.A., Blatch,G.L., and Dirr,H.W. (1998) A topologically conserved aliphatic residue in α-helix 6 stabilizes the hydrophobic core in domain II of glutathione transferases and is a structural determinant for the unfolding pathway. *Biochem.J.*, 336, 413-418.

70. Liu,S., Zhang,P., Ji,X., Johnson,W.W., Gilliland,G.L., and Armstrong,R.N. (1992) Contribution of tyrosine 6 to the catalytic mechanism of isoenzyme 3-3 of glutathione S-transferase. *J.Biol.Chem.*, 267, 4296-4299.

71. Atkins,W.M., Wang,R.W., Bird,A.W., Newton,D.J., and Lu,A.Y.H. (1993) The catalytic mechanism of glutathione S-transferase (GST). Spectroscopic determination of the pK_a of TYR-9 in rat α1-1 GST. *J.Biol.Chem.*, 268, 19188-19191.

72. Caccuri,A.M., Ascenzi,P., Antonini,G., Parker,M.W., Oakley,A.J., Chiessi,E., Nuccetelli,M., Battistoni,A., Bellizia,A., and Ricci,G. (1996) Structural flexibility modulates the activity of human glutathione transferase P1-1. Influence of a poor co-substrate on dynamics and kinetics of human glutathione transferase. *J.Biol.Chem.*, 271, 16193-16198.

73. Caccuri,A.M., Antonini,G., Board,P.G., Flanagan,J., Parker,M.W., Paolesse,R., Turella,P., Federici,G., Lo Bello,M., and Ricci,G. (2001) Evolutionary strategy for optimization of GSH binding and catalysis in Alpha, Pi, Mu and Theta glutathione transferases. *Chem Biol Interact*, 133, 163-166.

74. Ji,X., Johnson,W.W., Sesay,M.A., Dickert,L., Prasad,S.M., Ammon,H.L., Armstrong,R.N., and Gilliland,G.L. (1994) Structure and function of the xenobiotic substrate binding site of a glutathione S-transferase as revealed by x-ray crystallographic analysis of product complexes with the diastereomers of 9-(S-glutathionyl)-10-hydroxy-9-10-dihydrophenanthrene. *Biochemistry*, 33, 1043-1052.

75. Caccuri,A.M., Antonini,G., Nicotra,M., Battistoni,A., Lo Bello,M., Board,P.G., Parker,M.W., and Ricci,G. (1997) Catalytic mechanism and role of hydroxyl residues in the active site of theta class glutathione S-transferases. Investigation of Ser-9 and Tyr-113 in a glutathione S-transferase from the Australian sheep blowfly, *Lucilia cuprina*. *J.Biol.Chem.*, 272, 29681-29686.

76. Rossjohn,J., McKinstry,W.J., Oakley,A.J., Verger,D., Flanagan,J., Chelvanayagam,G., Tan,K.-L., Board,P.G., and Parker,M.W. (1998) Human theta class glutathione transferase: the crystal structure reveals a sulfate-binding pocket within a buried active site. *Structure*, 6, 309-322.

77. Casalone,E., Allocati,N., Ceccarelli,I., Masulli,M., Rossjohn,J., Parker,M.W., and Di Ilio,C. (1998) Site-directed mutagenesis of the *Proteus mirabilis* glutathione transferase B1-1 G-site. *FEBS Lett.*, 423, 122-124.

78. Bhargava,M.M., Listowsky,I., and Arias,I.M. (1978) Ligandin. Bilirubin binding and glutathione *S*-transferase activity are independent processes. *J.Biol.Chem.*, 253, 4112-4115.

79. Oakley,A.J., Lo Bello,M., Nuccetelli,M., Mazzetti,A.P., and Parker,M.W. (1999) The ligandin (non-substrate) binding site of human Pi class glutathione

transferase is located in the electrophile binding site (H-site). *J.Mol.Biol.*, 291, 913-926.

80. Singh,S.P., Janecki,A.J., Srivastava,S.K., Awasthi,S., Awasthi,Y.C., Xia,S.J., and Zimniak,P. (2002) Membrane association of glutathione *S*-transferase mGSTA4-4, an enzyme that metabolizes lipid peroxidation products. *J.Biol.Chem.*, 277, 4232-4239.

81. Barr,R.K., Kendrick,T.S., and Bogoyevitch,M.A. (2002) Identification of the critical features of a small peptide inhibitor of JNK activity. *J.Biol.Chem.*, 277, 10987-10997.

82. Goberdhan,D.C.I., Wilson,C. (1998) JNK, cytoskeletal regulator and stress response kinase? A *Drosophila* perspective. *BioEssays*, 20, 1009-1019.

83. Gustin,M.C., Albertyn,J., Alexander,M., and Davenport,K. (1998) MAP kinase pathways in the yeast *Saccharomyces cerevisiae*. *Microbiol.Mol.Biol.Rev.*, 62, 1264-1300.

84. Davis,R.J. (2000) Signal transduction by the JNK group of MAP kinases. *Cell*, 103, 239-252.

85. Adler,V., Yin,Z., Fuchs,S.Y., Benezra,M., Rosario,L., Tew,K.D., Pincus,M.R., Sardana,M., Henderson,C.J., Wolf,C.R., Davis,R.J., and Ronai,Z. (1999) Regulation of JNK signaling by GSTp. *EMBO J.*, 18, 1321-1334.

86. Cho,S.-G., Lee,Y.H., Park,H.-S., Ryoo,K., Kang,K.W., Park,J., Eom,S.-J., Kim,M.J., Chang,T.-S., Choi,S.-Y., Shim,J., Kim,Y., Dong,M.-S., Lee,M.-J., Kim,S.G., Ichijo,H., and Choi,E.-J. (2001) Glutathione *S*-transferase Mu modulates the stress-activated signals by suppressing apoptosis signal-regulating kinase 1. *J.Biol.Chem.*, 276, 12749-12755.

87. Kodym,R., Calkins,P., and Story,M. (1999) The cloning and characterization of a new stress response protein. A mammalian member of afamily of θ class glutathione S-transferase-like proteins. *J.Biol.Chem.*, 274, 5131-5137.

88. Lyon,R.P., Hill,J.J., and Atkins,W.M. (2003) Novel class of bivalent glutathione *S*-transferase inhibitors. *Biochemistry*, 42, 10418-10428.

89. Schaeffer,H.J., Weber,M.J. (1999) Mitogen-activated protein kinases: Specific messages from ubiquitous messengers. *Mol.Cell.Biol.*, 19, 2435-2444.

90. Kyriakis,J.M. (1998) Making the connection: coupling of stress-activated ERK/MAPK (extracellular-signal-regulated kinase/mitogen-activated protein kinase) core signalling modules to extracellular stimuli and biological responses. *Biochem.Soc.Symp.*, 64, 29-48.

91. Barr,R.K., Bogoyevitch,M.A. (2001) The c-Jun N-terminal protein kinase family of mitogen-activated protein kinases (JNK MAPKs). *IJBCB*, 33, 1047-1063.

92. Kyriakis,J.M., Avruch,J. (2001) Mammalian mitogen-activated protein kinase signal transduction pathways activated by stress and inflammation. *Physiol.Rev.*, 81, 807-869.

93. Ip,Y.T., Davis,R.J. (1998) Signal transduction by the c-Jun N-terminal kinase (JNK)-from inflammation to development. *Curr.Opin.Cell Biol.*, 10, 205-219.

94. Whitmarsh,A.J., Davis,R.J. (1996) Transcription factor AP-1 regulation by mitogen-activated protein kinase signal transduction pathways. *J.Mol.Med.*, 74, 589-607.

95. Lu,X., Nemoto,S., and Lin,A. (1997) Identification of c-Jun NH2-terminal protein kinase (JNK)-activating kinase 2 as an activator of JNK but not p38. *J.Biol.Chem.*, 272, 24751-14754.

96. Tournier,C., Whitmarsh,A.J., Cavanagh,J., Barrett,T., and Davis,R.J. (1997) Mitogen-activated protein kinase kinase 7 is an activator of the c-Jun NH2-terminal kinase. *Proc.Natl.Acad.Sci.USA*, 94, 7337-7342.

97. Tournier,C., Whitmarsh,A.J., Cavanagh,J., Barrett,T., and Davis,R.J. (1999) The *MKK7* gene encodes a group of c-Jun NH2 -terminal kinase kinases. *Mol.Cell.Biol.*, 19, 1569-1581.

98. Hibi,M., Lin,A., Smeal,T., Minden,A., and Karin,M. (1993) Identification of an oncoprotein- and UV-responsive protein kinase that binds and potentiates the c-Jun activation domain. *Genes Develop.*, 7, 2135-2148.

99. Gupta,S., Campbell,D., Derijard,B., and Davis,R.J. (1995) Transcription factor ATF2 regulation by the JNK signal transduction pathway. *Science*, 267, 389-393.

100. Whitmarsh,A.J., Shore,P., Sharrocks,A.D., and Davis,R.J. (1995) Integration of MAP kinase signal transduction pathways at the serum response element. *Science*, 269, 403-407.

101. Minden,A., Karin,M. (1997) Regulation and function of the JNK subgroup of MAP kinases. *Biochim.Biophys.Acta*, 1333, F85-F104.

102. Gupta,S., Barrett,T., Whitmarsh,A.J., Cavanagh,J., Sluss,H.K., Derijard,B., and Davis,R.J. (1996) Selective interaction of JNK protein kinase isoforms with transcription factors. *EMBO J.*, 15, 2760-2770.

103. Sluss,H.K., Han,Z., Barrett,T., Davis,R.J., and Ip,Y.T. (1996) A JNK signal transduction pathway that mediates morphogenesis and immune response in *Drosophila*. *Genes Develop.*, 10, 2745-2758.

104. Sluss,H.K., Han,Z., Barrett,T., Davis,R.J., and Ip,Y.T. (1996) A JNK signal transduction pathway that mediates morphogenesis and immune response in *Drosophila*. *Genes Develop.*, 10, 2745-2758.

105. Riesgo-Escovar,J.R., Hafen,E. (1997) *Drosophila* Jun kinase regulates expression of *Decapentaplegic* via the ETS-domain protein Aop and the AP-1 transcription factor DJun during dorsal closure. *Genes Develop.*, 11, 1717-1727.

106. Holland,P.M., Suzanne,M., Campbell,J.S., Noselli,S., and Cooper,J.A. (1997) MKK7 is a stress-activated mitogen-activated protein kinase kinase functionally related to *hemipterous*. *J.Biol.Chem.*, 272, 24994-24998.

107. Glise,B., Bourbon,H., and Noselli,S. (1995) *hemipterous* encodes a novel Drosophila MAP kinase kinase, required for epithelial cell sheet movement. *Cell*, 83, 451-461.

108. Glise,B., Noselli,S. (1997) Coupling of Jun amino-terminal kinase and decapentaplegic signaling pathways in *Drosophila* morphogenesis. *Genes Develop.*, 11, 1738-1747.

109. Hou,X.S., Goldstein,E.S., and Perrimon,N. (1997) *Drosophila* Jun relays the Jun amino-terminal kinase signal transduction pathway to the Decapentaplegic signal transduction pathway in regulating epithelial cell sheet movement. *Genes Develop.*, 11, 1728-1737.

110. Kockel,L., Zeitlinger,J., Staszewski,L.M., Mlodzik,M., and Bohmann,D. (1997) Jun in *Drosophila* development: redundant and nonredundant functions and regulation by two MAPK signal transduction pathways. *Genes Develop.*, 11, 1748-1758.

111. Noselli,S., Agne`s,F. (1999) Roles of the JNK signaling pathway in *Drosophila* morphogenesis. *Current Opinion in Genetics & Development*, 9, 466-472.

112. Xie,X., Gu,Y., Fox,T., Coll,J.T., Fleming,M.A., Markland,W., Caron,P.R., Wilson,K.P., and Su,M.S.S. (1998) Crystal structure of JNK3: a kinase implicated in neuronal apoptosis. *Structure*, 6, 983-991.

113. Pearson,G., Robinson,F., Gibson,T.B., Xu,B., Karandikar,M., Berman,K., and Cobb,M.H. (2001) Mitogen-activated protein (MAP) kinase pathways: regulation and physiological functions. *Endocrine Reviews*, 22, 153-183.

114. Chen,R.-H., Abate,C., and Blenis,J. (1993) Phosphorylation of the c-Fos transrepression domain by mitogen-activated protein kinase and 90-kDa ribosomal S6 kinase. *Proc.Natl.Acad.Sci.USA*, 90, 10952-10956.

115. Hai,T., Curran,T. (1991) Cross-family dimerization of transcription factors Fos/Jun and ATF/CREB alters DNA binding specificity. *Proc.Natl.Acad.Sci.USA*, 88, 3720-3724.

116. Xia,C.L., Cowell,I.G., Dixon,K.H., Pemble,S.E., Ketterer,B., and Taylor,J.B. (1991) Glutathione transferase π its minimal, promoter and downstream cis-acting element. *Biochem.Biophys.Res.Comm.*, 176, 233-240.

117. Yokoyama,Y., Sagara,M., Sato,S., and Saito,Y. (1998) Value of glutathione S-transferase p and the oncogene products c-Jun, c-Fos, c-H-Ras, and c-Myc as a prognostic indicator in endometrial carcinomas. *Gynecol.Oncol.*, 68, 280-287.

118. Seimiya,H., Mashima,T., Toho,M., and Tsuruo,T. (1997) c-Jun NH2-terminal kinase-mediated activation of interleukin-1β converting enzyme/CED-3-like protease during anticancer drug-induced apoptosis. *J.Biol.Chem.*, 272, 4631-4636.

119. Chen,Y.-R., Wang,X., Templeton,D., Davis,R.J., and Tan,T.-H. (1996) The role of c-Jun N-terminal kinase (JNK) in apoptosis induced by ultraviolet C and γ Radiation. Duration of JNK activation may determine cell death and proliferation. *J.Biol.Chem.*, 271, 31929-31936.

120. Juo,P., Kuo,C.J., Reynolds,S.E., Konz,R.F., Raingeaud,J., Davis,R.J., Biemann,H.-P., and Blenis,J. (1997) Fas activation of the p38 mitogen-activated protein kinase signalling pathway requires ICE/CED-3 family proteases. *Mol.Cell.Biol.*, 17, 24-35.

121. Lenczowski,J.M., Dominguez,L., Eder,A.M., King,L.B., Zacharchuk,C.M., and Ashwell,J.D. (1997) Lack of a role for Jun kinase and AP-1 in Fas-induced apoptosis. *Mol.Cell.Biol.*, 17, 170-181.

122. Xia,Z., Dickens,M., Raingeaud,J., Davis,R.J., and Greenberg,M.E. (1995) Opposing effects of ERK and JNK-p38 MAP kinases on apoptosis. *Science*, 270, 1326-1331.

123. Butterfield,L., Storey,B., Maas,L., and Heasley,L.E. (1997) c-Jun NH2 -terminal kinase regulation of the apoptotic response of small cell lung cancer cells to ultraviolet radiation. *J.Biol.Chem.*, 272, 10110-10116.

124. Stronach,B.E., Perrimon,N. (1999) Stress signaling in *Drosophila*. *Oncogene*, 18, 6172-6182.

125. Sharrocks,A.D., Yang,S.-H., and Galanis,A. (2000) Docking domains and substrate specificity determination for MAP kinases. *TIBS*, 25, 448-453.

126. Tanoue,T., Adachi,M., Moriguchi,T., and Nishida,E. (2000) A conserved docking motif in MAP kinases common to substrates, activators and regulators. *Nature Cell Biology*, 2, 110-116.

127. Xu,B., Stippec,S., Robinson,F.L., and Cobb,M.H. (2001) Hydrophobic as well as charged residues in both MEK1 and ERK2 are important for their proper docking. *J.Biol.Chem.*, 276, 26509-26515.

128. Tanoue,T., Maeda,R., Adachi,M., and Nishida,E. (2001) Identification of a docking groove on ERK and p38 MAP kinases that regulates the specificity of docking interactions. *EMBO J.*, 20, 466-479.

129. Eblen,S.T., Catling,A.D., Assanah,M.C., and Weber,M.J. (2001) Biochemical and biological functions of the N-terminal, noncatalytic domain of extracellular signal-regulated kinase 2. *Mol.Cell.Biol.*, 21, 249-259.

130. Brunet,A., Pouyssegur,J. (1996) Identification of MAP kinase domains by redirecting stress signals into growth factor responses. *Science*, 272, 1652-1655.

131. Bardwell,A.J., Flatauer,L.J., Matsumoto,K., Thorner,J., and Bardwell,L. (2001) A conserved docking site in MEKs mediates high-affinity binding to

MAP kinases and cooperates with a scaffold protein to enhance signal transmission. *J.Biol.Chem.*, 276, 10374-10386.

132. Enslen,H., Brancho,D.M., and Davis,R.J. (2000) Molecular determinants that mediate selective activation of p38 MAP kinase isoforms. *EMBO J.*, 19, 1301-1311.

133. Fantz,D.A., Jacobs,D., Glossip,D., and Kornfeld,K. (2001) Docking sites on substrate proteins direct extracellular signal regulated kinase to phosphorylate specific residues. *J.Biol.Chem.*, 276, 27256-27265.

134. Whitmarsh,A.J., Cavanagh,J., Tournier,C., Yasuda,J., and Davis,R.J. (1998) A mammalian scaffold complex that selectively mediates MAP kinase activation. *Science*, 281, 1671-1674.

135. Harding,T.C., Xue,L., Bienemann,A., Haywood,D., Dickens,M., Tolkovsky,A.M., and Uney,J.B. (2001) Inhibition of JNK by overexpression of the JNK binding domain of JIP-1 prevents apoptosis in sympathetic neurons. *J.Biol.Chem.*, 276, 4531-4534.

136. Neel,B.G., Tonks,N.K. (1997) Protein tyrosine phosphatases in signal transduction. *Curr.Opin.Cell Biol.*, 9, 193-204.

137. Jin,D.-Y., Teramoto,H., Giam,C.-Z., Chun,R.F., Gutkind,J.S., and Jeang,K.-T. (1997) A human suppressor of c-jun N-terminal kinase 1 activation by tumor necrosis factor α. *J.Biol.Chem.*, 272, 25816-25823.

138. Wang,T., Arifoglu,P., Ronai,Z., and Tew,K.D. (2001) Glutathione *S*-transferase P1-1 (GSTP1-1) inhibits c-Jun N-terminal kinase (JNK1) signaling through interaction with the C terminus. *J.Biol.Chem.*, 276, 20999-21003.

139. Elsby,R., Kitteringham,N.R., Goldring,C.E., Lovatt,C.A., Chamberlain,M., Henderson,C.J., Wolf,C.R., and Park,B.K. (2003) Increased constitute c-Jun N-terminal kinase signaling in mice lacking glutathione *S*-transferase Pi. *J.Biol.Chem.*, 278, 22243-22249.

140. Ishisaki,A., Hayashi,H., Suzuki,S., Ozawa,K., Mizukoshi,E., Miyakawa,K., Suzuki,M., and Imamura,T. (2001) Glutathione *S*-transferase Pi is a dopamine-inducible suppressor of dopamine-induced apoptosis in PC12 cells. *Journal of Neurochemistry*, 77, 1362-1371.

141. Bernardini,S., Bernassola,F., Cortese,C., Ballerini,S., Melino,G., Motti,C., Bellincampi,L., Iori,R., and Federici,G. (2001) Glutathione *S*-transferase P1-1 involvement during apoptosis induced by H_2O_2 and etoposide. *Chem Biol Interact*, 133, 308-311.

142. Yin,Z., Ivanov,V.N., Habelhah,H., Tew,K., and Ronai,Z. (2000) Glutathione *S*-transferase p elicits protection against H_2O_2 -induced cell death via coordinated regulation of stress kinases. *Cancer Res.*, 60, 4053-4057.

143. Vararattanavech,A., Ketterman,A. (2003) Multiple roles of glutathione binding-site residues of glutathione S-transferase. *Protein and Peptide Letters*, 10, 441-448.

144. Wolter,S., Mushinski,J.F., Saboori,A.M., Resch,K., and Kracht,M. (2001) Inducible expression of a constitutively active mutant of MAP kinase kinase (MKK) 7 specifically activates JUN N-terminal protein kinase (JNK), alters expression of at least nine genes, and inhibits cell proliferation. *J.Biol.Chem.*.

145. Bradford,M.M. (1976) A rapid and sensitive method for the quantitation of microgram quantities of protein utilizing the principle of protein-dye binding. *Anal.Biochem.*, 72, 248-254.

146. Habig,W.H., Pabst,M.J., and Jakoby,W.B. (1974) Glutathione S-transferases. The first enzymatic step in mercapturic acid formation. *J.Biol.Chem.*, 249, 7130-7139.

147. Zhang,K., Chaillet,J.R., Perkins,L.A., and Halazonetis,T.D. (1990) *Drosophila* homolog of the mammalian *jun* oncogene is expressed during embryonic

development and activates transcription in mammalian cells. *Proc.Natl.Acad.Sci.USA*, 87, 6281-6285.

148. Nilsson,L.O., Gustafsson,A., and Mannervik,B. (2000) Redesign of substrate-selectivity determining modules of glutathione transferase A1–1 installs high catalytic efficiency with toxic alkenal products of lipid peroxidation. *Proc.Natl.Acad.Sci.USA*, 97, 9408-9412.

149. Pal,A., Gu,Y., Pan,S.-S., Ji,X., and Singh,S.V. (2001) C-terminal region amino acid substitutions contribute to catalytic differences between murine class alpha glutathione transferases mGSTA1-1 and mGSTA2-2 toward anti-diol epoxide isomers of benzo[c]phenanthrene. *Biochemistry*, 40, 7047-7053.

150. Udomsinprasert,R., Ketterman,A.J. (2002) Expression and Characterization of a Novel Class of Glutathione S-Transferase from *Anopheles dirus*. *Insect Biochem.Molec.Biol.*, 32, 425-433.

151. Ketterman,A.J., Prommeenate,P., Boonchauy,C., Chanama,U., Leetachewa,S., Promtet,N., and Prapanthadara,L. (2001) Single amino acid changes outside the active site significantly affect activity of glutathione S-transferases. *Insect Biochem.Molec.Biol.*, 31, 65-74.

152. Anderson,W.B., Board,P.G., Gargano,B., and Anders,M.W. (1999) Inactivation of Glutathione Transferase Zeta by Dichloroacetic Acid and Other Fluorine-Lacking r-Haloalkanoic Acids. *Chem.Res.Toxicol.*, 12, 1144-1149.

153. Tong,Z., Board,P.G., and Anders,M.W. (1998) Glutathione transferase zeta catalyses the oxygenation of the carcinogen dichloroacetic acid to glyoxylic acid. *Biochem.J.*, 331, 371-374.

154. Tzeng,H.-F., Blackburn,A.C., Board,P.G., and Anders,M.W. (2000) Polymorphism- and Species-Dependent Inactivation of Glutathione Transferase Zeta by Dichloroacetate. *Chem.Res.Toxicol.*, 13, 231-236.

155. Thom,R., Dixon,D.P., Edwards,R., Cole,D.J., and Lapthorn,A.J. (2001) The Structure of a Zeta Class Glutathione S-Transferase from Arabidopsis thaliana: Characterisation of a GST with Novel Active-site Architecture and a Putative Role in Tyrosine Catabolism. *J.Mol.Biol.*, 308, 949-962.

156. Polekhina,G., Board,P.G., Blackburn,A.C., and Parker,M.W. (2001) Crystal Structure of Maleylacetoacetate Isomerase/Glutathione Transferase Zeta Reveals the Molecular Basis for Its Remarkable Catalytic Promiscuity. *Biochemistry*, 40, 1567-1576.

157. Dixon,M., Webb,E.C. (1979) Enzymes. Academic Press Inc., New York, pp. 332-467.

158. Allardyce,C.S., McDonagh,P.D., Lian,L.-Y., Wolf,C.R., and Roberts,G.C.K. (1999) The role of tyrosine-9 and the C-terminal helix in the catalytic mechanism of Alpha-class glutathione S-transferases. *Biochem.J.*, 343, 525-531.

159. Ferrell,J.E.Jr. (1996) Tripping the switch fantastic: how a protein kinase cascade can convert graded inputs into switch-like outputs. *TIBS*, 21, 460-466.

160. Nuccetelli,M., Mazzetti,A.P., Rossjohn,J., Parker,M.W., Board,P., Caccuri,A.M., Federici,G., Ricci,G., and Lo Bello,M. (1998) Shifting substrate specificity of human glutathione transferase (from class pi to class alpha) by a single point mutation. *Biochem.Biophys.Res.Comm.*, 252, 184-189.

161. Buschmann,T., Potapova,O., Bar-Shira,A., Ivanov,V.N., Fuchs,S.Y., Henderson,S., Fried,V.A., Minamoto,T., Alarcon-Vargas,D., Pincus,M.R., Gaarde,W.A., Holbrook,N.J., Shiloh,Y., and Ronai,Z. (2003) Jun NH2-terminal kinase phosphorylation of p53 on Thr-81 is important for p53 stabilization and transcriptional activities in response to stress. *Mol.Cell.Biol.*, 21, 2743-2754.

162. Fuchs,S.Y., Adler,V., Pincus,M.R., and Ronai,Z. (1998) MEKK1/JNK signaling stabilizes and activates p53. *Proc.Natl.Acad.Sci.USA*, 95, 10541-10546.

163. Fuchs,S.Y., Tappin,I., and Ronai,Z. (2000) Stability of the ATF2 transcription factor is regulated by phosphorylation and dephosphorylation. *J.Biol.Chem.*, 275, 12560-12564.

164. Hemingway,J., Hawkes,N., Prapanthadara,L., Jayawardena,K.G.I., and Ranson,H. (1998) The role of gene splicing, gene amplification and regulation in mosquito insecticide resistance. *Phil.Trans.R.Soc.Lond.B*, 353, 1695-1699.

165. Jeng,S.S., Wan,W.C., and Chang,C.F. (1978) Existence of an estrogen-like compound in the ovary of the shrimp *Parapenaeus fissurus*. *Gen.Comp.Endocrinol.*, 36, 211-214.

166. Ziegler,R., Ibrahim,M.M. (2001) Formation of lipid reserves in fat body and eggs of the yellow fever mosquito, *Aedes aegypti*. *Journal of Insect Physiology*, 47, 623-627.

167. Briegel,H., Gut,T., and Lea,A.O. (2003) Sequential deposition of yolk components during oogenesis in an insect, *Aedes aegypti* (Diptera: Culicidae). *J.Insect Physiol.*, 49, 249-260.

168. Leaver,M.J., Wright,J., and George,S.G. (1997) Structure and expression of a cluster of glutathione S-transferase genes from a marine fish, the plaice (*Pleuronectes platessa*). *Biochem.J.*, 321, 405-412.

169. Warnecke,C., Willich,T., Holzmeister,J., Bottari,S.P., and Fleck,E. (1999) Efficient transcription of the human angiotensin II type 2 receptor gene requires intronic sequence elements. *Biochem.J.*, 340, 17-24.

170. Anders,M.W., Anderson,W.B., Tzeng,H.-F., and Board,P.G. (2001) Glutathione transferase zeta: novel xenobiotic substrates and enzyme inactivation. *Chem Biol Interact*, 133, 211-216.

171. Berhane,K., Widersten,M., Engstrom,A., Kozarich,J.W., and Mannervik,B. (1994) Detoxication of base propenals and other a,b-unsaturated aldehyde

products of radical reactions and lipid peroxidation by human glutathione transferases. *Proc.Natl.Acad.Sci.USA*, 91, 1480-1484.

172. Ishikawa,T., Esterbauer,H., and Sies,H. (1986) Role of cardiac glutathione transferase and of the glutathione S-conjugate export system in biotransformation of 4-hydroxynonenal in the heart. *J.Biol.Chem.*, 261, 1576-1581.

173. Yang,Y., Cheng,J.-Z., Singhal,S.S., Saini,M., Pandya,U., Awasthi,S., and Awasthi,Y.C. (2001) Role of glutathione *S*-transferases in protection against lipid peroxidation. Overexpression of hGSTA2-2 in K562 cells protects against hydrogen peroxide induced apoptosis and inhibits JNK and caspase 3 activation. *J.Biol.Chem.*, 276, 19220-19230.

174. Ranson,H., Claudianos,C., Ortelli,F., Abgrall,C., Hemingway,J., Sharakhova,M.V., Unger,M., Collins,F.H., and Feyereisen,R. (2002) Evolution of supergene families associated with insecticide resistance. *Science*, 298, 179-181.

175. Fournier,D., Bride,J.-M., Poirie,M., Berge,J.-B., and Plapp,F.W. (1992) Insect glutathione S-transferases. Biochemical characteristics of the major forms from houseflies susceptible and resistant to insecticides. *J.Biol.Chem.*, 267, 1840-1845.

176. Yasuda,J., Whitmarsh,A.J., Cavanagh,J., Sharrma,M., and Davis,R.J. (1999) The JIP group of mitogen-activated protein kinase scaffold proteins. *Mol.Cell.Biol.*, 19, 7245-7254.

177. Nihalani,D., Meyer,D., Pajni,S., and Holzman,L.B. (2001) Mixed lineage kinase-dependent JNK activation is governed by interactions of scaffold protein JIP with MAPK module components. *EMBO J.*, 20, 3447-3458.

178. Adler,V., Pincus,M.R., Minamoto,T., Fuchs,S.Y., Bluth,M.J., Brandt-Rauf,P.W., Friedman,F.K., Robinson,R.C., Chen,J.M., Wang,X.W., Harris,C.C., and

Ronai,Z. (1997) Conformation-dependent phosphorylation of p53. *Proc.Natl.Acad.Sci.USA*, 94, 1686-1691.

179. Ma,B., Elkayam,T., Wolfson,H., and Nussinov,R. (2003) Protein–protein interactions: Structurally conserved residues distinguish between binding sites and exposed protein surfaces. *Proc.Natl.Acad.Sci.USA*, 100, 5772-5777.

180. Hu,Z., Ma,B., Wolfson,H., and Nussinov,R. (2000) Conservation of polar residues as hot spots at protein interfaces. *Proteins*, 39, 331-342.

181. Mever,M., Wilson,P., and Schomburg,D. (1996) Hydrogen bonding and molecular surface shape complementarily as a basis for protein docking. *J.Mol.Biol.*, 264, 199-210.

182. Hansson,L.O., Bolton-Grob,R., Massoud,T., and Mannervik,B. (1999) Evolution of differential substrate specificities in mu class glutathione transferases probed by DNA shuffling. *J.Mol.Biol.*, 287, 265-276.

183. Stites,W.E. (1997) Protein-protein interactions: Interface structure, binding thermodynamics, and mutational analysis. *Chem Rev*, 97, 1233-1250.

184. Fayos,R., Melacini,G., Burns,L., Scott,J.D., and Jennings,P.A. (2003) Induction of flexibility through protein-protein interactions. *J.Biol.Chem.*.

185. Oakley,A.J., Lo Bello,M., Ricci,G., Federici,G., and Parker,M.W. (1998) Evidence for an induced-fit mechanism operating in Pi class glutathione transferases. *Biochemistry*, 37, 9912-9917.

186. Neuefeind,T., Huber,R., Dasenbrock,H., Prade,L., and Bieseler,B. (1997) Crystal structrure of herbicide-detoxifying maize glutathione S-transferase-I in Complex with lactoylglutathione: evidence for an induced-fit mechanism. *J.Mol.Biol.*, 274, 446-453.

187. Manoharan,T.H., Gulick,A.M., Puchalski,R.B., Servias,A.L., and Fahl,W.E. (1992) Structural studies on human glutathione S-transferase π.

Substitution mutations to determine amino acids necessary for binding glutathione. *J.Biol.Chem.*, 267, 18940-18945.

188. Tan,K.-L., Chelvanayagam,G., Parker,M.W., and Board,P.G. (1996) Mutagenesis of the active site of the human theta-class glutathione transferase GSTT2-2: catalysis with different substrates involves different residues. *Biochem.J.*, 319, 315-321.

189. Wallace,L.A., Burke,J., and Dirr,H.W. (2000) Domain-domain interface packing at conserved Trp-20 in class α glutathione transferase impacts on protein stability. *Biochim.Biophys.Acta*, 1478, 325-332.

190. Stenberg,G., Abdalla,A.-M., and Mannervik,B. (2000) Tyrosine 50 at the subunit interface of dimeric human glutathione transferase P1-1 is a structural key residue for modulating protein stability and catalytic function. *Biochem.Biophys.Res.Comm.*, 271, 59-63.

191. Robertson,A.D. (2002) Intramolecular interactions at protein surfaces and their impact on protein function. *TIBS*, 27, 521-526.

192. Xia,H., Gu,Y., Pan,S.S., Ji,X., and Singh,S.V. (2001) Amino acid substitutions at positions 207 and 221 contribute to catalytic differences between murine glutathione S-transferase A1-1 and A2-2 toward (+)-anti-7,8-dihydroxy-9,10-epoxy-7,8,9, 10-tetrahydrobenzo[a]pyrene. *Biochemistry*, 38, 19824-19830.

193. Wilhelm,D., Bender,K., Knebel,A., and Angel,P. (1997) The level of intracellular glutathione is a key regulator for the induction of stress-activated signal transduction pathways including Jun N-terminal protein kinases and p38 kinase by alkylating agents. *Mol.Cell.Biol.*, 17, 4792-4800.

194. Ward,N.E., Pierce,D.S., Chung,S.E., Gravitt,K.R., and O'Brian,C.A. (1998) Irreversible inactivation of protein kinase C by glutathione. *J.Biol.Chem.*, 273, 12558-12566.

195. Liu,B., Hannun,Y.A. (1997) Inhibition of the neutral magnesium-dependent sphingomyelinase by glutathione. *J.Biol.Chem.*, 272, 16281-16289.

APPENDIX

Publications from the Ph.D. project

1. **Udomsinprasert,R**.; Bogoyevitch,M.A.; Ketterman,A.J. (2004). Reciprocal regulation of glutathione *S*-transferase spliceforms and the *Drosophila* c-Jun N-terminal Kinase pathway components. Biochem.J. 383, 483-490.

2 **Udomsinprasert,R**.; Pongjaroenkit,S.; Wongsantichon,J.; Oakley,A.J.; Prapanthadara,L.; Wilce,M.C.J.; Ketterman,A.J. (2005) Identification, characterization and structure of a new delta class glutathione transferase isoenzyme. Biochem.J. In Press Immediate publication doi: 10.1040/BJ20042015.

Reciprocal regulation of glutathione S-transferase spliceforms and the *Drosophila* c-Jun N-terminal kinase pathway components

Rungrutai UDOMSINPRASERT*, Marie A. BOGOYEVITCH† and Albert J. KETTERMAN*[1]

*Institute of Molecular Biology and Genetics, Mahidol University, Salaya Campus, Nakorn Pathom 73170, Thailand, and †Cell Signalling Laboratory, Biochemistry and Molecular Biology, University of Western Australia, 35 Stirling Highway, Crawley, WA 6009, Australia

In mammalian systems, detoxification enzymes of the GST (glutathione S-transferase) family regulate JNK (c-Jun N-terminal kinase) signal transduction by interaction with JNK itself or other proteins upstream in the JNK pathway. In the present study, we have studied GSTs and their interaction with components of the JNK pathway from *Diptera*. We have evaluated the effects of four Delta class *Anopheles dirus* GSTs, GSTD1-1, GSTD2-2, GSTD3-3 and GSTD4-4, on the activity of full-length recombinant *Drosophila* HEP (mitogen-activated protein kinase kinase 7; where HEP stands for hemipterous) and the *Drosophila* JNK, as well as the reciprocal effect of these kinases on GST activity. Interestingly, even though these four GSTs are alternatively spliced products of the same gene and share > 60 % identity, they exerted different effects on JNK activity. GSTD1-1 inhibited JNK activity, whereas the other three GST isoforms activated JNK. GSTD2-2, GSTD3-3 and GSTD4-4 were inhibited 50–80 % by HEP or JNK but GSTD1-1 was not inhibited by JNK. However, there were some similarities in the actions of HEP and JNK on these GSTs. For example, binding constants for HEP or JNK inhibiting a GST were similar (20–70 nM). Furthermore, after incubation of the GSTs with JNK, both JNK and the GSTs changed catalytic properties. The substrate specificities of both GSTs and JNK were also altered after their co-incubation. In addition, glutathione modulated the effects of JNK on GST activity. These results emphasize that different GST spliceforms possess different properties, both in their catalytic function and in their regulation of signalling through the JNK pathway.

Key words: c-Jun N-terminal kinase (JNK), *Drosophila*, glutathione S-transferase, hemipterous (HEP; MKK7), JNK activity regulation, mosquito.

INTRODUCTION

GSTs (glutathione S-transferases; EC 2.5.1.18) are a superfamily of multifunctional enzymes involved in normal cellular metabolism as well as in the detoxification of various hydrophobic endogenous and xenobiotic compounds [1]. The central importance of GSTs in detoxification lies in their unique capacity to conjugate glutathione with a wide variety of compounds [2]. This detoxification reaction is of critical importance in cell survival. As a consequence, GSTs have been found in virtually all organisms and are currently grouped into at least ten classes based on their primary sequence similarity, substrate specificity, immunological properties, and tertiary and quaternary structures [3]. Changes in glutathione levels have also been associated with the activation of a stress response [4] and GSTs can protect against electrophiles and oxidative stress by altering cellular glutathione levels [1]. GSTs also have glutathione peroxidase activity under conditions of oxidative stress and they have been further implicated in a range of physiological roles such as signal transduction, cell proliferation, differentiation and apoptosis [5].

Various classes of GSTs have been shown to be involved in these broader physiological roles. For example, GST Omega protected cells from apoptosis induced by Ca^{2+} mobilization from intracellular stores through its ability to regulate the Ca^{2+} channel activity of the ryanodine receptor [6]. Since the Bcl-2 family member Bax regulates programmed cell death by promoting apoptosis [7], a role for GST Theta in regulation of apoptotic cell death has also been suggested following its identification as a Bax-interacting protein [8].

Other interactions of GSTs to alter intracellular signal-transduction events have been reported. Most often these implicate GST in the regulation of the JNK (c-Jun N-terminal kinase) signal-transduction pathway. JNK is a member of the MAPK (mitogen-activated protein kinase) family, which is conserved across all eukaryotes ranging from yeast and insects to mammals [9]. JNK has been implicated in a variety of biological functions in response to stress, and the transmission of signals through the JNK pathway is achieved by sequential phosphorylation and activation of the pathway kinase components, the MKKKs (MAP kinase kinase kinase), the MKKs and the MAPKs. The activation of JNK relays extracellular cues to transcription factors such as c-Jun [10], activating transcription factor 2 [11] and Elk1 [12], thereby regulating gene expression, cellular homoeostasis, differentiation, apoptosis and cell death. Not only is the induction of c-*jun* and c-*fos* transcription dependent on JNK, but Jun and Fos can also induce the transcription of xenobiotic-metabolizing enzymes such as GST [13]. Thus c-Jun is directly involved in GST Pi expression *in vivo* [14]. This suggests a role of JNK in the induction of a cellular defence programme against cytotoxic xenobiotics.

JNK pathway components and GSTs are evolutionally conserved across mammals and insects. Different mammalian GST classes such as GST Pi and GST Mu have been reported to interact with different stress kinase proteins in the JNK pathway. For example, GST Pi is a JNK regulatory protein, and its association with JNK maintains a low basal level of JNK activity in the non-stressed cell [15]. The lack of GST Pi increased constitutive JNK activity *in vivo* and, therefore, regulated the expression of genes that were specific downstream targets of the JNK pathway [16].

Abbreviations used: ASK1, apoptosis signal-regulating kinase 1; CDNB, 1-chloro-2,4-dinitrobenzene; DCNB, 1,2-dichloro-4-nitrobenzene; GST, glutathione S-transferase; HEP, hemipterous; JNK, c-Jun N-terminal kinase; MAPK, mitogen-activated protein kinase; MKK, MAP kinase kinase; PNBC, *p*-nitrobenzyl chloride; PNPB, *p*-nitrophenyl bromide.

[1] To whom correspondence should be addressed (email frakt@mahidol.ac.th).

Moreover, GST Pi co-ordinates ERK/p38/IKK activation as part of the mechanism underlying its ability to elicit protection against H_2O_2-induced cell death [17]. In contrast, GST Mu interacts with ASK1 (apoptosis signal-regulating kinase 1), an upstream activating kinase of JNK that participates in cell death [18].

In the present study, we evaluate the interaction of GST and kinase proteins in a *Dipteran* system using four different spliceforms of *Anopheles dirus* Delta class GSTs and two different *Drosophila* kinase proteins, *Drosophila* HEP7 (where HEP stands for hemipterous) and *Drosophila* JNK (JNK). The *Drosophila* JNK pathway, viewed as a linear cascade [19], comprises the *Hemipterous* (HEP or DMKK7) [20], *basket* (JNK) [21] and *D-Jun* [22], which are homologous proteins with mammalian MKK7, JNK and c-Jun respectively. The four *Anopheles* GSTs used in the present study are alternatively spliced products from a single gene [23]. To elucidate the mechanism by which GSTs modulate the JNK signalling pathway, we assessed both GST and kinase activities to provide evidence for direct protein–protein interactions and to measure the binding affinity. Our results show that the GSTs interact with protein kinases, the different GST isoforms appear to possess different regulatory mechanisms in the JNK pathway and JNK interaction also affects GST activities. This is the first report of the reciprocal regulation of GST and JNK pathway activities.

EXPERIMENTAL

Preparation of DNA constructs

The alternatively spliced products, GSTD1-1, GSTD2-2, GSTD3-3 and GSTD4-4, were cloned into a pET3a vector [24]. The recombinant proteins in the *Drosophila* JNK pathway consisting of *Drosophila* HEP7 (HEP; GenBank® accession number AAB63449.1), *Drosophila* JNK (JNK and also known as *basket*; GenBank® accession number AAB97094.1) and the transactivation domain of *Drosophila* Jun (amino acids 1–104; Jun 1–104; GenBank® accession number P18289) were obtained by reverse transcriptase–PCR from adult *Drosophila melanogaster*. The PCR products were then cloned into a pET28b vector (Stratagene). The HEP recombinant plasmid was also used as the template for a site-directed mutagenesis method to construct a constitutively active HEP mutant (HEP_{3E}). The mammalian MKK7-β1 isoform mutant ($MKK7_{3E}$) has constitutive kinase activity after the substitutions of Ser^{271}, Thr^{275} and Ser^{277} to Glu [25]; we therefore altered the three homologous residues (Ser^{348}, Thr^{352} and Ser^{354}) of *Drosophila* HEP7 to Glu by two-step PCR using a Quik Change™ site-directed mutagenesis kit (Stratagene). All recombinant clones were identified by restriction-digest of the plasmids and confirmed by full-length sequencing in both directions using a BigDye™ Terminator Cycle Sequencing kit (PerkinElmer).

Preparation of recombinant proteins

GST proteins were expressed and purified using either GSTrap or S-hexyl-glutathione affinity chromatography [24]. The four recombinant proteins, HEP, HEP_{3E}, JNK and Jun 1–104, were expressed as histidine fusion proteins. The JNK and Jun 1–104 recombinant proteins were expressed as soluble proteins and purified using a standard Ni^{2+}-nitrilotriacetate column method (Amersham Biosciences). In contrast, HEP and HEP_{3E} recombinant proteins were expressed mainly in inclusion bodies. Therefore these HEP and HEP_{3E} were purified using Ni^{2+}-nitrilotriacetate column chromatography under denaturing conditions and renatured by slow dialysis using the Roti®-Fold reagent (Carl Roth GmbH+, Karlsruhe, Germany). Protein concentrations were determined using the BioRad protein reagent with BSA as the standard [26].

GST activity assays

GST activity was measured by the conjugation of GSH with the hydrophobic substrates CDNB (1-chloro-2,4-dinitrobenzene; Aldrich), DCNB (1,2-dichloro-4-nitrobenzene; Fluka, Buchs, Switzerland), PNBC (*p*-nitrobenzyl chloride; Aldrich) and PNPB (*p*-nitrophenyl bromide; Aldrich) [24]. We used the CDNB conjugation as our standard assay because GST-specific activity for this substrate was highest [24].

Effects of protein kinases HEP and JNK on GST activity

The effects of HEP and JNK on GST activity were examined by incubating GSTs and kinase proteins in a 1:1 molar ratio at room temperature (27–30 °C) for 5 min. GST activity was measured in the presence and absence of kinase proteins. The effects on GST activity were evaluated by the following methods.

(i) *The percentage inhibition of GST activity*. The percentage inhibition was determined by measuring GST activity in the presence of HEP or JNK as well as without kinase proteins as the control.

(ii) *The type of inhibition and affinity binding* (K_i). GST and kinase protein interactions were performed by varying the concentration of CDNB from 0.05 to 3.0 mM and measuring the kinetic parameters for CDNB and GSH conjugation [24]. The kinetic parameters and K_i were determined by both linear and non-linear regression analysis using GraphPad Prism 2.01 software.

(iii) *The change of GST substrate specificity by JNK*. GST and JNK were incubated in a 1:1 molar ratio and the effects of JNK on GST activity were determined using the hydrophobic substrates for GST, as mentioned above. A positive or negative change of GST activity towards a substrate, when compared with activity in the absence of JNK, indicated a substrate selectivity change of GST.

(iv) *The effect of GSH on GST activity in the presence of JNK*. A 1:1 molar ratio of GST/JNK was incubated at room temperature for 5 min in the presence and absence of 2 mM GSH. The GST activity was determined towards its hydrophobic substrates as described above.

In vitro protein kinase assays

Constitutively active HEP_{3E} was used to activate JNK and then both HEP_{3E} and Jun 1–104 were assessed as JNK substrates [21,22]. HEP_{3E}/JNK/Jun 1–104 in 1:2:10 molar ratio were incubated in 20 mM Hepes, 20 mM $MgCl_2$, 20 mM β-glycerophosphate (pH 7.6), containing 500 μM dithiothreitol, 100 μM sodium orthovanadate, supplemented with 20 μM ATP and 3 μCi of [γ-^{32}P]ATP. The phosphorylation reactions were performed for 25 min at room temperature and separated by SDS/PAGE. Phosphorylated proteins were visualized by autoradiography and quantified by Cerenkov counting.

Effects of GST on protein kinase activity

The recombinant GSTs were incubated with kinase proteins in a 10:1 molar ratio for 10 min at room temperature. Kinase activity was then measured as described above.

RESULTS

JNK and HEP can inhibit the activity of Delta GST spliceforms

Previous studies have shown that GSTs of the mammalian Pi and Mu classes are capable of modulating the JNK pathway through

Table 1 Effect of HEP and JNK proteins on GST activity

The recombinant proteins of HEP and JNK were incubated with the different GST splice forms in 1:1 molar ratio for 5 min at room temperature. The percentage inhibition of GST activity was calculated using a reaction that contained no kinase proteins as control. No inhibition of GST activity of GSTD1-1 by JNK protein was detected. Results are means ± S.D. for at least four independent experiments.

GST	Inhibition of GSTs by HEP (%)	Inhibition of GSTs by JNK (%)
D1-1	54.64 ± 3.83	No inhibition detected
D2-2	53.29 ± 7.71	85.35 ± 6.72
D3-3	23.71 ± 1.88	44.64 ± 6.92
D4-4	29.27 ± 2.99	68.45 ± 4.00

their inhibition of JNK and interaction with ASK respectively [18]. In the present study, we have evaluated whether GSTs of the *Dipteran* Delta class could interact with two kinases from *Drosophila*, either JNK or its upstream kinase HEP, by measuring both the effects of the kinases on GST activity and the effects of the GSTs on kinase activity.

Previously, a comprehensive study of six GST isoforms yielded estimates of total GST concentrations in eukaryotic cells, depending on tissue type, ranging from 0.1 to 1.4 nmol of GST/mg of total soluble protein [27]. From our laboratory data, we estimate *Drosophila* SL2 cells to contain 66 pg of soluble protein/cell. Assuming a tissue culture cell volume of 1 pl [28], a total GST cell concentration of 7–90 μM can be estimated. A single MAPK protein has been estimated to have cellular concentrations of 1–3 μM [28]. In *Anopheles gambiae*, it has been reported that, probably, there are 32 different soluble GST encoding transcripts with 31 being found in the adult mosquito [29]. This is similar to the 37 putative GST genes identified in *Drosophila* [29]. It was also shown that, depending on the specific tissue/cell type, a single GST isoform can vary between 0.15 and 45 μM [27]. However, these concentration determinations do not address the issue of compartmental localization known to be important in controlling message propagation down signal-transduction pathways. We therefore chose an intermediate concentration range and used the ratio 1:1 for the GST/JNK experiments.

We began with an evaluation of the effects of JNK and HEP on the activity of four Delta GST spliceforms. Alternative splicing is a major mechanism of generating protein diversity in higher eukaryotes [30]. These four GSTs possess 61–77 % amino acid identity and are products of the *Adgst1AS1* gene [23,24]. They share an untranslated exon 1 and a translated exon 2 that code for 45 amino acids at the N-terminus. These two exons are spliced to one of four alternative exons 3, namely 3A, 3B, 3C or 3D. This generates four different mature transcripts coding for proteins containing 209–219 amino acids that have been called D4-4, D3-3, D2-2 and D1-1 respectively. These spliceforms therefore differ in their C-terminal amino acids only.

As shown in Table 1, GST activities, as assessed using the standard CDNB assay, were decreased in the presence of a 1:1 molar concentration of HEP. The activities of the GST spliceforms GSTD1-1 and GSTD2-2 were the greatest affected, but even the inhibition of GSTD3-3 and GSTD4-4 was >20 %. A parallel series of experiments in which JNK was incubated with each Delta GST spliceform also showed that JNK could inhibit the activity of GSTD2-2, GSTD3-3 and GSTD4-4 towards CDNB. However, under these assay conditions, no inhibition of GSTD1-1 activity could be observed (Table 1). The differences in the effects of the HEP and JNK on the activities of the GST spliceforms would appear to be the result of different interactions with the different amino acids in the C-terminus of each GST spliceform.

Table 2 Mechanism of GST and kinase protein interaction

The type of inhibition and affinity binding (K_i) of GST and kinase protein interaction were studied by varying the concentration of CDNB from 0.05 to 3.0 and measuring kinetic parameters under the standard conditions for each GST enzyme. Results are means ± S.E.M. for at least four independent experiments.

GST	Type of inhibition	K_i HEP-GST (nM)	K_i JNK-GST (nM)
D1-1	Non-competitive	50.0 ± 2.84	Not determined
D2-2	Non-competitive	21.3 ± 5.18	73.9 ± 20.1
D3-3	Non-competitive	43.6 ± 7.19	76.8 ± 15.4
D4-4	Non-competitive	125.0 ± 45.2	218 ± 86.3

Mechanism of GST inhibition by HEP and JNK

A more detailed kinetic study of inhibition was undertaken to yield data on the affinity of binding (K_i) and the mechanism of interaction for these four GST spliceforms and the kinases HEP and JNK (Table 2). With the exception of the JNK and GSTD1-1, which showed no inhibition of GST activity, the inhibition of the GST spliceforms by JNK or by HEP was non-competitive with respect to its substrate CDNB. This indicated that the interaction with each kinase did not block the GST active site despite inhibiting its transferase activity. This interaction was also of high affinity, with estimates of K_i in the range of 20–70 nM for GSTD1-1, GSTD2-2 and GSTD3-3 (Table 2). For GSTD4-4, K_i values were higher, being in the range of 100–200 nM; however, all of these interactions exhibited approx. 3–4 orders of magnitude greater affinity than the interactions of GSTs with glutathione [24]. Furthermore, these results show that HEP interacts with all the GST Delta spliceforms tested. JNK also interacts with GSTD2-2, GSTD3-3 and GSTD4-4, but it was not possible to observe an interaction of JNK with GSTD1-1 in this experiment.

Modulation of protein kinase activity in the presence of GST Delta spliceforms

We next tested the reciprocal regulation of GST Delta spliceforms on protein kinase activity. We began by assessing JNK activity towards its physiological substrate Jun. As shown in Figure 1(A), GSTD1-1 inhibited the ability of JNK to phosphorylate Jun by approx. 50 %. In contrast, the inclusion of GSTD2-2, GSTD3-3 or GSTD4-4 increased JNK activity by up to 170 %. Thus despite JNK not inhibiting GSTD1-1 activity towards CDNB (Table 1), GSTD1-1 was capable of inhibiting JNK activity towards Jun (Figure 1A).

We next repeated these protein kinase assays, but without the inclusion of the Jun substrate protein. Thus we could assess the actions of the GST Delta spliceforms on both HEP_{EE} and JNK activity using the ability of HEP_{EE} to phosphorylate JNK as well as the ability of JNK to phosphorylate HEP_{EE} [21]. As shown in Figure 1(B), the incubation of JNK alone did not result in its significant autophosphorylation. Similarly, prolonged incubation of HEP_{EE} alone did not result in its significant autophosphorylation (results not shown). The inclusion of HEP_{EE} with JNK resulted in weak phosphorylation of both HEP_{EE} and JNK proteins. When the GST Delta spliceforms were also included, the most striking differences were noted with GSTD2-2 and GSTD3-3, which increased the phosphorylation of both HEP_{EE} and JNK proteins up to 6-fold. Furthermore, GSTD1-1 and GSTD4-4 seemed to inhibit the phosphorylation of HEP_{EE}, without inhibiting the phosphorylation of JNK. These results therefore show that GSTs can affect the activities of both JNK towards HEP_{EE} and HEP_{EE} towards JNK. They also show that GSTs were not JNK substrates because no phosphorylated GST protein was observed even after prolonged

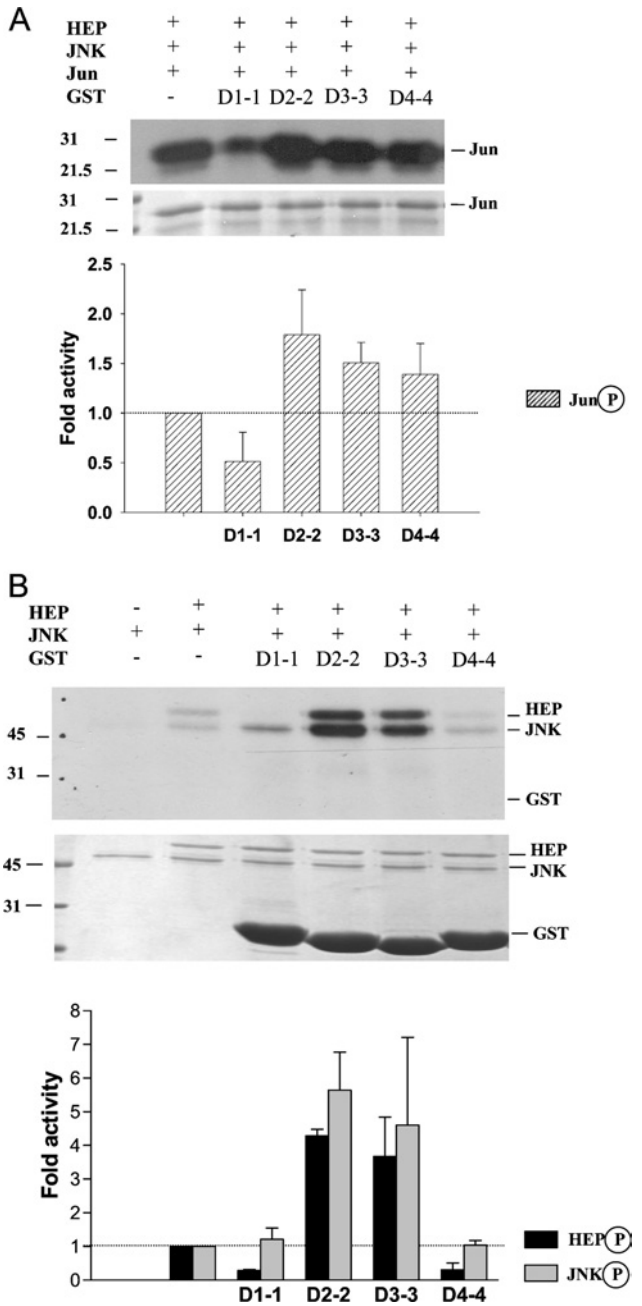

Figure 1 GST spliceforms are both positive and negative regulators of JNK activity

(**A**) The experiment was performed using GST/HEP_{3E}/JNK/Jun 1–104 in 10:1:2:10 molar ratio. GST was incubated with constitutively active HEP_{3E} for 10 min at room temperature before adding JNK and Jun with 3 μCi of [γ-^{32}P]ATP for 25 min of phosphorylation time at room temperature. Proteins were then separated by SDS/PAGE, and JNK activity was visualized by autoradiography of the ^{32}P-labelled Jun. The upper panel is an autoradiograph showing Jun phosphorylation in the presence and absence of different GST isoforms. The lower panel depicts SDS/polyacrylamide gel showing the sample loading for Jun. The histogram quantifies the effects of GSTs on Jun phosphorylation when compared with the reaction in the absence of these GSTs. Figures shown are representative of at least three independent experiments. (**B**) The experiment was performed using GST/HEP_{3E}/JNK in 10:1:2 molar ratio. GST was incubated with constitutively active HEP_{3E} for 10 min at room temperature before adding JNK with 3 μCi of [γ-^{32}P]ATP for 25 min of phosphorylation time at room temperature. Proteins were then separated by SDS/PAGE, and kinase activity was visualized by autoradiography of the ^{32}P-labelled substrates. The JNK protein was a substrate for HEP as well as HEP being a substrate for JNK [21]. The autoradiograph in the upper panel shows HEP and JNK phosphorylation in the presence and absence of different GST isoforms. The lower panel is an SDS/polyacrylamide gel showing the sample loading for HEP and JNK. The histogram quantifies the effects of the GSTs on HEP and JNK phosphorylation. Figures shown are representative of at least three independent experiments.

Table 3 Specific activity of GST splice forms using various hydrophobic substrates

Results are means ± S.E.M. for at least five separate assays. The substrate concentrations used were: CDNB, 1 mM; DCNB, 1 mM; PNBC, 1.2 mM and PNPB, 0.1 mM.

	Specific activity [μmol · min^{-1} · (mg of protein)$^{-1}$]			
GST	CDNB	DCNB	PNBC	PNPB
D1-1	6.54 ± 0.53	0.070 ± 0.002	1.05 ± 0.191	0.002 ± 0.002
D2-2	45.1 ± 3.41	0.177 ± 0.006	17.1 ± 1.09	0.047 ± 0.010
D3-3	67.5 ± 1.97	0.312 ± 0.023	2.96 ± 0.292	0.002 ± 0.007
D4-4	41.8 ± 1.40	0.042 ± 0.011	2.73 ± 0.105	0.023 ± 0.002

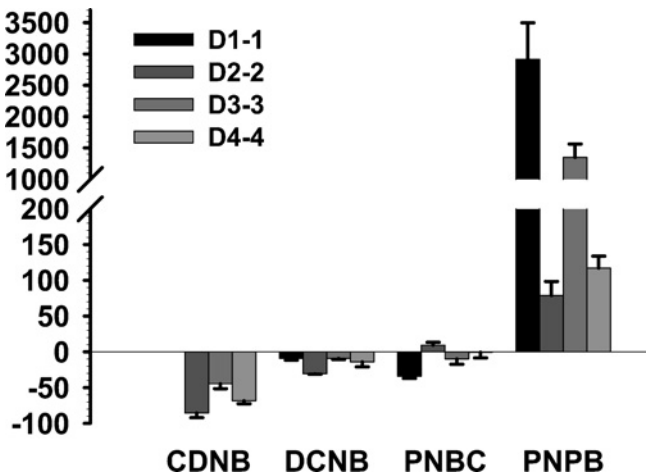

Figure 2 JNK changes the substrate specificity of GST spliceforms

GST and JNK were incubated in 1:1 molar ratio for 5 min at room temperature. GST activity was measured using various hydrophobic co-substrates. The percentage change in GST activity (*y*-axis) was determined by comparing the reactions in the presence and absence of JNK. The specific activity of each GST for the substrates in the absence of JNK is shown in Table 3. There was no activity change in GSTD1-1 activity using CDNB as the co-substrate due to the lack of a JNK effect (Table 1). Results shown are representative of at least four independent experiments with similar results.

exposure of the autoradiographs. This is consistent with these GST proteins lacking a consensus phosphorylation site for MAPKs, namely S/TP or PXS/TP [31].

JNK affected GST substrate specificity

We next evaluated whether JNK changed the substrate specificity of the Delta GST spliceforms. First, the specific activity of each Delta GST spliceform was determined for the substrates CDNB, DCNB, PNBC and PNPB in the absence of any JNK protein. The results are presented in Table 3. The results illustrate the striking differences in the enzymic properties of these four GSTs. For example, a 10-fold difference in specific activity was noted for the CDNB substrate. Similarly, 8-fold differences for DCNB, 17-fold differences for PNBC substrate and >20-fold differences for PNPB are noted. These differences must arise from the differences in amino acids at the C-terminus. These C-terminal residues contribute to the H-site and have been shown to determine substrate specificity for different compounds within each class and amongst different classes [32–34].

The changes in GST substrate specificity after incubation with JNK are shown in Figure 2. Some striking differences were observed. For example, GSTD1-1 activity towards CDNB was not

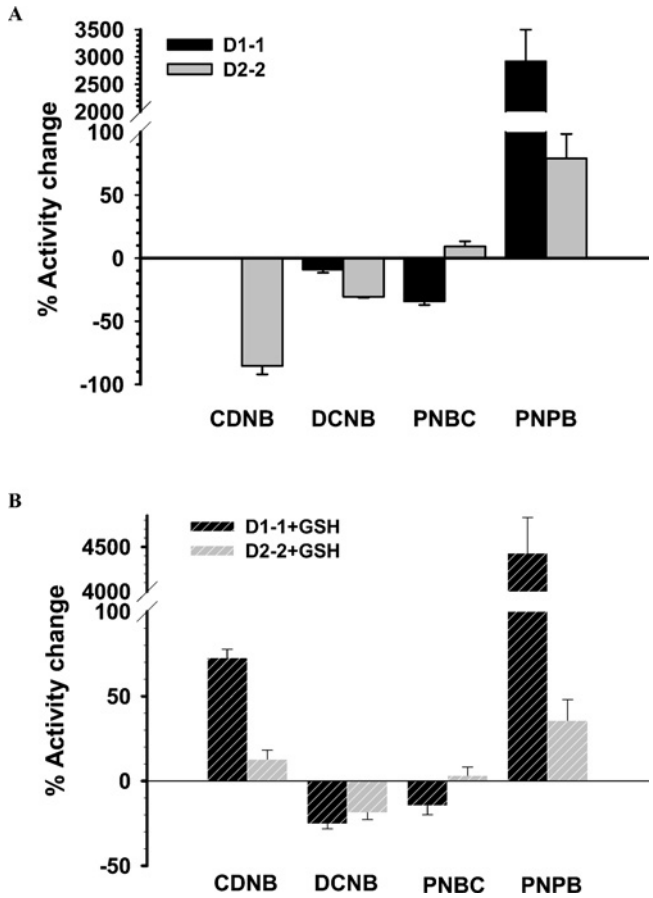

Figure 3 Presence of glutathione changed the JNK effects on GST activity

Effects of JNK on GST were determined in the absence and presence of GSH. GST and JNK were incubated in 1:1 molar ratio in the presence and absence of 2 mM GSH for 5 min at room temperature. GST activity was measured using various hydrophobic co-substrates. The percentage change in GST activity was then calculated: (**A**) specific activity of GSTD1-1 and GSTD2-2 affected by JNK, and it was employed for comparison with the reaction containing GSH, as shown in (**B**).

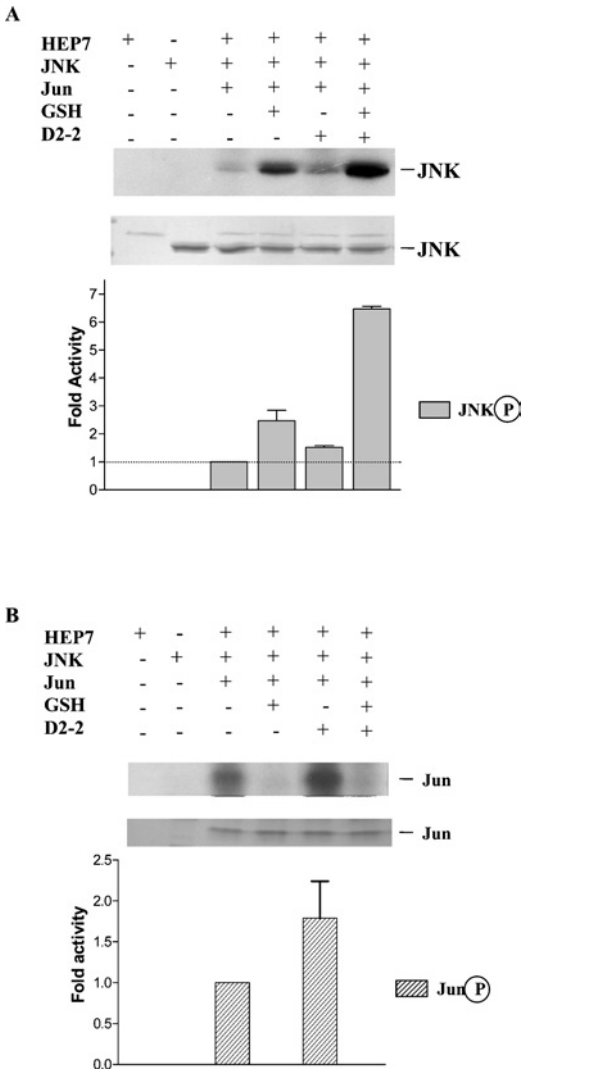

Figure 4 Presence of glutathione changed the GST effects on JNK activity

GST/HEP/JNK/Jun 1–104 in 10:1:2:10 molar ratio were incubated in the presence and absence of 10 mM GSH with 3 μCi of [γ-^{32}P]ATP for 25 min of phosphorylation time at room temperature. (**A**) The autoradiograph in the upper panel shows JNK phosphorylation in the presence and absence of GSH. The lower panel depicts an SDS/polyacrylamide gel showing the sample loading for JNK. The histogram quantifies in fold activity the GST's effect on JNK phosphorylation. (**B**) The autoradiograph in the upper panel shows Jun phosphorylation in the presence and absence of GSH. The lower panel depicts an SDS/polyacrylamide gel showing the sample loading for Jun. The histogram quantifies the GST's effects on Jun phosphorylation. Figures shown are representative of at least three independent experiments.

influenced when incubated in the presence of JNK; nonetheless, it was significantly increased (approx. 2500-fold) towards PNPB. Similarly, incubation with JNK increased GSTD2-2 activity using PNBC and PNPB, whereas it was decreased on using other substrates. Both D3-3 and D4-4 displayed an increase in activity towards PNPB; however, the activities were decreased towards other substrates. These results suggest that the JNK interaction provokes a set of different conformational changes in each GST, thus affecting the active-site topologies, for instance, changes in hydrophobicity and size through residue movement [35], in a dissimilar manner.

Effect of glutathione on GST–JNK interaction

Under normal cellular conditions, intracellular GSH concentrations are supposed to be in the range 1–10 mM. At these concentrations, GSH would usually be bound to the GST active site [36] and, therefore, we evaluated whether the presence of GSH would alter the effects of GSTs on JNK activities. In the presence of 2 mM GSH, JNK had different effects on the Delta GST spliceforms for the GST substrates, CDNB, DCNB, PNBC and PNPB (Figure 3). Specifically, when activities of the GSTD1-1 and GSTD2-2 spliceforms were assessed after preincubation in the absence (Figure 3A) and presence (Figure 3B) of glutathione, the most striking differences were noted for activities towards the CDNB substrate. GSTD1-1 was now activated by JNK after preincubation in the presence of GSH, and GSTD2-2 was also activated rather than inhibited. We suggest that the known changes of GSH binding that result in GST-induced-fit conformational changes [37] could contribute to the changes noted in the GST–JNK interaction. These changes will be observed differently depending on the GST-specific isoforms and substrate employed.

GSH also affected JNK activity by inducing JNK autophosphorylation (Figure 4A), but attenuated Jun phosphorylation (Figure 4B). As shown in the presence of Jun, the autophosphorylation of JNK was decreased; however, the GST and GSH-induced-fit conformational change induced a 3.5-fold increase in JNK autophosphorylation. The results also identify glutathione as a critical molecule directly involved in JNK regulation by

controlling JNK substrate selectivity and specificity of interaction. Direct interaction of GSH and kinases has been reported previously for several isoforms of protein kinase C that were shown to be inhibited by GSH [38]. High GSH concentrations have been shown to inhibit the sphingomyelin/ceramide cycle where generation of ceramide leads to cell-cycle arrest and apoptosis [39]. In addition, the depletion of GSH in the cell during oxidative stress exerted negative regulation over protein kinase C isoenzymes [38] as well as the JNK/p38 pathway [4]. GSH has been shown to be a potent inhibitor of JNK activation, suggesting the existence of specific cellular components involved in JNK activation in response to different forms of cellular stress [4]. We suggest GSTs may be one of these components.

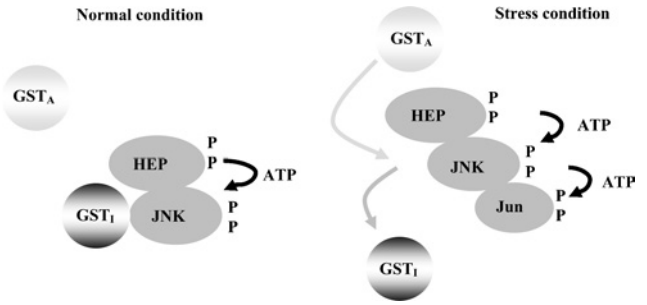

Figure 5 A proposed mechanism of GST regulation of stress kinase proteins through a dissociation/association process

The different isoforms of GSTs possess different JNK effector properties. GST$_I$ refers to a JNK inhibitor and GST$_A$ represents a JNK activator. The JNK regulation occurs on stress. Left panel: under normal conditions, GST$_I$ inhibits JNK and maintains JNK at basal level activity [15]. Right panel: once stress occurs, a mechanism to dissociate GST$_I$ from JNK comes into effect. GST$_A$ may now associate with JNK or an upstream activating kinase and increase or modulate the kinase cascade response.

DISCUSSION

In the present study, we characterized the non-enzymic function of GST in the regulation of stress-activated kinase proteins of the JNK pathway as well as the reciprocal regulation of GST by proteins of the JNK pathway. In insects, HEP is a homologue of mammalian MKK7, whereas the single *Drosophila* JNK or basket protein corresponds to the ten human JNK isoforms with a 61–75 % amino acid identity [21]. Furthermore, GSTs in insects currently fall into six classes, with the Delta class being the best studied [29,40,41]. Here, we have concentrated on the study of four spliceforms of a single Delta class GST, GSTD1-1, GSTD2-2, GSTD3-3 and GSTD4-4. Interestingly, the splicing of these GSTs generates products that share the same N-terminal 45 amino acids of the conserved glutathione-binding region [24]. Any differences in the actions of these spliceforms must therefore arise from the C-terminal regions of these proteins and we have previously shown that their substrate specificities, steady-state kinetics with respect to both GSH and CDNB and inhibition kinetics to the pyrethroid insecticide permethrin are very different [24].

Results of the present study have extended our previous studies by demonstrating an interaction between the *Dipteran* GSTD1-1, GSTD2-2, GSTD3-3 and GSTD4-4 and the JNK pathway components, JNK and HEP. Our inhibition study showed different interactions of these kinases with the GST splice products, particularly as seen with the inhibition of several of the GST spliceforms by JNK (Table 1). We observed, using the standard CDNB assay, that GSTD1-1 showed no inhibition, whereas the remaining GSTs were inhibited by their preincubation with JNK protein. We suggest that the interaction with the kinase could change the GST conformation and this results in different GST enzymic activity.

This is also the first report of the activation of JNK activity by their preincubation with GST. Previously, GSTs have been reported to serve as negative regulators in the JNK pathway, acting either on JNK or ASK1 [15,18]. In the present study, we report that although some alternatively spliced GSTs inhibit JNK activity, other spliceforms may also function as JNK activator proteins. These results again highlight the functional diversity of the GST spliceforms. Moreover, our study shows that the GSTs can associate with the immediate JNK upstream activator kinase in *Drosophila*, HEP. Hence, GST may play additional roles in the regulation of kinase proteins in the JNK pathway through an, as yet, unknown mechanism.

As a consequence of the different effects of GSTD4-4 on JNK activity, as shown by an increased phosphorylation of c-Jun (Figure 1A) and a decreased phosphorylation of HEP (Figure 1B), we suggest that the GSTs such as GSTD4-4 may contribute to a change in JNK substrate selectivity. Intriguingly, GST could be a pivotal molecule to switch the JNK downstream cascade direction by changing activation of transcriptional machinery components and thereby gene expression. One critical determinant of MAPK specificity and efficacy is the docking motif on the kinase surface, which interacts with the substrate target site. A structural change of JNK after interaction with GST may impact on this region critical for specificity determination [42,43]. Nonetheless, JNK has many functions in controlling cell stress responses, and it is possible that the GST–JNK interaction changes substrate specificities of JNK for other JNK substrates such as activating transcription factor 2 [11], Elk-1 [12] or p53 [44]. The GST–JNK interaction would therefore function as a switch or modulator for the various JNK processes on stimulation by cellular stresses (Figure 5). Owing to the nature of the signalling process, there must be other molecules participating in the regulation of the GST–JNK interaction. Since there are various classes and isoforms of GSTs [1,2] and JNKs [9] that are widely distributed in different tissues, the signalling specificity of GST–JNK interactions may also be controlled by the specific classes and isoforms present in any particular cell type. Previously, it was shown that distinct classes of GSTs played particular roles by interacting with different kinase proteins [15,18]. In the present study, we report that different isoforms of the same class of GST interact with JNK and modulate JNK activity in different ways. The variety of GST isoforms may be one of the keys determining signal specificity and controlling a particular cells biological response.

The GST–JNK interaction may occur through the C-terminus of JNK, which has been reported as being important for providing direct protein–protein interaction with GSTP1-1 [45]. JNK has also been shown to interact electrostatically with other signalling molecules through a conserved docking motif called the common docking domain [46]. The conserved polar residues within the common docking domain may serve as energetic hot spots, which increase the specific protein–protein interaction [47,48]. In addition, hydrogen bonding and molecular surface shape complementarity are vital criteria that determine protein docking [49]. Thus the variation in surface residues of a GST interacting with a particular JNK may induce distinct conformational changes, yielding functional changes in both proteins. A shift in substrate specificity arising from the association of GST and JNK, in addition to the presence of different GST isoforms generated in the course of natural molecular evolution [50], would be a useful feature for a detoxification mechanism already well known for recognizing diverse substrate compounds.

In summary, the results show that distinct isoforms of GSTs specifically interact with JNK with different effects. Intriguingly, even though the studied GST isoforms are alternatively spliced products sharing $>60\%$ amino acid identity, the GST proteins displayed contrary roles in the regulation of JNK. It suggests that the specific isoforms of GSTs present may be important in controlling the final cellular response. The present study provides new insight into the mechanism of GSTs in regulating and conferring specificity of stress kinase proteins in the JNK pathway.

We are particularly grateful to Associate Professor Dr W. Chulalakasananukul (Genetics Program, Department of Botany, Chulalongkorn University, Bangkok, Thailand) for donating the *D. melanogaster* adults used in cloning of the *Drosophila* HEP, JNK and Jun. This work was supported by the Thailand Research Fund (TRF), a Royal Golden Jubilee Scholarship (R. U.) and Royal Golden Jubilee Grant (R. U.).

REFERENCES

1 Hayes, J. D. and Pulford, D. J. (1995) The glutathione S-transferase supergene family: regulation of GST and the contribution of the isoenzymes to cancer chemoprotection and drug resistance. CRC Crit. Rev. Biochem. Mol. Biol. **30**, 445–600
2 Armstrong, R. N. (1997) Structure, catalytic mechanism, and evolution of the glutathione transferases. Chem. Res. Toxicol. **10**, 2–18
3 Sheehan, D., Meade, G., Foley, V. M. and Dowd, C. A. (2001) Structure, function and evolution of glutathione transferases: implications for classification of non-mammalian members of an ancient enzyme superfamily. Biochem. J. **360**, 1–16
4 Wilhelm, D., Bender, K., Knebel, A. and Angel, P. (1997) The level of intracellular glutathione is a key regulator for the induction of stress-activated signal transduction pathways including Jun N-terminal protein kinases and p38 kinase by alkylating agents. Mol. Cell. Biol. **17**, 4792–4800
5 Ketterer, B. (2001) A bird's eye view of the glutathione transferase field. Chem. Biol. Interact. **138**, 27–42
6 Dulhunty, A., Gage, P., Curtis, S., Chelvanayagam, G. and Board, P. (2001) The glutathione transferase structural family includes a nuclear chloride channel and a ryanodine receptor calcium release channel modulator. J. Biol. Chem. **276**, 3319–3323
7 Fesik, S. W. (2001) Insights into programmed cell death through structural biology. Cell (Cambridge, Mass.) **103**, 273–282
8 Kampranis, S. C., Damianova, R., Atallah, M., Toby, G., Kondi, G., Tsichlis, P. N. and Makris, A. M. (2000) A novel plant glutathione *S*-transferase/peroxidase suppresses Bax lethality in yeast. J. Biol. Chem. **275**, 29207–29216
9 Barr, R. K. and Bogoyevitch, M. A. (2001) The c-Jun N-terminal protein kinase family of mitogen-activated protein kinases (JNK MAPKs). Int. J. Biochem. Cell Biol. **33**, 1047–1063
10 Hibi, M., Lin, A., Smeal, T., Minden, A. and Karin, M. (1993) Identification of an oncoprotein- and UV-responsive protein kinase that binds and potentiates the c-Jun activation domain. Genes Dev. **7**, 2135–2148
11 Gupta, S., Campbell, D., Dérijard, B. and Davis, R. J. (1995) Transcription factor ATF2 regulation by the JNK signal transduction pathway. Science **267**, 389–393
12 Whitmarsh, A. J., Shore, P., Sharrocks, A. D. and Davis, R. J. (1995) Integration of MAP kinase signal transduction pathways at the serum response element. Science **269**, 403–407
13 Xia, C. L., Cowell, I. G., Dixon, K. H., Pemble, S. E., Ketterer, B. and Taylor, J. B. (1991) Glutathione transferase π its minimal promoter and downstream cis-acting element. Biochem. Biophys. Res. Commun. **176**, 233–240
14 Yokoyama, Y., Sagara, M., Sato, S. and Saito, Y. (1998) Value of glutathione S-transferase p and the oncogene products c-Jun, c-Fos, c-H-Ras, and c-Myc as a prognostic indicator in endometrial carcinomas. Gynecol. Oncol. **68**, 280–287
15 Adler, V., Yin, Z., Fuchs, S. Y., Benezra, M., Rosario, L., Tew, K. D., Pincus, M. R., Sardana, M., Henderson, C. J., Wolf, C. R. et al. (1999) Regulation of JNK signaling by GSTp. EMBO J. **18**, 1321–1334
16 Elsby, R., Kitteringham, N. R., Goldring, C. E., Lovatt, C. A., Chamberlain, M., Henderson, C. J., Wolf, C. R. and Park, B. K. (2003) Increased constitute c-Jun N-terminal kinase signaling in mice lacking glutathione *S*-transferase Pi. J. Biol. Chem. **278**, 22243–22249
17 Yin, Z., Ivanov, V. N., Habelhah, H., Tew, K. and Ronai, Z. (2000) Glutathione *S*-transferase p elicits protection against H_2O_2-induced cell death via coordinated regulation of stress kinases. Cancer Res. **60**, 4053–4057
18 Cho, S.-G., Lee, Y. H., Park, H.-S., Ryoo, K., Kang, K. W., Park, J., Eom, S.-J., Kim, M. J., Chang, T.-S., Choi, S.-Y. et al. (2001) Glutathione *S*-transferase Mu modulates the stress-activated signals by suppressing apoptosis signal-regulating kinase 1. J. Biol. Chem. **276**, 12749–12755
19 Stronach, B. E. and Perrimon, N. (1999) Stress signaling in *Drosophila*. Oncogene **18**, 6172–6182
20 Holland, P. M., Suzanne, M., Campbell, J. S., Noselli, S. and Cooper, J. A. (1997) MKK7 is a stress-activated mitogen-activated protein kinase kinase functionally related to *hemipterous*. J. Biol. Chem. **272**, 24994–24998
21 Sluss, H. K., Han, Z., Barrett, T., Davis, R. J. and Ip, Y. T. (1996) A JNK signal transduction pathway that mediates morphogenesis and immune response in *Drosophila*. Genes Dev. **10**, 2745–2758
22 Zhang, K., Chaillet, J. R., Perkins, L. A. and Halazonetis, T. D. (1990) *Drosophila* homolog of the mammalian *jun* oncogene is expressed during embryonic development and activates transcription in mammalian cells. Proc. Natl. Acad. Sci. U.S.A. **87**, 6281–6285
23 Pongjaroenkit, S., Jirajaroenrat, K., Boonchauy, C., Chanama, U., Leetachewa, S., Prapanthadara, L. and Ketterman, A. J. (2001) Genomic organization and putative promotors of highly conserved glutathione S-transferases originating by alternative splicing in *Anopheles dirus*. Insect Biochem. Mol. Biol. **31**, 75–85
24 Jirajaroenrat, K., Pongjaroenkit, S., Krittanai, C., Prapanthadara, L. and Ketterman, A. J. (2001) Heterologous expression and characterization of alternatively spliced glutathione *S*-transferases from a single *Anopheles* gene. Insect Biochem. Mol. Biol. **31**, 867–875
25 Wolter, S., Mushinski, J. F., Saboori, A. M., Resch, K. and Kracht, M. (2002) Inducible expression of a constitutively active mutant of mitogen activated protein kinase kinase 7 specifically activates c-JUN NH2-terminal protein kinase, alters expression of at least nine genes, and inhibits cell proliferation. J. Biol. Chem. **277**, 3576–3584
26 Bradford, M. M. (1976) A rapid and sensitive method for the quantitation of microgram quantities of protein utilizing the principle of protein-dye binding. Anal. Biochem. **72**, 248–254
27 Rowe, J. D., Nieves, E. and Listowsky, I. (1997) Subunit diversity and tissue distribution of human glutathione S-transferase: interpretations based on electrospray ionization-MS and peptide sequence-specific antisera. Biochem. J. **325**, 481–486
28 Ferrell, Jr, J. E. (1996) Tripping the switch fantastic: how a protein kinase cascade can convert graded inputs into switch-like outputs. TIBS **21**, 460–466
29 Ding, Y., Ortelli, F., Rossiter, L. C., Hemingway, J. and Ranson, H. (2003) The *Anopheles gambiae* glutathione transferase supergene family: annotation, phylogeny and expression profiles. BMC Genomics **4**, 35–50
30 Nurtdinov, R. N., Artamonova, I. I., Mironov, A. A. and Gelfand, M. S. (2003) Low conservation of alternative splicing patterns in the human and mouse genomes. Hum. Mol. Genet. **12**, 1313–1320
31 Pearson, G., Robinson, F., Gibson, T. B., Xu, B., Karandikar, M., Berman, K. and Cobb, M. H. (2001) Mitogen-activated protein (MAP) kinase pathways: regulation and physiological functions. Endocr. Rev. **22**, 153–183
32 Allardyce, C. S., McDonagh, P. D., Lian, L.-Y., Wolf, C. R. and Roberts, G. C. K. (1999) The role of tyrosine-9 and the C-terminal helix in the catalytic mechanism of Alpha-class glutathione S-transferases. Biochem. J. **343**, 525–531
33 Nilsson, L. O., Gustafsson, A. and Mannervik, B. (2000) Redesign of substrate-selectivity determining modules of glutathione transferase A1-1 installs high catalytic efficiency with toxic alkenal products of lipid peroxidation. Proc. Natl. Acad. Sci. U.S.A. **97**, 9408–9412
34 Pal, A., Gu, Y., Pan, S.-S., Ji, X. and Singh, S. V. (2001) C-terminal region amino acid substitutions contribute to catalytic differences between murine class alpha glutathione transferases mGSTA1-1 and mGSTA2-2 toward anti-diol epoxide isomers of benzo[c]phenanthrene. Biochemistry **40**, 7047–7053
35 Nuccetelli, M., Mazzetti, A. P., Rossjohn, J., Parker, M. W., Board, P., Caccuri, A. M., Federici, G., Ricci, G. and Lo Bello, M. (1998) Shifting substrate specificity of human glutathione transferase (from class pi to class alpha) by a single point mutation. Biochem. Biophys. Res. Commun. **252**, 184–189
36 Oakley, A. J., Rossjohn, J., Lo Bello, M., Caccuri, A. M., Federici, G. and Parker, M. W. (1997) The three-dimensional structure of the human pi class glutathione S-transferase P1-1 in complex with the inhibitor ethacrynic acid and its glutathione conjugate. Biochemistry **36**, 576–585
37 Oakley, A. J., Harnnoi, T., Udomsinprasert, R., Jirajaroenrat, K., Ketterman, A. J. and Wilce, M. C. J. (2001) The crystal structures of glutathione S-transferases isozymes 1-3 and 1-4 from *Anopheles dirus* species B. Protein Sci. **10**, 2176–2185
38 Ward, N. E., Pierce, D. S., Chung, S. E., Gravitt, K. R. and O'Brian, C. A. (1998) Irreversible inactivation of protein kinase C by glutathione. J. Biol. Chem. **273**, 12558–12566
39 Liu, B. and Hannun, Y. A. (1997) Inhibition of the neutral magnesium-dependent sphingomyelinase by glutathione. J. Biol. Chem. **272**, 16281–16287
40 Fournier, D., Bride, J.-M., Poirié, M., Bergé, J.-B. and Plapp, F. W. (1992) Insect glutathione S-transferases. Biochemical characteristics of the major forms from houseflies susceptible and resistant to insecticides. J. Biol. Chem. **267**, 1840–1845
41 Ranson, H., Claudianos, C., Ortelli, F., Abgrall, C., Hemingway, J., Sharakhova, M. V., Unger, M., Collins, F. H. and Feyereisen, R. (2002) Evolution of supergene families associated with insecticide resistance. Science **298**, 179–181

42 Sharrocks, A. D., Yang, S.-H. and Galanis, A. (2000) Docking domains and substrate specificity determination for MAP kinases. TIBS **25**, 448–453
43 Tanoue, T., Maeda, R., Adachi, M. and Nishida, E. (2001) Identification of a docking groove on ERK and p38 MAP kinases that regulates the specificity of docking interactions. EMBO J. **20**, 466–479
44 Adler, V., Pincus, M. R., Minamoto, T., Fuchs, S. Y., Bluth, M. J., Brandt-Rauf, P. W., Friedman, F. K., Robinson, R. C., Chen, J. M., Wang, X. W. et al. (1997) Conformation-dependent phosphorylation of p53. Proc. Natl. Acad. Sci. U.S.A. **94**, 1686–1691
45 Wang, T., Arifoglu, P., Ronai, Z. and Tew, K. D. (2001) Glutathione *S*-transferase P1-1 (GSTP1-1) inhibits c-Jun N-terminal kinase (JNK1) signaling through interaction with the C terminus. J. Biol. Chem. **276**, 20999–21003
46 Tanoue, T., Adachi, M., Moriguchi, T. and Nishida, E. (2000) A conserved docking motif in MAP kinases common to substrates, activators and regulators. Nat. Cell Biol. **2**, 110–116
47 Ma, B., Elkayam, T., Wolfson, H. and Nussinov, R. (2003) Protein-protein interactions: structurally conserved residues distinguish between binding sites and exposed protein surfaces. Proc. Natl. Acad. Sci. U.S.A. **100**, 5772–5777
48 Hu, Z., Ma, B., Wolfson, H. and Nussinov, R. (2000) Conservation of polar residues as hot spots at protein interfaces. Proteins **39**, 331–342
49 Meyer, M., Wilson, P. and Schomburg, D. (1996) Hydrogen bonding and molecular surface shape complementarity as a basis for protein docking. J. Mol. Biol. **264**, 199–210
50 Hansson, L. O., Bolton-Grob, R., Massoud, T. and Mannervik, B. (1999) Evolution of differential substrate specificities in mu class glutathione transferases probed by DNA shuffling. J. Mol. Biol. **287**, 265–276

Received 30 March 2004/28 June 2004; accepted 13 July 2004
Published as BJ Immediate Publication 14 July 2004, DOI 10.1042/BJ20040519

Identification, characterization and structure of a new Delta class glutathione transferase isoenzyme

Rungrutai UDOMSINPRASERT*[1], Saengtong PONGJAROENKIT†[1], Jantana WONGSANTICHON*, Aaron J. OAKLEY‡, La-aied PRAPANTHADARA§, Matthew C. J. WILCE‡ and Albert J. KETTERMAN*[2]

*Institute of Molecular Biology and Genetics, Mahidol University, Salaya Campus, 25/25 Putthamonthol Road 4, Salaya, Nakon Pathom 73170, Thailand, †Department of Biology, Faculty of Science, Maejo University, Chiangmai 50290, Thailand, and ‡Department of Pharmacology/Crystallography Centre, University of Western Australia, Crawley 6009, Australia, and §Research Institute for Health Sciences, Chiangmai University, Chiangmai 50200, Thailand

The insect GST (glutathione transferase) supergene family encodes a varied group of proteins belonging to at least six individual classes. Interest in insect GSTs has focused on their role in conferring insecticide resistance. Previously from the mosquito malaria vector *Anopheles dirus*, two genes encoding five Delta class GSTs have been characterized for structural as well as enzyme activities. We have obtained a new Delta class GST gene and isoenzyme from *A. dirus*, which we name adGSTD5-5. The adGSTD5-5 isoenzyme was identified and was only detectably expressed in *A. dirus* adult females. A putative promoter analysis suggests that this GST has an involvement in oogenesis. The enzyme displayed little activity for classical GST substrates, although it possessed the greatest activity for DDT [1,1,1-trichloro-2,2-bis-(*p*-chlorophenyl)ethane] observed for Delta GSTs. However, GST activity was inhibited or enhanced in the presence of various fatty acids, suggesting that the enzyme may be modulated by fatty acids. We obtained a crystal structure for adGSTD5-5 and compared it with other Delta GSTs, which showed that adGSTD5-5 possesses an elongated and more polar active-site topology.

Key words: *Anopheles dirus*, crystal structure, Delta class glutathione transferase, enzyme characterization, glutathione transferase gene, regulatory element.

INTRODUCTION

The insect GST (glutathione transferase) (EC 2.5.1.18) supergene family encodes a diverse set of proteins belonging to at least six individual classes (Delta, Epsilon, Sigma, Theta, Zeta, Omega and several unclassified genes) [1]. Interest in insect GSTs has focused on their role in conferring insecticide resistance [2] and in protecting against cellular damage by oxidative stress [3]. Many resistant insects are associated with elevated levels of GST activity [4]. In *Anopheles dirus*, two genes encoding five GSTs isoenzymes from the Delta class have been acquired previously and characterized for structural as well as enzyme activities [5–8]. To this end, we have identified a new Delta class GST isoenzyme from *Anopheles dirus* species B, which we named adGSTD5-5 (in insect GST nomenclature, 'D' refers to the Delta class and '5-5' refers to the homodimeric isoenzyme [9,10]). The availability of the *A. dirus* genome sequence has also enabled a putative promoter prediction, which suggests that this GST is involved in developmental-stage regulation. Moreover, the adGSTD5-5 enzyme was expressed and studied for structural as well as functional characteristics. The crystal structure of adGSTD5-5 was also obtained. Our data therefore reveal an overview of an evolutionarily conserved enzyme from gene to protein function.

MATERIALS AND METHODS

Genomic isolation of *gstD5*

A. dirus genomic library construction and screening was performed as described previously [7]. Using lower stringency hybridization, the presence of another GST gene was revealed on the phage clone of *adgst1AS1*. The recombinant phage clone 8A.2 was sequenced further until the complete sequence of 15 694 bp for the insert was obtained (GenBank® accession number AF251478).

adGSTD5-5 expression construct

The mRNAs were isolated from the fourth instar larvae, pupae, male and female adults by using TRIzol® reagent (Invitrogen) as described in the manufacturer's instructions. First-strand cDNA was synthesized by using Superscript II reverse transcriptase (Gibco BRL) and the oligo(dT)$_{15}$ primer [5′-GGCGGTCGACATATG(dT)$_{15}$-3′] (Proligo Singapore Pty), as described in the instruction manual. The N-terminus primer (5′-CACGCCG**CATATG**ACGACGGTGCTGTACTATC-3′) and C-terminus primer (5′-CGCCGTCGA**CATATG**CTACTGCTTCAACTTCGA-3′) were designed from the N-terminus and C-terminus of the amino acid coding region. The initial codon (ATG) and stop codon (TAG) are underlined, and the NdeI recognition site also incorporated in both primers is shown in bold. The PCR amplification (35 cycles of 94 °C for 1 min, 60 °C for 30 s and 72 °C for 1 min, and then a final extension step at 72 °C for 7 min) was performed on a PE system 2400 (PerkinElmer). The PCR product was purified from gel by GENECLEAN® II kit (BIO 101, La Jolla, CA, U.S.A.) following the manufacturer's instructions. The purified PCR product was digested with NdeI, and ligated into pET3a (Novagen) at the NdeI site. The ligated reaction was transformed into *Escherichia coli* DH5α cells. Then the recombinant clones were sequenced in both directions. Finally, the recombinant clones were transformed into *E. coli* BL21(DE3)pLysS competent cells for protein expression. The expression and purification of the recombinant enzyme was performed as described previously [11].

Abbreviations used: CDNB, 1-chloro-2,4-dinitrobenzene; DDT, 1,1,1-trichloro-2,2-bis-(*p*-chlorophenyl)ethane; GST, glutathione transferases; RMSD, root mean square deviation.

[1] These authors contributed equally to this work.

[2] To whom correspondence should be addressed (email frakt@mahidol.ac.th).

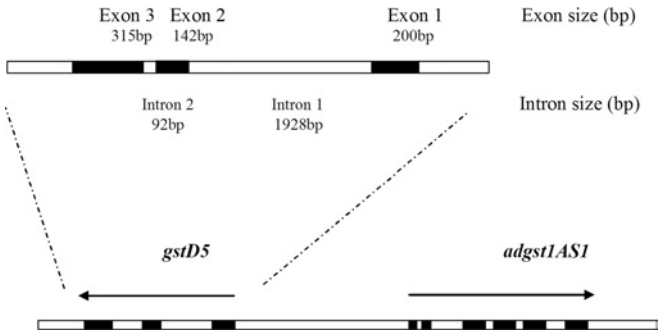

Figure 1 ***adgst1AS1*** **and** ***gstD5*** **gene organization of 8A.2 clone**

The *gstD5* gene is located 4620 bp upstream, with the opposite orientation to *adgst1AS1*. The 15694 bp genomic sequence has GenBank® accession number AF251478.

Characterization of the recombinant adGSTD5-5 enzyme

GST assay

Steady-state kinetics were studied for adGSTD5-5 at varying concentrations of CDNB (1-chloro-2,4-dinitrobenzene) and GSH in 0.1 M phosphate buffer, pH 6.5. The reaction was monitored at 340 nm, $\varepsilon = 9600\ M^{-1} \cdot cm^{-1}$. Apparent kinetic parameters, k_{cat}, K_m and k_{cat}/K_m were determined by fitting the collected data to a Michaelis–Menten equation by non-linear regression analysis using GraphPad Prism (GraphPad software, San Diego, CA, U.S.A.) [8,12]. The cumene hydroperoxide assay was performed by the method of Wendel [13]. The inhibition studies were performed using the GST assay conditions of 3 mM CDNB and 10 mM GSH (except for adGSTD2-2 and adGSTD6-6, where 15 mM GSH was used) in the absence and presence of various concentrations of inhibitors. Inhibitor solutions were diluted appropriately to maintain a constant concentration of organic solvent, if used, when the inhibitor concentration was varied. Protein quantification was determined by the method of Bradford [14] using the Bio-Rad reagent with BSA as the standard protein.

Crystallization

Culture trays (Flow Laboratories, McLean, VA, U.S.A.) sealed with petroleum jelly and siliconized coverslips (Hampton Research, Laguna Niguel, CA, U.S.A.) were used to grow crystals by the hanging-drop vapour-diffusion method. The well contained a 1 ml solution containing 1.6–2 M Li_2SO_4, 1 mM $CuCl_2$ and 100 mM sodium phosphate buffer, pH 6.5–7.5. A 1 μl aliquot of protein (13.1 mg/ml), 1 μl of 10 mM glutathione sulphonic acid and 1 μl of well solution were applied to the bipyramidal crystals (0.1–0.2 mm) that appeared within 24 h of setting up the tray.

Data collection

Crystals were transferred to artificial mother liquor containing 20 % (v/v) glycerol before snap-freezing at 100 K using an Oxford Cryo-Cooler. Data were collected using a Mar345 Image Plate system (marresearch GmbH, Norderstedt, Germany) with Cu-Kα X-rays from a Rigaku Ru-200 rotating anode generator equipped with Ni-focusing mirrors.

Structure solution and refinement

The adGST1-6 (adGSTD6-6) monomer solved at 2.15 Å (1 Å = 0.1 nm) resolution (Protein Date Bank code 1V2A) was used as a search model for molecular replacement using Molrep [15]. All structure refinement was performed using CNS [16] and model building in O [17]. A random selection of 5 % of reflections was chosen as a Free-R set to test the validity of various refinement steps. Alignment of adGSTD5-5 with adGSTD3-3 and adGSTD4-4 was performed using Deep View Swiss-PdbViewer version 3.7 (http://www.expasy.org/spdbv/) to obtain the RMSD (root mean square deviation) of the α-carbon backbone [18]. The Figures were created with Accelrys DS ViewerPro 5.0.

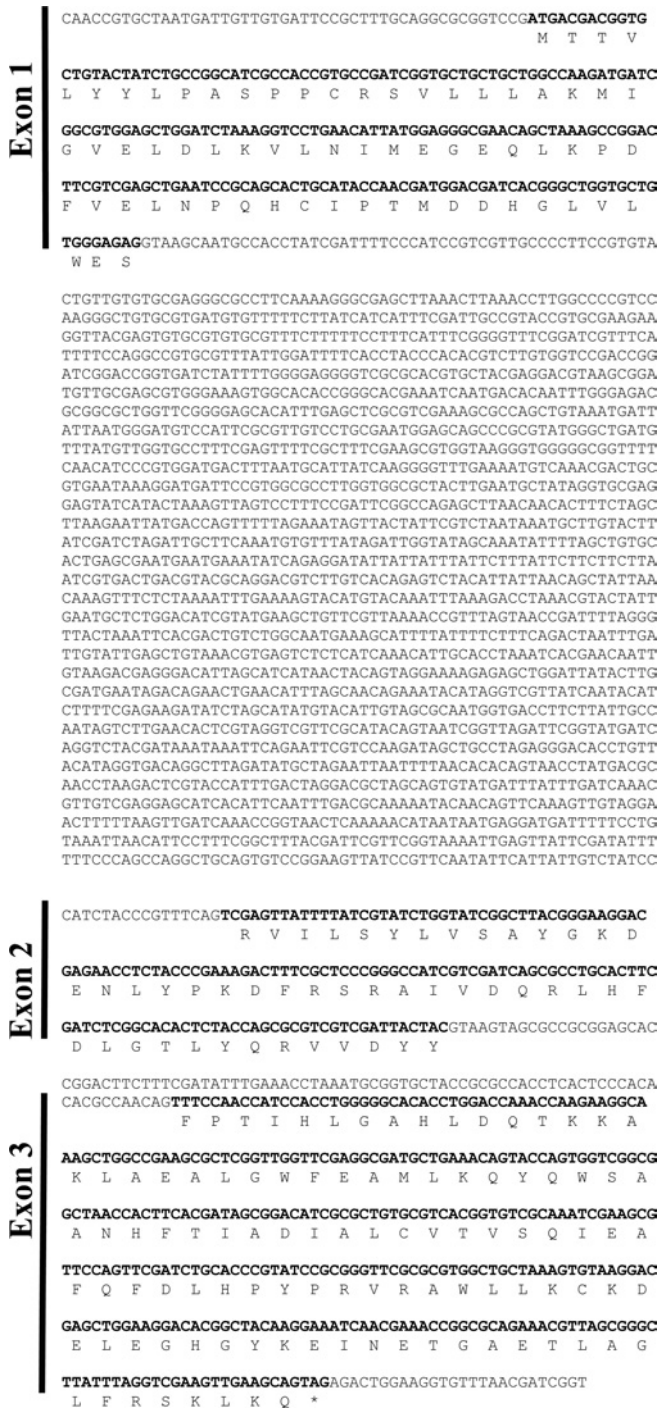

Figure 2 **The** ***gstD5*** **gene organization is composed of three coding regions that code for one GST protein**

The coding sequence is shown in bold, with the translated amino acid sequence below. The last codon of exon 1 is split, with the last base of the codon in exon 2.

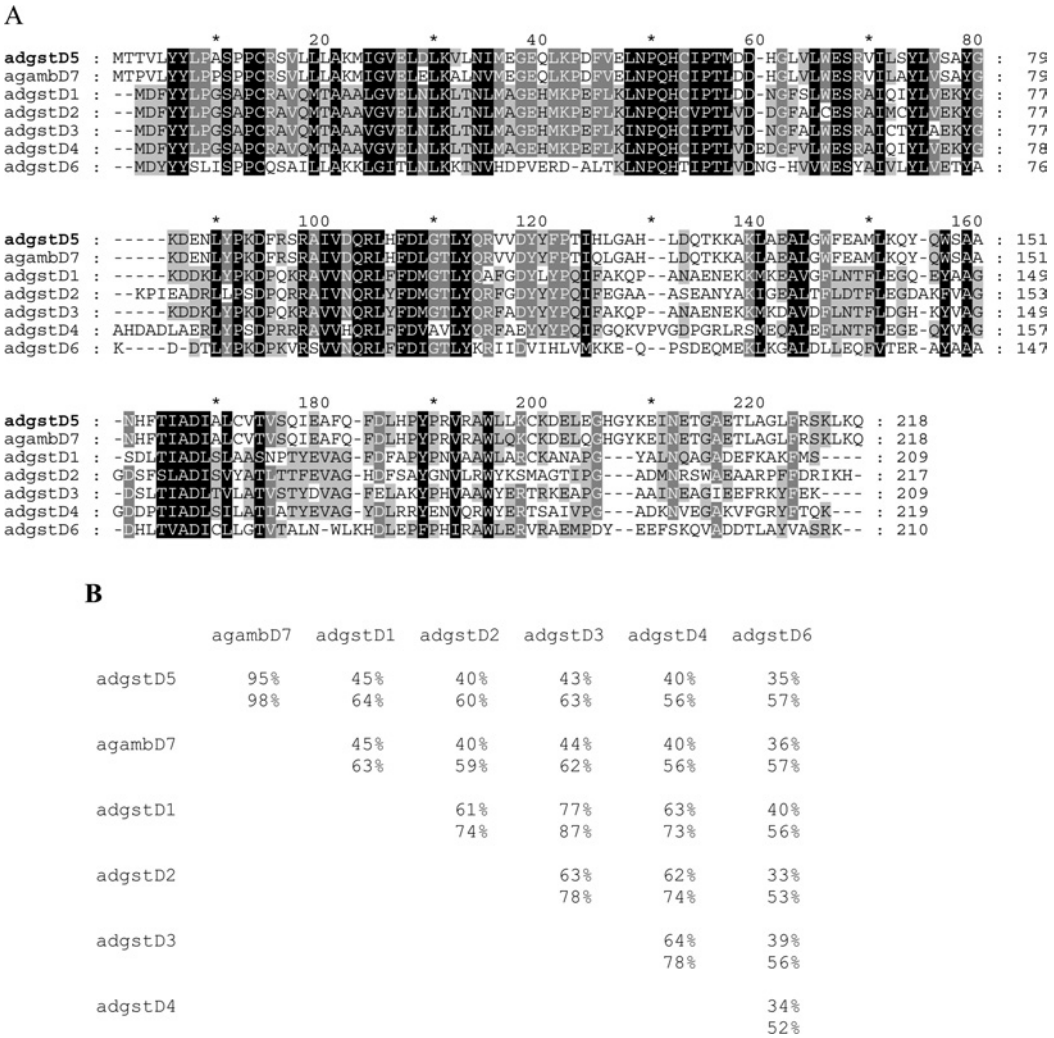

Figure 3 Amino acid sequence comparison of *A. dirus* adGSTD5-5 and the orthologous enzyme of AgadGSTD7 from *A. gambiae* (agambD7) and five previously obtained *A. dirus* Delta GSTs using GeneDoc version 2.6

The sequences are adGSTD1-1, adGSTD2-2, adGSTD3-3, adGSTD4-4 and adGSTD6-6 (GenBank® accession numbers AF273041, AF273038, AF273039, AF273040 and AY014406 respectively [6,8]). (**A**) The dashes indicate gaps in the sequence. Black shading indicates 100 % conserved residues for the seven sequences, dark grey indicates 80 % conserved, and light grey indicates 60 % conserved. (**B**) Matrix table of percentage amino acid identities (top value) and percentage amino acid similarities (bottom value) for the sequences aligned in (**A**).

RESULTS AND DISCUSSION

Genomic organization and isolation cDNA of *adgstD5*

A BLAST analysis of the 15 694 bp complete sequence of phage clone 8A.2 revealed a new GST gene, *adgstD5*, from the malaria vector *A. dirus*. This gene was named *adgstD5* for A. dirus GST class Delta protein coding sequence 5. The *adgstD5* gene is located upstream and is in reverse orientation to the *adgst1AS1* gene (Figure 1). Previously, we had a partial sequence for the phage insert, which suggested that the second gene was downstream, as well as possibly of the same Delta class GST as *adgst1AS1* and therefore was called *gst1-5* for insect GST class one enzyme five [7]. The derived amino acid sequence of the three coding exons is shown in Figure 2. The BLAST analysis yielded the highest identity to aggst1-7 (now referred to as gstD7), the product of the *aggst1β* gene of *Anopheles gambiae* [19]. The percentage amino acid identity for these two enzymes is 95 % and the percentage similarity is 98 % (Figure 3). The two mosquito malaria vectors *A. dirus* and *A. gambiae* have been diverged for several million years, the first in Southeast Asia and the second in Africa. The high degree of sequence conservation between the two *Anopheles* species suggests that this GST isoenzyme has a role in the metabolism of a compound that is a common metabolic product or a significant component in the environment in many living cells. A comparison with the available *A. gambiae* genome data shows that the adGSTD5 protein has 29–45 % amino acid identity with other Delta GSTs and 9–36 % with GSTs from the remaining classes. The percentage amino acid similarity to the Delta GSTs is 49–66 %. Therefore this GST is most like the Delta class GSTs; however, this gene encodes a singular GST protein with marginal amino acid identity with other Delta class GSTs.

Putative promoters of *adgstD5*

Previously, intronless GST genes have been reported in *Drosophila*; however, later introns were identified, as well as a 5′ untranslated region exon [20]. Our data of the exon composition of *adgstD5* define only the coding region. An additional possible 5′ and 3′ splice site were identified by BCM Gene Finder [21]. This

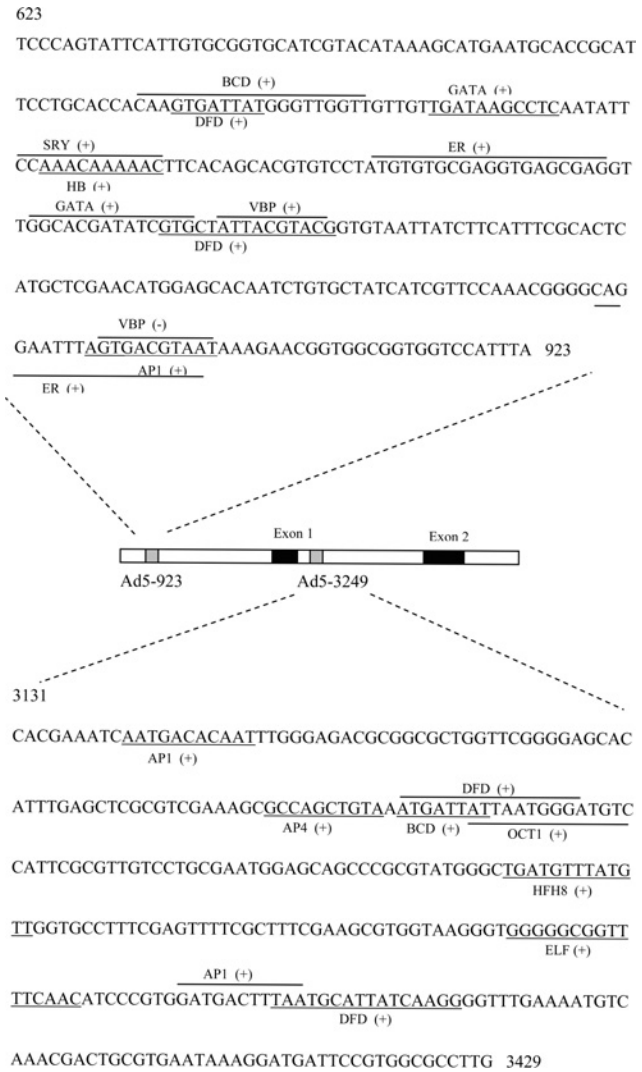

Figure 4 Sequence of two putative promoters of *gstD5* (Ad5-923 and Ad5-3429)

Potential transcription-factor-binding sites were mapped on the region of these two putative promoters by the MatInspector program. BCD, bicoid; ELF, grainyhead protein of *Drosophila*; ER, oestrogen receptor; HFH8, forkhead domain protein; SRY, sex-determining region Y; VBP, vitellogenin-binding protein. The binding site of each potential transcription factor is underlined or overlined. The (+) indicates the binding site on the sense strand, while (−) indicates the binding site on the antisense strand.

suggests a possible 5′ splice site (TG/**GT**GGTT) and 3′ splice site (TTGC**AG**/GC) (bold indicates the usually conserved splice site codon cleavage points) 771 bp and 11 bp upstream of exon 1 respectively. This implies that there is an exon that may be a 5′ untranslated region. Analysis also revealed two putative promoters, Ad5-923 and Ad5-3429, which may be defined as regulatory promoters of *adgstD5*, and are required to fulfil the core promoter activity in specific physiological circumstances (Figure 4).

Ad5-923 contains several binding sites for developmentally regulated transcription factors, such as hunchback, *Dfd*, AP-1 and GATA-1 (Figure 4). Also of interest are several binding sites of oestrogen receptor and oestrogen-dependent protein (oestrogen-receptor- and vitillogenin-binding protein) and maternal-effect protein in Ad5-923. It has been reported that there is an oestrogen-like compound in another arthropod, the ovary of shrimp (*Parapenaeus fissurus*) [22]. Searching the *Drosophila* genome database for an oestrogen receptor sequence yielded one sequence (CG 7404 gene product) on chromosome 3 that was distinct from the ecdysone receptor gene which is located on chromosome 2. BLAST analysis of the CG 7404 gene product provided the highest score to an oestrogen-related receptor β (41 % identity and 53 % similarity). These data imply that oestrogen-like compounds in insects may function in a similar way to vertebrate oestrogen. It is possible that the type of transcription factor binding sites detected in Ad5-293 may have contributed to the specific expression of Adgst5 mRNA in adult female mosquitoes.

Oocyte development in female mosquitoes involves lipid synthesis at extra-ovarian sites, such as the fat body, transfer and then incorporation into oocytes [23,24]. In *Aedes aegypti*, the dry weight of oocytes consists of 35 % lipids, 80 % of which has been transported from fat body [23,24]. The accumulation and transport of the lipid reserves in adult female mosquitoes would create an oxidative stress burden that could be alleviated by increased GST expression. The presence of an oestrogen-response element upstream of the *GSTA* gene was proposed to have a possible role in sexually maturing female plaice oocyte development [25]. The authors suggested that the enormous mobilization of lipids during lipovitellin synthesis in females presents a specific requirement of a GST-mediated detoxification mechanism to deal with lipid peroxidation, since up to 50 % of total fish egg lipid is composed of polyunsaturated fatty acids originating from the mother [25]. Ad5-923 contained both the oestrogen-response element and a vitellogenin-binding-protein element, which suggests that *adgstD5* might be involved in oogenesis, as was proposed for the fish GST.

Currently, the number of genes known to be regulated by elements outside the 5′ flanking region is constantly increasing. These intronic regulators often direct cell-type-specific or developmentally regulated gene expression [26]. Ad5-3429 is located within the intron, and contains several binding sites for factors that are reported to be involved in embryo or tissue development; that is, bicoid, HFH8, Elf, oct, *dfd* and AP-1 (activator protein 1) (Figure 4). This putative promoter therefore may be involved in developmental-stage regulation.

Expression and characterization of the recombinant adGSTD5-5 enzyme

Induction of the *E. coli* culture gave a high yield of recombinant adGSTD5-5 protein expression (250–300 mg/l of *E. coli* culture). However, adGSTD5-5 had a very weak affinity for GST-affinity chromatography medium compared with other GST isoenzymes from *A. dirus*, so the final yield of purified GST was low (1–3 mg/l of *E. coli* culture).

The characterization of the recombinant adGSTD5-5 was intrinsically problematic, as the enzyme possessed low detectable activities, suggesting the enzyme possessed very different substrate specificities compared with the other *A. dirus* GSTs. The adGSTD5-5 enzyme had an intermediate specific activity in GSH conjugation with the classical GST substrate CDNB. The K_m for GSH was the lowest observed for all six *A. dirus* GSTs (Table 1), suggesting the highest affinity binding to GSH. An estimated V_{max} of 167 μmol/min per mg and K_m of 14.9 mM are given only for purposes of comparison, as the data was collected well below the K_m value owing to CDNB solubility limits. The fairly high K_m for CDNB indicated low-affinity binding for this substrate. Cumene hydroperoxide activity was measured for adGSTD5-5 and also, for comparison, adGSTD4-4. The adGSTD5-5 activity of 0.293 ± 0.004 μmol/min per mg of protein (mean $\pm$ S.D.) was 6-fold greater than the 0.050 ± 0.009 μmol/min per mg of protein determined for adGSTD4-4. Our study of a range of compounds shown previously to be substrates for cytosolic GSTs

Table 1 Kinetic parameters of *A. dirus* GSTs

The data for adGSTD1-1, adGSTD2-2, adGSTD3-3, adGSTD4-4 and adGSTD6-6 have been reported previously [6,8,11].

			CDNB		GSH	
Isoenzyme	V_{max} (μmol/min per mg)	k_{cat} (s^{-1})	K_m (mM)	k_{cat}/K_m ($mM^{-1} \cdot s^{-1}$)	K_m (mM)	k_{cat}/K_m ($mM^{-1} \cdot s^{-1}$)
adGSTD5-5	167 ± 48	69	14.9 ± 4.9	5	0.21 ± 0.01	400
adGSTD1-1	12.9 ± 0.6	5.03	0.10 ± 0.03	48.4	0.86 ± 0.2	5.86
adGSTD2-2	63.9 ± 3.50	25.9	0.21 ± 0.03	121	1.30 ± 0.15	20
adGSTD3-3	67.5 ± 1.97	26.9	0.10 ± 0.01	269	0.40 ± 0.05	67
adGSTD4-4	40.3 ± 1.89	16.9	0.52 ± 0.67	32	0.83 ± 0.08	20
adGSTD6-6	2.2 ± 0.3	0.9	5.3 ± 0.8	0.2	1.8 ± 0.4	0.5

Table 2 Inhibition study of CDNB activity

The CDNB activity was measured in the absence and presence of the respective compound at the concentration given. The data presented represent the means ± S.D. for at least three independent experiments. ND, not detected.

		Inhibition (%)					
Compound	Concentration (mM)	adGSTD5-5	adGSTD1-1	adGSTD2-2	adGSTD3-3	adGSTD4-4	adGSTD6-6
Dichloroacetic acid	0.5	16.84 ± 3.22	ND	ND	ND	ND	ND
Cumene hydroperoxide	2.5	37.17 ± 1.19	30.36 ± 9.53	60.44 ± 2.15	28.94 ± 4.82	29.53 ± 3.77	28.27 ± 2.56
p-Nitrobenzyl chloride	1.0	33.40 ± 6.07	43.38 ± 5.17	37.60 ± 3.67	55.36 ± 1.84	49.77 ± 1.35	9.52 ± 1.98
p-Nitrophenyl bromide	0.1	35.72 ± 1.50	24.30 ± 14.52	17.28 ± 0.88	33.39 ± 3.78	31.33 ± 3.10	3.17 ± 3.85
Ethacrynic acid	0.1	84.67 ± 0.71	100 ± 0	99.57 ± 0.59	98.31 ± 0.10	100 ± 0	86.36 ± 1.65
	0.01	55.22 ± 0.66	99.46 ± 1.54	94.88 ± 1.32	81.61 ± 0.76	85.49 ± 1.58	57.73 ± 3.09
	0.001	40.28 ± 3.16	81.88 ± 4.14	64.16 ± 3.74	37.95 ± 1.99	46.45 ± 3.39	37.55 ± 1.40
S-Hexylglutathione	0.1	71.98 ± 1.76	94.93 ± 0.65	97.08 ± 0.92	67.84 ± 1.10	76.91 ± 0.26	64.14 ± 3.58
	0.01	24.87 ± 3.93	63.18 ± 3.21	75.44 ± 0.61	32.07 ± 1.58	20.09 ± 1.24	35.03 ± 2.46
Permethrin	0.01	35.56 ± 1.68	20.37 ± 1.90	27.36 ± 5.45	35.87 ± 1.87	47.73 ± 3.08	11.70 ± 1.87
Deltamethrin	0.01	40.15 ± 2.17	11.01 ± 7.51	30.72 ± 3.53	35.28 ± 3.05	49.30 ± 2.37	15.87 ± 5.29
λCyhalothrin	0.01	39.96 ± 1.19	21.88 ± 10.66	29.11 ± 2.88	26.38 ± 1.73	40.50 ± 1.40	23.26 ± 5.58

Table 3 DDTase activity of the recombinant GST isoenzymes from *A. dirus*

The DDTase activity is expressed as nmol of DDE (dichlorodiphenyldichloroethylene) formation/mg of enzyme protein. The CDNB specific activity is in μmol/min per mg of protein.

Isoenzyme	DDTase activity	CDNB activity	DDTase/CDNB
adGSTD5-5	78.77 ± 13.19	19.2	4.11
adGSTD1-1	<1.0	12.2	–
adGSTD2-2	1.87 ± 0.82	39.7	0.05
adGSTD3-3	2.66 ± 0.29	64.6	0.04
adGSTD4-4	7.50 ± 1.68	38.3	0.20
adGSTD6-6	1.28 ± 0.22	1.37	0.93

from the classes described previously, including 1,2-dichloro-4-nitrobenzene, *p*-nitrophenethyl bromide and ethacrynic acid, revealed that there was no detectable activity with these known GST substrates, even at 10-fold increased enzyme concentration compared with that used in the CDNB assay. Nevertheless, adGSTD5-5 did interact with these substrates as well as pyrethroid insecticides, as shown by inhibition of CDNB activity (Table 2). Intriguingly, only adGSTD5-5 was inhibited by dichloroacetic acid, which is the specific substrate for Zeta class GSTs in dechlorination of dichloroacetic acid to glyoxylic acid [27–31]. However, this dechlorination activity was undetectable for adGSTD5-5. Despite low GSH-conjugating activity, adGSTD5-5 possessed the greatest DDT [1,1,1-trichloro-2,2-bis-(*p*-chlorophenyl)ethane] dehydrochlorination activity of the six recombinant GSTs that we have currently obtained (Table 3). The DDTase activity was 11–62-fold different among the five

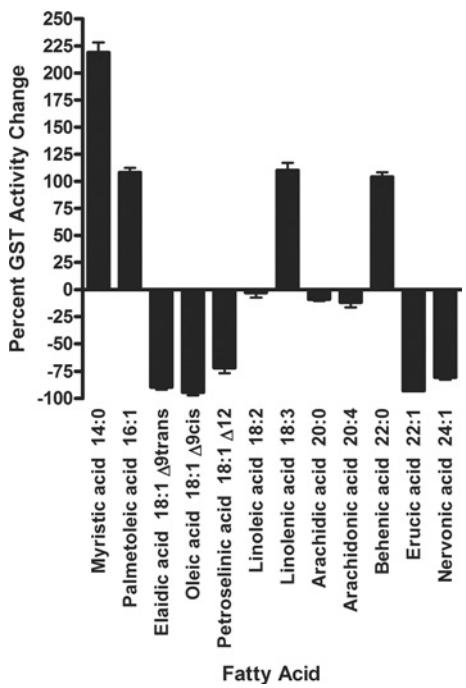

Figure 5 Fatty acid effects on adGSTD5-5 CDNB activity

The final concentration of fatty acids tested was 50 μM in the standard CDNB assay. Data show the changed enzyme activity for CDNB in the presence of the respective fatty acid, where negative values show inhibition and positive values show activation relative to the absence of any fatty acid.

Table 4 X-ray data reduction statistics

Values in parentheses refer to the highest resolution bin (2.59–2.50 Å).

Parameter	Value
R-factor (%)	7.8 (39.6)*
$I/\sigma I$	12.9 (2.6)
Number of observations	37582 (3682)
Number of unique observations	9605 (963)
Multiplicity	3.9 (3.8)
Completeness (%)	95.6 (97.9)

Table 5 Model statistics

Values in parentheses refer to the highest resolution bin (2.66–2.50 Å).

Parameter	Value
R-factor	0.233 (0.351)
R-free	0.265 (0.407)
Non-hydrogen atoms in model:	
Protein	1732
Glutathione sulphonic acid	23
Water	44
Cu^{2+} ions	3
Mean B-factor	45.5
B-factor from Wilson plot	41.8
RMSD from ideal values	
Bond lengths	0.007 Å
Bond angles	1.4°
Dihedral angles	20.8°
Improper angles	0.82°

A. dirus GSTs, and adGSTD1-1 had no detectable activity (Table 3). A ratio of DDTase/CDNB activity showed that the adGSTD5-5 enzyme possessed a 4–100-fold greater DDT substrate preference compared with the other GSTs. Altogether, these data illustrate that adGSTD5-5 displays catalytic properties distinct from the insect GST isoenzymes defined previously. Two additional classes of soluble GSTs, Omega and Zeta, were also described recently with unusual enzymatic activities in a variety of organisms, including mammals [32–34]. This suggests that gene rearrangement in combination with structural evolution presumably constitutes an evolutionary function of the GST enzymes operating in Nature [35]. The mechanism of catalysis and the residues involved are yet to be investigated for adGSTD5-5.

Various mammalian GST isoforms have been shown to be highly active in conjugating toxic lipid alkenals and purine and pyrimidine alkenals, all of which are believed to arise in cells as a consequence of oxidative processes [36,37]. Interestingly, adGSTD5-5 contained the putative regulatory elements involved in detoxification of lipid peroxidation. Therefore we investigated the role of heterologously expressed adGSTD5-5 involved in detoxification of potentially deleterious fatty acid metabolites by assaying the effect of polyunsaturated fatty acids on GSH conjugation with CDNB. Our data demonstrated adGSTD5-5 interaction with several fatty acids (Figure 5). An interesting observation was that, although several fatty acids appeared to have little effect on CDNB activity, the remaining tested either inhibited activity by 72–94 % or enhanced activity by 104–219 %. This fatty acid interaction yielding varying effects on adGSTD5-5 implies that adGSTD5-5 may have a physiological role in protection against oxidative stress as reported previously for GST Alpha class isoenzymes that appear to be involved in the signalling mechanisms of apoptosis [38].

Structural determination of adGSTD5-5 enzyme

Molecular replacement was successful with the solution corresponding to the highest peak in the rotation function (5.97σ) and translation function (13.82σ) as shown in Table 4. The initial model (R-factor = 0.526, R-free = 0.515) was subjected to rigid body, positional and temperature-factor refinement, reducing the R-factor to 0.466 (R-free = 0.485). Sigma-A weighted $2F_o$-F_c and F_o-F_c electron density maps calculated from this model revealed a molecule in the G-site not present in the model. This was clearly a glutathione sulphonic acid molecule. Six cycles of positional refinement, B-factor refinement and model building were performed in which the amino acid sequence of the model was changed from that of adGSTD6-6 to adGSTD5-5. The final model includes amino acid residues 2–215, one glutathione sulphonic acid molecule and 44 water molecules. Statistics for this model are given in Table 5. The adGSTD5-5 structure obtained for this study is shown in Figure 6 (Protein Data Bank accession number 1R5A).

The tertiary structure obtained from crystallographic analysis showed the adGSTD5-5 protein to possess the canonical GST structure (Figure 7). The physiologically relevant state of the protein is a dimer, which is present in the crystal owing to a 2-fold symmetry operation. The overall structure is broadly similar to that of previously determined Delta class GST structures [5].

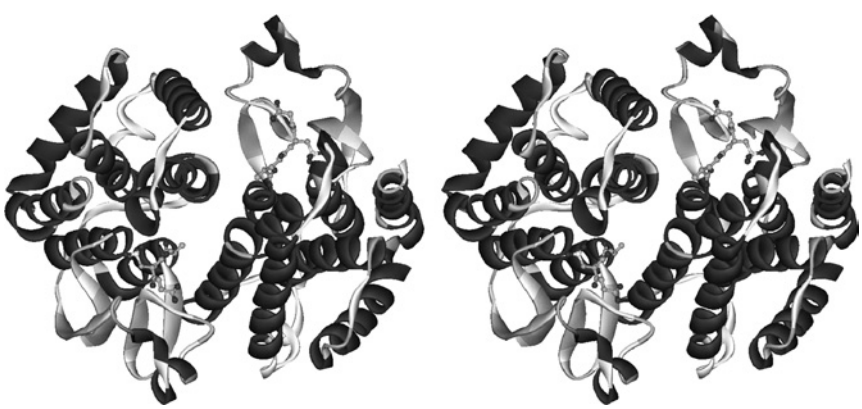

Figure 6 Stereo view of adGSTD5-5

The view is looking down on the 2-fold axis into the active site, with the glutathione sulphonic acid shown as a ball-and-stick figure. The co-ordinates for the tertiary structure have been deposited in the Protein Data Bank under the accession code 1R5A.

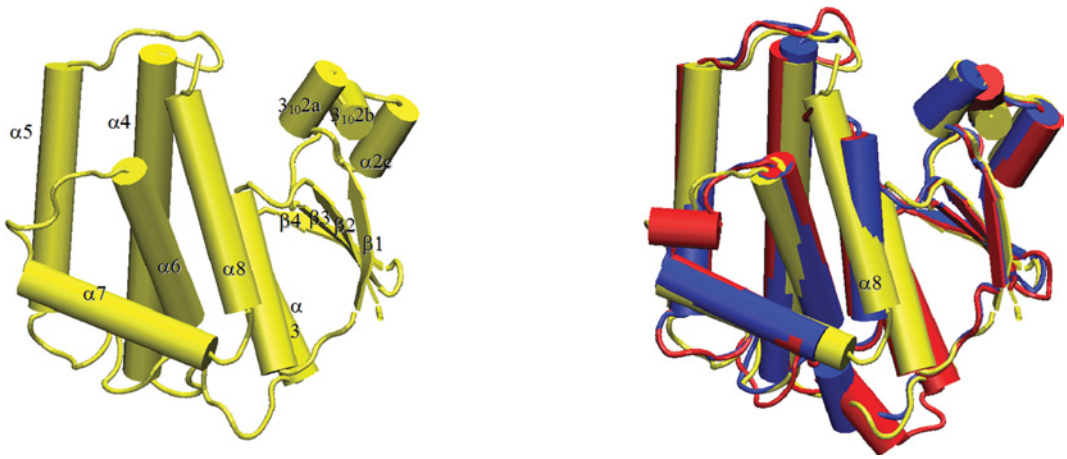

COLOUR

Figure 7 Cartoon representation of adGSTD5-5

Cylinders represent helices, arrows represent strands, and lines represent random coil. (**A**) adGSTD5-5, with secondary structure elements labelled. (**B**) Aligned *Anopheles* GSTs. adGSTD3-3 is in blue, adGSTD4 is in red, and adGSTD5-5 is in yellow.

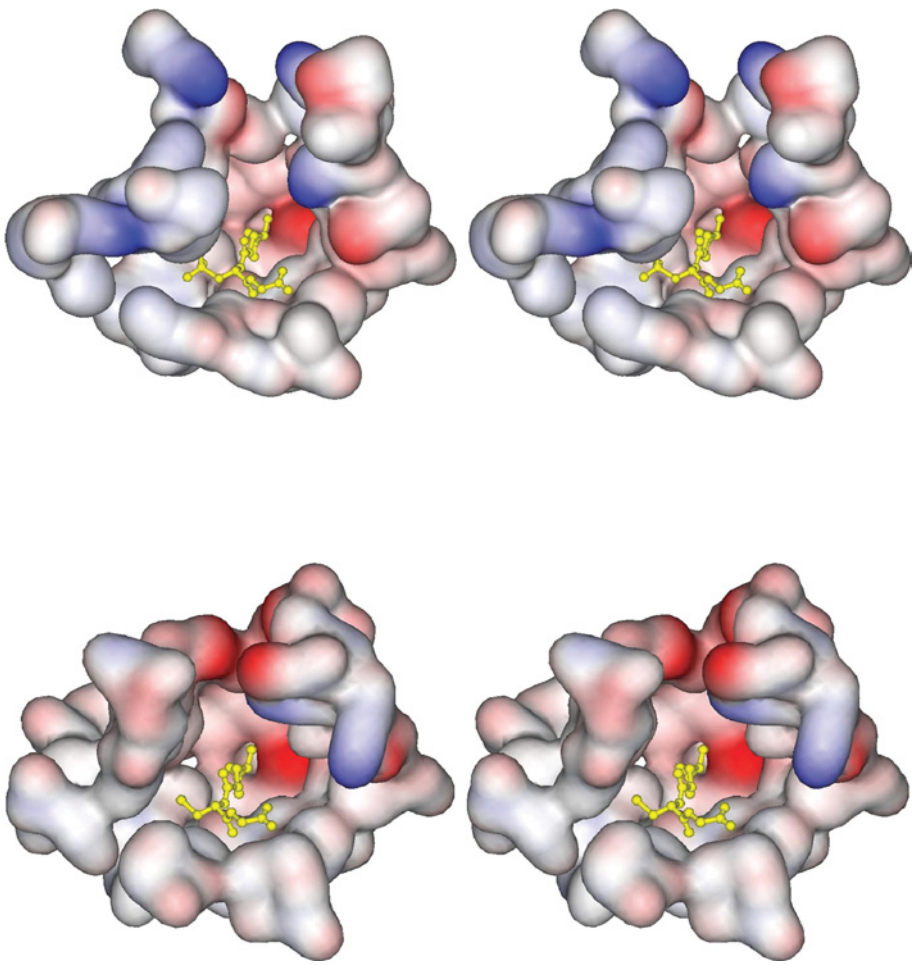

COLOUR

Figure 8 Stereo views of the electrostatic potential surface of the active-site pockets of adGSTD5-5 and adGSTD3-3

The two tertiary structures were aligned to illustrate the same view of the active site. The top panel shows adGSTD5-5, and the bottom panel shows adGSTD3-3. A yellow ball-and-stick representation shows the GSH in the pocket.

The G-site is formed mostly by residues from the N-terminal thioredoxin domain. Like other Delta class GSTs, a serine residue (Ser[11]) appears to be responsible for activating the GSH thiol residue in catalysis. However, in the absence of direct evidence such as site-directed mutagenesis, it is possible that a nearby serine, cysteine or tyrosine residue may be the major catalytic

residue. The presence of a histidine residue (His^{119}) was unexpected: GST H-sites normally being lined with hydrophobic residues. A water molecule sits in the H-site and is hydrogen-bonded to $His^{119}N\varepsilon2$.An alignment of the adGSTD5-5 tertiary structure with these two *A. dirus* GSTs, adGSTD3-3 and adGSTD4-4 (Protein Data Bank accession numbers 1JLV and 1JLW respectively), illustrates the conserved nature of GST tertiary structure. adGSTD5-5 possessed a RMSD of 1.42 Å and 1.25 Å for the α-carbon alignment with adGSTD3-3 and adGSTD4-4 respectively. There are significant differences between the packing of helix $\alpha8$ of adGSTD5-5 with the rest of the protein. As a result, this helix is closer to the C-terminal domain compared with other insect GST isoenzymes (Figure 7). This can be attributed to the substitution of packing residues in adGSTD5-5 to smaller amino acids. As such, the overall shape of the H-site is different in adGSTD5-5 compared with the adGSTD3-3 and adGSTD4-4 isoenzymes. A comparison of adGSTD5-5 and adGSTD3-3 showed 47 % identity in the 43 amino acids that make up the active-site pocket with an average RMSD of 0.616 Å for the identical amino acid residues. However, the shape of the two active-site pockets seems to be quite distinct, with the adGSTD5-5 pocket appearing to be elongated (Figure 8). In comparison, the adGSTD5-5 pocket also appears to be more polar, with an increase in both positive and negative charges that contributes to distinct orientations of GSH and substrate binding. These structurally unique features of adGSTD5-5, especially in the vicinity of the active site and the C-terminus, may define the substrate repertoire for this particular GST, whereby it displays an unusual enzymatic property. These results suggest that there is considerable structural plasticity in the active site of Delta class GSTs, and that their catalytic activities may not be restricted to hydrophobic co-substrates.

Conclusion

The adGSTD5-5 isoenzyme was identified and only detectably expressed in *A. dirus* adult females. A high degree of sequence conservation of this gene across several million years of divergent evolution between two Anopheline malaria vector species suggests that this GST isoenzyme performs an important function. A putative promoter analysis suggests that this GST has an involvement in oogenesis and in developmental-stage regulation. The enzyme displayed little activity for classical GST substrates, although it possessed the greatest activity for DDT, 10-fold, observed for Delta GSTs. However enzyme activity was increased or decreased by fatty acid interaction, suggesting that the GST activity may be modulated by fatty acids. A tertiary structure comparison revealed differences in active-site composition, with an elongated and more polar active-site topology.

This work was supported by the Thailand Research Fund, and R.U. was supported by a Royal Golden Jubilee Scholarship.

REFERENCES

1 Ding, Y., Ortelli, F., Rossiter, L. C., Hemingway, J. and Ranson, H. (2003) The *Anopheles gambiae* glutathione transferase supergene family: annotation, phylogeny and expression profiles. BMC Genomics **4**, 35–50

2 Vontas, J. G., Small, G. J. and Hemingway, J. (2001) Glutathione S-transferases as antioxidant defence agents confer pyrethroid resistance in *Nilaparvata lugens*. Biochem. J. **357**, 65–72

3 Zou, S., Meadows, S., Sharp, L., Jan, L. Y. and Jan, Y. N. (2000) Genome-wide study of aging and oxidative stress response in *Drosophila melanogaster*. Proc. Natl. Acad. Sci. U.S.A. **97**, 13726–13731

4 Prapanthadara, L., Hemingway, J. and Ketterman, A. J. (1993) Partial purification and characterization of glutathione S-transferases involved in DDT resistance from the mosquito *Anopheles gambiae*. Pestic. Biochem. Physiol. **47**, 119–133

5 Oakley, A. J., Harnnoi, T., Udomsinprasert, R., Jirajaroenrat, K., Ketterman, A. J. and Wilce, M. C. J. (2001) The crystal structures of glutathione S-transferases isozymes 1–3 and 1–4 from *Anopheles dirus* species B. Protein Sci. **10**, 2176–2185

6 Jirajaroenrat, K., Pongjaroenkit, S., Krittanai, C., Prapanthadara, L. and Ketterman, A. J. (2001) Heterologous expression and characterization of alternatively spliced glutathione *S*-transferases from a single *Anopheles* gene. Insect Biochem. Mol. Biol. **31**, 867–875

7 Pongjaroenkit, S., Jirajaroenrat, K., Boonchauy, C., Chanama, U., Leetachewa, S., Prapanthadara, L. and Ketterman, A. J. (2001) Genomic organization and putative promoters of highly conserved glutathione S-transferases originating by alternative splicing in *Anopheles dirus*. Insect Biochem. Mol. Biol. **31**, 75–85

8 Udomsinprasert, R. and Ketterman, A. J. (2002) Expression and characterization of a novel class of glutathione S-transferase from *Anopheles dirus*. Insect Biochem. Mol. Biol. **32**, 425–433

9 Mannervik, B., Awasthi, Y. C., Board, P. G., Hayes, J. D., Di Ilio, C., Ketterer, B., Listowsky, I., Morgenstern, R., Muramatsu, M., Pearson, W. R. et al. (1992) Nomenclature for human glutathione transferases. Biochem. J. **282**, 305–306

10 Chelvanayagam, G., Parker, M. W. and Board, P. G. (2001) Fly fishing for GSTs: a unified nomenclature for mammalian and insect glutathione transferases. Chem. Biol. Interact. **133**, 256–260

11 Ketterman, A. J., Prommeenate, P., Boonchauy, C., Chanama, U., Leetachewa, S., Promtet, N. and Prapanthadara, L. (2001) Single amino acid changes outside the active site significantly affect activity of glutathione S-transferases. Insect Biochem. Mol. Biol. **31**, 65–74

12 Prapanthadara, L., Koottathep, S., Promtet, N., Hemingway, J. and Ketterman, A. J. (1996) Purification and characterization of a major glutathione S-transferase from the mosquito *Anopheles dirus* (species B). Insect Biochem. Mol. Biol. **26**, 277–285

13 Wendel, A. (1981) Glutathione peroxidase. Methods Enzymol. **77**, 325–333

14 Bradford, M. M. (1976) A rapid and sensitive method for the quantitation of microgram quantities of protein utilizing the principle of protein-dye binding. Anal. Biochem. **72**, 248–254

15 Vagin, A. and Teplyakov, A. (2000) An approach to multi-copy search in molecular replacement. Acta Crystallogr. Sect. D Biol. Crystallogr. **56**, 1622–1624

16 Brunger, A. T., Adams, P. D., Clore, G. M., DeLano, W. L., Gros, P., Gross-Kunstleve, R. W., Jiang, J. S., Kuszewski, J., Nilges, M., Pannu, N. S. et al. (1998) Crystallography & NMR system: a new software suite for macromolecular structure determination. Acta Crystallogr. Sect. D Biol. Crystallogr. **54**, 905–921

17 Jones, T. A., Zou, J. Y., Cowan, S. W. and Kjeldgaard, M. (1991) Improved methods for building protein models in electron density maps and the location of errors in these models. Acta Crystallogr. Sect. A Found. Crystallogr. **47**, 110–119

18 Guex, N. and Peitsch, M. C. (1997) SWISS-MODEL and the Swiss-PdbViewer: an environment for comparative protein modeling. Electrophoresis **18**, 2714–2723

19 Ranson, H., Collins, F. and Hemingway, J. (1998) The role of alternative mRNA splicing in generating heterogeneity within the *Anopheles gambiae* class I glutathione S-transferase family. Proc. Natl. Acad. Sci. U.S.A. **95**, 14284–14289

20 Lougarre, A., Bride, J. M. and Fournier, D. (1999) Is the insect glutathione S-transferase I gene family intronless? Insect Mol. Biol. **8**, 141–143

21 Smith, R., Wiese, B., Wojzynski, M., Davison, D. and Worley, K. (1996) BCM search launcher – an integrated interface to molecular biology data base search and analysis services available on the World Wide Web. Genome Res. **6**, 454–462

22 Jeng, S. S., Wan, W. C. and Chang, C. F. (1978) Existence of an estrogen-like compound in the ovary of the shrimp *Parapenaeus fissurus*. Gen. Comp. Endocrinol. **36**, 211–214

23 Ziegler, R. and Ibrahim, M. M. (2001) Formation of lipid reserves in fat body and eggs of the yellow fever mosquito, *Aedes aegypti*. J. Insect Physiol. **47**, 623–627

24 Briegel, H., Gut, T. and Lea, A. O. (2003) Sequential deposition of yolk components during oogenesis in an insect, *Aedes aegypti* (Diptera: Culicidae). J. Insect Physiol. **49**, 249–260

25 Leaver, M. J., Wright, J. and George, S. G. (1997) Structure and expression of a cluster of glutathione S-transferase genes from a marine fish, the plaice (*Pleuronectes platessa*). Biochem. J. **321**, 405–412

26 Warnecke, C., Willich, T., Holzmeister, J., Bottari, S. P. and Fleck, E. (1999) Efficient transcription of the human angiotensin II type 2 receptor gene requires intronic sequence elements. Biochem. J. **340**, 17–24

27 Anderson, W. B., Board, P. G., Gargano, B. and Anders, M. W. (1999) Inactivation of glutathione transferase zeta by dichloroacetic acid and other fluorine-lacking α-haloalkanoic acids. Chem. Res. Toxicol. **12**, 1144–1149

28 Tong, Z., Board, P. G. and Anders, M. W. (1998) Glutathione transferase zeta catalyses the oxygenation of the carcinogen dichloroacetic acid to glyoxylic acid. Biochem. J. **331**, 371–374

29 Tzeng, H.-F., Blackburn, A. C., Board, P. G. and Anders, M. W. (2000) Polymorphism- and species-dependent inactivation of glutathione transferase zeta by dichloroacetate. Chem. Res. Toxicol. **13**, 231–236

30 Thom, R., Dixon, D. P., Edwards, R., Cole, D. J. and Lapthorn, A. J. (2001) The structure of a Zeta class glutathione S-transferase from *Arabidopsis thaliana*: characterisation of a GST with novel active-site architecture and a putative role in tyrosine catabolism. J. Mol. Biol. **308**, 949–962
31 Polekhina, G., Board, P. G., Blackburn, A. C. and Parker, M. W. (2001) Crystal structure of maleylacetoacetate isomerase/glutathione transferase zeta reveals the molecular basis for its remarkable catalytic promiscuity. Biochemistry **40**, 1567–1576
32 Board, P. G., Coggan, M., Chelvanayagam, G., Easteal, S., Jermiin, L. S., Schulte, G. K., Danley, D. E., Hoth, L. R., Griffor, M. C., Kamath, A. V. et al. (2000) Identification, characterization, and crystal structure of the omega class glutathione transferases. J. Biol. Chem. **275**, 24798–24806
33 Anders, M. W., Anderson, W. B., Tzeng, H.-F. and Board, P. G. (2001) Glutathione transferase zeta: novel xenobiotic substrates and enzyme inactivation. Chem. Biol. Interact. **133**, 211–216
34 Board, P., Baker, R. T., Chelvanayagam, G. and Jermiin, L. S. (1997) Zeta, a novel class of glutathione transferases in a range of species from plants to humans. Biochem. J. **328**, 929–935
35 Parker, M. W., McKinstry, W. J., Oakley, A. J., Polekhina, G., Rossjohn, J., Chelvanayagam, G., Board, P. G., Di Ilio, C., Caccuri, A. M., Ricci, G. and Lo Bello, M. (2001) Evolution of functional diversity as observed through structural studies of glutathione transferases. Chem. Biol. Interact. **133**, 8–12
36 Berhane, K., Widersten, M., Engström, Å., Kozarich, J. W. and Mannervik, B. (1994) Detoxication of base propenals and other α,β-unsaturated aldehyde products of radical reactions and lipid peroxidation by human glutathione transferases. Proc. Natl. Acad. Sci. U.S.A. **91**, 1480–1484
37 Ishikawa, T., Esterbauer, H. and Sies, H. (1986) Role of cardiac glutathione transferase and of the glutathione S-conjugate export system in biotransformation of 4-hydroxynonenal in the heart. J. Biol. Chem. **261**, 1576–1581
38 Yang, Y., Cheng, J.-Z., Singhal, S. S., Saini, M., Pandya, U., Awasthi, S. and Awasthi, Y. C. (2001) Role of glutathione *S*-transferases in protection against lipid peroxidation: overexpression of hGSTA2–2 in K562 cells protects against hydrogen peroxide induced apoptosis and inhibits JNK and caspase 3 activation. J. Biol. Chem. **276**, 19220–19230

Received 6 December 2004/14 February 2005; accepted 17 February 2005
Published as BJ Immediate Publication 17 February 2005, DOI 10.1042/BJ20042015

BIOGRAPHY

NAME	Miss Rungrutai Udomsinprasert
DATE OF BIRTH	1 March 1972
PLACE OF BIRTH	Samutsongkhram, Thailand
INSTITUTIONS ATTENDED	Mahidol University, 1990-1993
	Bachelor degree of Science (Medical Technology)
	Mahidol University, 1997-1999
	Master of Science
	(Molecular Genetics and Genetic Engineering)
	Mahidol University, 2001-2005
	Doctor of Philosophy
	(Molecular Genetics and Genetic Engineering)
RESEARCH GRANT	Royal Golden Jubilee Ph.D. Program
	(Thailand Research Fund)
	Scholarships for Doctoral Students and
	Graduate Program Staff for a Presentation Abroad 2003
	(Mahidol University)
	Research assistantships 2004
	(Mahidol University)
	Partial thesis scholarship 2004
	(Mahidol University)
HOME ADDRESS	42/1 Soi Monthonthong, Putthamonthon 2 Rd,
	Taveewatana, Bangkok, 10170, Thailand
	Tel. 0-2887-0600
	Email : rungrutaiu@yahoo.com